INTELLIGENT PERFORMANCE, ARCHITECTURE ANALYSIS, FUNCTIONAL SAFETY METRICS OF AUTOMATED STEERING SYSTEMS FOR AUTONOMOUS VEHICLES

by

SAIF YOSEIF SALIH

A dissertation submitted in partial fulfillment of the
requirements for the Ph.D. degree of

SYSTEMS ENGINEERING

2022

Oakland University
Rochester, Michigan

Doctoral Advisory Committee:

Richard Olawoyin, Ph.D., Chair
Christopher Cooley, Ph.D.
Debatosh Debnath, Ph.D.
Suzan ElSayed, Ph.D.

To my wife, Safa, and my kids, Rafal, Ahmed and Ali,

ACKNOWLEDGMENTS

Firstly, I would like to express my sincere gratitude to my advisor, Prof. Richard Olawoyin, for the continuous support, and significant contributions to my Ph.D. study and related research, for his wisdom, patience, motivation, and immense knowledge. His guidance and commitment to the highest standard inspired me in all the time of my research and writing of this Ph.D. dissertation and contributing to the state of the art of automated driving vehicles. Without his knowledge and assistance, none of this Ph.D. journey would have been successful. I could not have imagined having a better advisor and mentor for my Ph.D. study.

Besides my advisor, I would like to thank the rest of my advisory committee members: Prof. Christopher Cooley for his continuous support and advice through regular discussions that we had during my Ph.D. study; Prof. Debatosh Debnath and Prof. Suzan ElSayed for their insightful comments and encouragement.

Last but not the least, I would like to thank my family: my parents who supported me spiritually; my wife who encouraged and supported me to join the Ph.D. program and finish my degree; and my kids for their patience and be part of my life

Saif Yoseif Salih

ABSTRACT

INTELLIGENT PERFORMANCE, ARCHITECTURE ANALYSIS, AND FUNCTIONAL SAFETY METRICS OF AUTOMATED STEERING SYSTEMS FOR AUTONOMOUS VEHICLES

by

Saif Yoseif Salih

Adviser: Richard Olawoyin, Ph.D.

The increasing complexities and functionalities of the electrical and/or electronic (E/E) systems in present day automobiles, make it challenging for original equipment manufacturers (OEMs) and suppliers to ensure a high level of safety in the automotive critical safety systems. The steering systems represent a standard functionality on every vehicle to control the direction of the vehicle literally and provide more stability for the vehicle motion. High automated vehicles require intelligent steering systems in which more Advanced Driver Assistance Systems (ADAS) applications are linked together such as cameras, radars, Lidars, and global positioning system (GPS). These integrated systems and applications are required for environmental perception, communications, data fusion, planning, prediction, decision making, and actuation processes all in real-time. Therefore, hardware (HW) and software (SW) solutions are developed and implemented in compliance with ISO 26262 standard, Road Vehicles – Functional Safety. Due to the lack of the steering systems published information and the crucial role of the steering associated with complex functionalities challenges, this dissertation provides a case study of how the

steering systems of different automated driving levels can be complied with ISO 26262 given the emerging challenges imposed by the electric vehicle curb weight, increasing trend for the near future. The analysis focused on the safety lifecycle of the E/E components of the steering systems to ensure high availability of the steering systems and avoid any sudden loss of assistance (SLOA). Various safety mechanisms were evaluated and analyzed to improve the functional safety of the steering systems architecture and logic control paths. Based on the proposed controllability metrics performed in this dissertation, it was found that the hazard or malfunction of the steering systems shifted from the Automotive Safety Integrity Level (ASIL) B to ASIL C, the second most critical safety level. To comply with the ISO 26262 and to mitigate the residual risks of E/E systems failure, several solutions proposed in the concept for compliance with the standard such as redundant HW or SW in the controller path.

The controllability classes or categories of the high automated vehicles based on the vehicle global position related to the lane marker lines were investigated and redefined to accommodate for the machine or system in the loop controlling the dynamic driving task (DDT) in autonomous vehicle maneuvering. A new wheel offset marker concept was introduced when the vehicle is approaching the lane marker lines. Also, it was found that the are human factors challenges in SAE level 4 and 5 and the interaction between the driver and the automated control systems of the vehicle that require human machine interface (HMI) modalities. The driver – automated control system engagement in the steering system of the vehicles is one of the crucial control complex scenarios that add uncertainties and potential risks when handing over the steering control between the driver

and-or the automated control system with the allotted time. This study highlights the need to define the driver intervention in high-automated vehicle of SAE level 4 and 5 in order to sustain the traffic safety and keep the vehicle in the intended trajectory or path. This can be addressed by deploying HMI and the human factor implementation in ISO 26262 to standardize the driver-machine relation with the DDT in real time and interactive environment. Both manual and automated driving modes demand the functional safety implementation of the steering system to mitigate any system malfunction or failure.

An artificial neural network (ANN) model was developed to predict the steering torque commands and steering wheel angle (SWA) based on the steering system dataset and vehicle's parameters. ANN model was developed using Neural Network Training (nntraintool) toolbox of MATLAB to evaluate the intelligent steering system performance. The trained ANN model delivered a regression value of ~ 98.5 % versus the measured SWA. The results showed that the ANN was effective in predicting the steering wheel angle patterns based on the input dataset, considering the non-linearity and complexity of the steering system control. This finding helps to improve the functional safety of autonomous vehicles and introduce the concept of intelligent steering systems for path and trajectory planning. Therefore, ANN should be implemented as an abstraction layer in the control module and deployed in the control and actuation processes to support sensor data fusion and support the prediction and pattern recognition.

TABLE OF CONTENTS

TABLE OF CONTENTS—Continued

TABLE OF CONTENTS—Continued

TABLE OF CONTENTS—Continued

LIST OF TABLES

LIST OF TABLES—Continued

LIST OF FIGURES

LIST OF ABBREVIATIONS

ABS	Anti-Lock Brake System
ACC	Adaptive Cruise Control
ACV	Autonomous and Connected Vehicles
ADAS	Advanced Driver Assistance System
ADS	Automated Driving System
As	Steering Assistance Ratio
ASIC	Application Specific Integrated Circuit
ASIL	Automotive Safety Integrity Level
a_y	Lateral Acceleration
BEV	Battery Electric Vehicle
BIST	Built in Self-Test
C	Controllability
DDT	Driving Dynamic Tasks
DTC	Diagnostic Trouble Code
E	Exposure
ECU	Electronic Control Unit
EE	Electric and Electronic
EHPS	Electro-Hydraulic Power Steering
EPS	Electric Power Steering
ESC	Electronic Stability Control

FIT	Failure in Time
FPGA	Field Programmable Gate Array
F_y	Lateral Force on the Tire
g	Gravity (m/sec2)
GDU	Gate Driver Unit
GPS	Global Positioning System
HAD	Highly Automated Driving
HARA	Hazard Analysis and Risk Assessment
HW	Hardware
i_s	Kinetic Steering Ratio
ISO	International Organization of Standardization
LDW	Lane Departure Warning
LFM	Latent Fault Metric
LKA	Lane Keep Assistance
SLOA	Sudden Loss of Assistance
MPFL	Latent Multi Point Fault
MPV	Multi-Purpose Vehicle
Ms	Steering Torque around the Steering Axle
MTTF	Mean Time to Failure
NHTA	National Highway Transportation Administration
NHTSA	National Highway Traffic Safety Administration

OEM	Original Equipment Manufacturers
PCB	Printed Circuit Board
PLD	Programmable Logic Device
PMHF	Probabilistic Metric for Hardware Failure
PWM	Pulse Width Modulation
QM	Quality Management
RAM	Random Access Memory
RF	Residual Fault
ROM	Read Only Memory
rp	Pneumatic Trail
rτ	Constructive Trail
S	Severity
SAE	Society of Automotive Engineers
SbW	Steer by Wire
SoC	System on Chip
SOP	Start of Production
SPF	Single Point Fault
SPFM	Single Point Fault Metric
SUV	Sport Utility Vehicle
SW	Software

SWT	Steering Wheel Torque
DINS	Driver Information and Notification Systems
NMVCCS	National Motor Vehicle Crash Causation Survey
CVM	Control Vehicle Motion
SVM	Sense Vehicle Motion
AoU	Assumption of Use
GT	Gamma Technologies
HAV	Highly Automated Vehicles
RNN	Recurrent Neural Network
HCS	Hardware Computing Systems
V&V	Verification and Validation
MIMO	Multi-input Multi-out
T_s	Sample Time
T	Time Step
msec	Milliseconds
VHIL	Virtual Hardware in the Loop
FRSACC	Full Range Speed Adaptive Cruise Control
ARC	Alive Rolling Counters
CRC	Cyclic Redundancy Check
CMI	Computer Machine Interaction
TTC	Time to Collision

IGV	Intelligent Ground Vehicles
CAN	Controller Area Network
BSP	Board Support Package
NSP	Neural Signal Processors
ASM	Automotive Simulation Model
GUI	Graphical User Interface
BLF	Binary Log File
MDF	Measurement Data Format
MSE	Mean Square Error
VW	Vehicle Weight
γ	Camber Angle
SWS	Steering Wheel Speed
SWA	Steering Wheel Angle
SWT	Steering Wheel Torque
ANN	Artificial Neural Network
AI	Artificial Intelligence
ML	Machine Learning
DbW	Drive by Wire
VMT	Vehicle Mile Travelled

SUMMARY

The design, development and deployment of advanced functionalities of the highly automated steering systems is the key of highly automated and intelligent vehicles driving systems. These developments are enabled within the scope of the ISO 26262 – functional safety of the road vehicles holistic standard. Inherently, safe steering systems design means “the absence of unreasonable risk due to hazard caused by malfunctioning behavior of the electrical/electronic systems). In this dissertation, the sudden loss of the assistance of the vehicle steering systems and its safety integrity were analyzed and a new design guideline was proposed based on the experiment and the model results findings. The sudden loss of assistance of steering systems at higher rack forces and more advanced driver assistant systems functions leads to the recommendation to change the ASIL rating from ASIL B to ASIL C based on HARA and ISO 26262 metrics for the sudden loss of assistance scenario. New solutions were analyzed and results showed that the steering systems architecture needs redundancy in the control path to meet these emerging challenges. It is possible to achieve ASIL C for electric power steering (EPS) systems using various types of architectures at the level of control logic paths utilizing the redundancy concepts. ASIL C mitigation or risk reduction was achieved by incorporating a dual core microcontroller (µc) integrated with a power management and safety-monitoring unit at the same board. The proper implementation of this logic control path of dual core microcontroller integrated with power management and safety monitoring makes the EPS system simpler, faster, reliable and more cost effective. This

allows steering system designers to easily and effectively add and retrofit functional safety to the EPS systems for higher levels of automated vehicles in the future. The combination of safe acquisitions, decision making and actuation along with the ASIL decomposition simplify the hardware architecture for the market of highly available EPS systems and reduce the time to deploy highly available EPS systems compliant with the ISO 26262 Standard.

The analysis of model-based fault injection for the steering system of high-automated vehicles has shown that the steering wheel angle is of high importance and classified as an ASIL D subsystem based on the risk assessment and control metrics that were developed in chapter four. The finding of the modeling of chapter four also redefined the controllability classes or categories of the high automated vehicles based on the vehicle global position related to the lane marker lines to accommodate for the machine or system in the loop controlling the dynamic driving task (DDT) in autonomous vehicle maneuvering. A new wheel offset marker concept was introduced when the vehicle is approaching the lane marker lines. Also, it was found that the are human factors challenges in SAE level 4 and 5 and the interaction between the driver and the automated control systems of the vehicle that require human machine interface (HMI) modalities as explained in table 4.6 in chapter 4. The driver – automated control system engagement in the steering system of the vehicles is one of the crucial control complex scenarios that add uncertainties and potential risks when handing over the steering control between the driver and-or the automated control system with the allotted time. Even when the driver is in full control of the steering system, the ESP is still responsible for approximately

(~ 80%) of the SWT required to steer the vehicle. Therefore, the steering system design and functional safety metric require specific architecture redundancies in SW, HW and system levels for high availability and risk mitigation mechanisms. Chapter four highlighted the need to define the driver intervention in high-automated vehicle of SAE level 4 and 5 in order to sustain the traffic safety and keep the vehicle in the intended trajectory or path. This can be addressed by deploying HMI and the human factor implementation in ISO 26262 to standardize the driver-machine relation with the DDT in real time and interactive environment. Both manual and automated driving modes demand the functional safety implementation of the steering system to mitigate any system malfunction or failure. Therefore, the fault injection concept supports the safety mechanisms implementation and correctness of the system architectural design with respect to faults and failures during the start-up and the runtime. This improves the test coverage of developing safe control system to operate as designed and meet the safety requirements in compliance with the OEMs and government regulations. Moving from the conventional control systems to the artificial intelligence (AI) and the machine learning (ML) is another key enabler for the highly automated driving systems. It was demonstrated that the developed artificial neural network (ANN) in this dissertation can achieve an acceptable level and of safety performance of the complex functions of the steering systems. In chapter five, the problem of predicting the steering wheel torque commands and the steering wheel angles scenarios for autonomous vehicles has been considered and explored. High fidelity dSPACE hardware-in-the-loop simulator bench dataset of steering system input and output parameters from vehicle were collected and

used to build the ANN model for training and validation of the steering column torque commands and the steering wheel angle. The performance of the ANN model to predict the steering command based on the dataset was validated with a regression value of ~ 98.5 % versus the measured steering wheel angle. The results show that the ANN and ML can effectively predict the steering patterns accurately given the fact that the non-linearity and complexity of the steering system control. This improves the safety highly automated driving system vehicles and confirm the feasibility of the concept of intelligent steering systems for path and trajectory planning based on the prediction patterns of the steering systems peripheral signals and parameters. Artificial intelligence finds its way to the most critical safety systems of the automotive for higher reliability and performance. Therefore, the ANN should be implemented as an abstraction layer in the control module to support sensor data fusion and support the prediction, pattern recognition and the vehicle intended trajectory.

CHAPTER ONE

INTRODUCTION

The vehicle traffic accidents and collisions still claim tens of lives on the roads in the United States and Worldwide despite the recent development and the automation evolutionary process of the automobiles and vehicular safety features over the past decade. In 2020, there were approximately 1.5 million deaths due to road accidents worldwide according to the National Highway Traffic Safety Administration (NHTSA) under the Fatality Analysis Reporting System (FARS) [1]. The Fatality Analysis Reporting System is a nationwide census that provides NHTSA, Congress and the American public yearly reports and data on fatal injuries suffered in motor vehicle traffic crashes and accidents statistics [2]. Table 1.1 reports the motorists and non-motorists killed in traffic crash accidents in the United States each year from 2014 to 2020 posted by the NHTSA [3]. It is clear that the fatality crash rates increased constantly from 2017 to 2019, however, the fatality rate decreased from 2017 to 2019. To exclude the effect of the vehicle mile travelled (VMT), which is used to calculate the fatality rates, the % change column in table 1.1 was calculated based on the fatality column to reflect the changes more accurately based on the causality statistics. The decrease of the fatalities from 2017 to 2019 shown in table 1.1 was due to the deployment of driver assistance technologies and safety systems that increased drivers and pedestrian's safety and reduced the human errors and the severity of crashes [3]. However, the fatality rate for 2020 was 1.37 fatalities per 100 million VMT, up from 1.11 fatalities per 100 million

VMT in 2019. The projected fatality and fatality rate for 2020 would be the greatest since 2007 and it is a 7.2 % increase compared with 2019. This shows a significant increase in deaths during 2020 despite the decline of VMT due to restrictions imposed in 2020 to curb the spread of COVID-19.

Table 1.1. US Traffic Fatality Data Report [3].

Year	Fatality Crashes	Fatality	% Change	Fatality Rate
2014	30,019	32,744	-0.5 %	1.08
2015	30,855	35,484	+ 8.4 %	1.15
2016	31,770	37,806	+6.5 %	1.19
2017	32,028	37,473	-0.9 %	1.17
2018	32,353	36,560	-1.7 %	1.13
2019	33,244	36,096	-2.0 %	1.11
2020	34,866	38,680	+7.2 %	1.37

The main behaviors driving an increase in deaths in 2020 include impaired driving, speeding and failure to wear which are related to the driver. To make the ground transportation driving system safer and more reliable, the ADAS equipped with active and passive safety systems are developed and deployed in modern vehicles with higher levels of automation. Consequently, ADAS and automated driving come with benefits and aim at assisting and improving the driver's control over the vehicle by avoiding undesired situations, such the Anti-lock Brake System (ABS), Traction Control System (TCS), and the Electric Power Steering. The automated driving technology presents some

significant human-factors challenges that escalate OEMs, suppliers, and developers to work together to define the key concepts of driving taxonomy, human-machine interface technology and the driver information and notification systems (DINS) [4].

The ground transportation ecosystem consists of three main elements: the driver, vehicle, and the environment or surrounding interaction with each other as shown in figure 1.1. Every element has its properties.

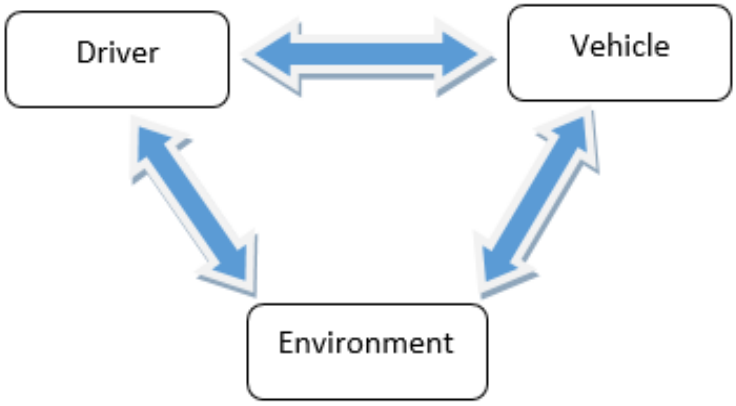

Figure 1.1. Ground transportation ecosystem main elements interacting with each other.

The characteristics are as followings:

1- The driver has knowledge, skills, driver traits, states, and expectancy and reaction response to upcoming events in real-time.

2- The vehicle has HMI, driver vehicle interface (DVI), support systems, connected and automated vehicle (CAV) systems that interact back and forth with the driver.

3- The environment has roads, traffic, weather, surrounding, and connected infrastructure and represent the domain that contains the driver and the vehicle together.

According to a recent study that investigated critical reasons for crashes published by the National Motor Vehicle Crash Causation Survey (NMVCCS) that the drivers cause approximately ~94 % (±2.2%) of the crashes at the national level in the United States. The driver-related critical reasons are broadly classified into recognition errors, decision errors, performance errors, and non-performance errors [5]. The critical reason was assigned to vehicles and the environment were ~2 % and ~3 % respectively. To achieve a "zero crash future," more recent developments in "advanced active safety systems" have introduced additional sensors such as onboard cameras, radars, LIDARS, infrared cameras, steering wheel angle and speed sensors, etc., and additional actuators such as active steering using electric motor assist, active suspensions and advanced emergency braking system [6]. The integration of these on-board sub-systems aims to drive the vehicle partially or fully autonomously by controlling the throttle of the propulsion system and the chassis (Steering and braking modules) [7, 8]. A new ambitious approach towards using drive by wire (DbW) where most mechanical components are replaced by E/E components. This is the reason that the Road Vehicles – Functional Safety (Parts 1-11) ISO26262 Standard was developed to provide a standard for generic functional safety management in the 2nd edition of 2018 for automotive electrical and electronic applications and control systems as shown in figure 1.2 [9].

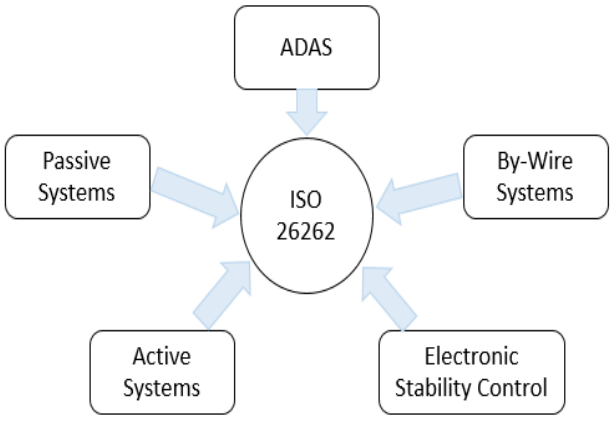

Figure 1.2. ISO 26262 road vehicle- functional safety automotive electrical and electronic systems and components.

1.1 Motivation and Background

Functional safety has become one of the most significant challenges for autonomous and connected vehicles (ACV) due to the advancement in the automotive industry and the complexity of implemented control systems. The automotive industry is transforming from conventional driving technology (where the driver's functionalities; brain, eyes, feet and hands) are part of the control loop to partially or fully autonomous vehicle development, where the microcontrollers (µc) and systems on the chip (SoC) are in the control loop (also referred as self-driving vehicles).

The Society of Automotive Engineers (SAE) - levels of autonomy defines SAE level 1 and 2 as partial autonomy, which requires the driver to execute or supervise the longitudinal and the lateral vehicle motion control at all times. The conditional driving automation of level 3 is where the driver and the system can exchange the vehicle control

with the fallback feature if the automated system fails. SAE level 4 is referred to as high driving automation, where the automated driving system performs all driving operations under specific driving modes and the fallback system is able to appropriately perform without any expectation of the driver to intervene. Full driving automation or SAE level 5 is defined as sustained and unconditional performance by the automated driving system of the entire driving dynamic tasks. Thus, the driver, if presented in the vehicle, may perform other tasks while a dedicated control system controls the vehicle or even there is no need for the driver in the vehicle at all [10]. Table 1.2 shows SAE level 0 through 5.

Table 1.2. SAE levels of automation [10].

SAE level	SAE name	Long., Lateral Control	Monitor environment	Backup	System capability
0	Manual	Driver	Driver	Driver	-
1	Assistance	Driver + System	Driver	Driver	Some driving modes
2	Partial	System	Driver	Driver	Some driving modes
Automated Driving System Monitors Driving Environment					
3	Automation with conditions	System	System	Driver	Some driving modes
4	Advanced Automation	System	system	system	Some driving modes
5	Complete automation	system	system	system	All driving mode

The automated driving control system mainly consists of electrical and electronic (E/E) components linked to sensors, actuators, and other mechanical components such as gears, drivetrains, throttle valves, brake modules, steering rack and pitman arms. Thus, more

stringent safety methodologies are deployed in certain control systems of the vehicle such as the electronic control unit (ECU) of the brake, steering, and the propulsion systems. The quantity of these ECU modules are increasing in modern vehicles, numbering into the hundreds of units interacting with each other and with the surroundings. As a result of more complexity of automated driving system architecture, software and hardware interaction and interfacing in the control systems which increases the risk of both systematic and random hardware failures. In order to reduce these risks and minimize any potential failure or loss of control, ISO 26262 guides the automotive original equipment manufacturers and suppliers (tier 1 and 2) to ensure adequate and acceptable levels of safety procedures are implemented. ISO 26262 consists of eleven parts as shown in figure 1.3 [11].

The main purpose of the ISO 26262 is to provide a standard for generic functional safety management for automotive electrical and electronic applications and systems. The ISO 26262 Standard provides guidelines and instructions throughout the product development process of the V model, from the conceptual development through decommissioning phase [11]. It explains in detail how to reduce the level of risk of a system, component or sub-component to acceptable level by setting the safety goals (SG) and developing suitable safety mechanisms (SM) to monitor, detect and mitigate any faults, errors, and failures in these E\E systems. It also provides an overview to manage the documentation flow of the product development processes, which consist of management, development which consist of management, development, production

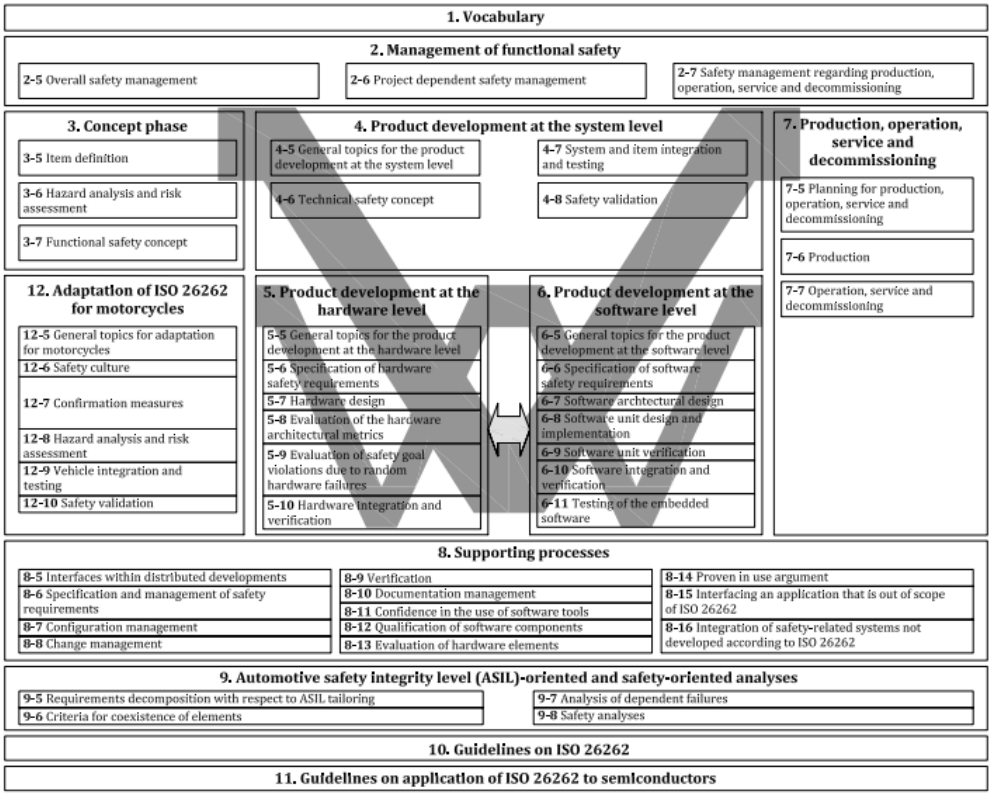

Figure 1.3. Generic parts of ISO 26262 standard [11].

operation, service and decommission. Therefore, complying with ISO 26262 will reduce the risk of systematic failures of the E/E and control the random hardware faults and failures to acceptable levels without any violation for the predetermined safety goals. The safety goals and measures are achieved and complied with through the implementation of safety plans, and later the safety mechanism to manage, process, and support technical requirements of the safety concepts. Part 3 of the ISO 26262 Standard deals with the ASIL computation and safety-oriented analysis. ASIL classification can be calculated and determined by the controllability (C), the severity (S) and the exposure (E) [11-13].

The ASIL rating specifies or identifies the item's necessary safety requirements for achieving a tolerable level of residual risk in case of a system malfunction. In addition, it details the potential hazards, the safety goals, and the level of criticality if a specific component or algorithm fails under specific operational scenarios. One of the most critical safety systems in the autonomous and connected vehicle is the body control module (BCM), which consists of longitudinal control module e.g. adaptive cruise control (ACC), anti-lock brake system; and the lateral control module e.g. power steering and electronic stability controls. These chassis control modules are managed and controlled by dedicated electronic control units, which consist mainly of E/E components connected to sensors and actuators by the general purposes inputs and outputs (GPIOs). The highly automated driving of SAE levels 4 requires the control system to continue the driving task even with the failures presented in system components; hardware (HW), software (SW) or both to continue the vehicle control [14]. Therefore, a fail-operational system must control the vehicle so that no safety violations will occur, whether in regards to the driver, passengers and other road users. This includes any functions and features of the fallback level to ensure the safety goals are maintained and to prevent any violations of the safety goals. However, in SAE level 2 and 3, the backup is the driver (human) in case of system malfunction as shown in table 1.2. This means that the driver must compensate for the system assistance at any time during the maneuver, in case of a SLOA by putting the required steering wheel torque (SWT) to maneuver the vehicle. The SWT, which is the driver's power to control the steering wheel, is transmitted to the torsion bar and rack & pinion gears. This power then is detected by a torque sensor and transmits

to the EPS ECU. The ECU then applies electric current (amount of power assist) according to the SWT and car speed and other predefined parameters. The National Highway Traffic Safety Administration published different values for the human driver steering capability under different driving conditions [15]. However, the maximum human SWT capability that can be applied on the steering wheel was not clear [15]. Different vehicles and/or vehicle configuration are capable of imposing different demands on the drivers' torque input, which can reach up to 60 N.m. The amount of steering assistance that the electric motor puts into the system is controlled so that the driver could steer the vehicle easily and comfortably. The EPS provides up to ~80% of the required steering torque to steer the vehicle under all speed and road conditions. Therefore, the driver is expected to provide the remaining ~20% [16]. There a lack of the human torque capability to steer or turn the steering wheel of the vehicle and this dissertation developed a framework to measure and report it in chapter three.

With the deployment of the new technology of ADAS and autonomous vehicles controlling systems during the last decade, the concept of sensor fusion has been used in the higher autonomy level vehicles, in which multiple channels and sources information are connected and processed [17]. It enables the control module of the vehicle to anticipate future events beforehand based on pattern recognition and dataset training .such as the model predictive control (MPC) and the recurrent neural network (CNN) Consequently, it alerts the driver before performing any maneuver or action to avoid any potential danger or risk. In higher autonomy levels, the electronic control units make decisions based on the perception input and the programmed algorithm that reside in their

µc and systems on the chip. This is where artificial intelligence (AI) and machine learning (ML) have effectively played a key role in building a vehicular sensory platform with sensor fusion, decision maker, and actuation streams and pipelines.

The parallel advancement and innovation in theory and hardware, High performance computer (HPC) systems in automotive applications have enabled the range of applications such as MPC and AI to be executed in real-time basis in automotive applications and controlling systems. Using the state-of-the-art math optimization solvers and rapid prototyping systems have enabled the control modules to perform complex calculations at a sufficient rate to meet the safety requirements of highly automated vehicles (HAV). This is the reason that the Ethernet and internet protocols (IPs) applications are recently used in the on-board communication and diagnostic such as diagnostic over internet protocol (DoIP) [18]. One solution that addresses the ecosystem of highly automated vehicles is what is now referred to as Vehicle-to-Everything (V2E) or (V2X) [19]. Horani et al studied the V2X communication for improved vision of ADAS function in challenging weather and proposed a vehicle-to-infrastructure (V2I) framework. The study explored the possibility of using a video data shared over V2I communication to detect the lane markers in adverse weather condition [19, 20]. They captured reference images in good visibility conditions in which lane marker lines were extracted and aligned to the sensed images using image registration technique over a dedicated short-range communication (DSRC) protocol. Another implementation of the V2E communication is when the vehicle is approaching a congested traffic or intersection. The vehicle ahead can send traffic data via vehicle-to-vehicle V2V

communication so that nearby vehicles use this as a priori and make decisions before arriving at that point [21]. The exchange of traffic data between vehicles and the sourroundings provide a unique opportunity to the ADAS applications and ground intelligent transportation systems (GITS).

The integration of the vehicle on board and off board streams and data pipelines for vehicle positioning, traffic and surroundings information represent a promising solution for ADAS functions of autonomous vehicles (AV). Within that extent, the AI, ML, and communications are the essential components of this novel platform. This requires a new ecosystem where the cloud or the servers can be reached faster and with lower latency and delay. The intelligent traffic management (ITM) using multiple input-multiple output (MIMO) technology for AV was studied by Raiyn J. and shown to offer better results by reducing the delay than a sectored antenna in the field of 5G [22]. However, this increases theunreliability and vulnerability of the intelligent transport system (ITS) which must be able to handle not only the natural disturbance, but also attacks of malicious nature [23]. Cybersecurity is another crucial aspect that be carefully considered in V2X communication of the AV.

The automation of the automobiles is an evolutionary process with the most recent advancement of AI, neural network processing (NSP) and deep machine learning (DML). Over the last decade, a significant progress has been made in the domain of the AI and DML pertaining to autonomous vehicles. This includes various fields such as perception, localization, mapping, trajectory planning, actuation and predictive control systems of the autonomous vehicles. Automated longitudinal and lateral control of the

vehicle require sensor data infusion, high available control architecture and monitoring system on the actuators to ensure the safety of the driver and other road users. There are several automation approaches for the lateral control of the vehicle in the literature. One recently proposed method is to use a camera based deep neural network (DNN) as an end-to-end self-driving system [24]. In order to predict the steering wheel angle, which controls the vehicle laterally, a neural network was created by NVIDIA to train images of the road ahead and predict the steering angles [25]. The drawback of this approach is that the network relies on the perception systems of the vehicle i.e. cameras and radars that are susceptible to the environment, weather conditions and signal noise and interfaces. In a related study, captured images of the highway maneuvers were trained using the ANN in the perception system [26]. Also, most of the published data and research utilizes the ANN, ML and AL in subsystems level such as perception or data fusion. It was reported that steering commands associated with road identical images were non-unique because images offsets the non-linear behavior of the yaw rate angle and not considering the vehicle speed in the input data. This dissertation develops a new framework to use the adaptive MPC and the ANN based on the end to end (ETE) automated control system rather than focusing in a specific subsystem level.

CHAPTER TWO

LITERATURE REVIEW

Automated and intelligent transportation driving systems have attracted extensive attention and interest from academia, industry, and the public. Traffic safety and fuel efficiency is the main motivation for automated and connected vehicles. The connected automated vehicles are considered as mitigations of issues such as traffic congestion, road safety, and inefficient fuel consumption and pollutant emissions that the current road transportation system suffers from [27]. Some challenges reported by multi research groups can be summarized as the followings [27]:

1. Ideal working conditions of the communication channel (e.g., no packet loss, communication failure, noise, etc.).
2. Perfect knowledge of vehicle dynamics (vehicle parameters, road friction conditions, etc.).
3. Perfect knowledge of the positions of the vehicles. Hence, additional investigation is required to understand how the aforementioned uncertainties affect cooperating driving scenarios.

The society of automotive engineering standard SAE J3016 which is also known as (Surface Vehicle Recommended Practice) defines the dynamic driving task as: “all of the real-time operational and tactical functions required to operate a vehicle in on-road traffic [28]. In the context of driving automation systems, SAE J3016 provides detailed definitions for six levels of driving automotion, ranging from no driving automation

(level 0) to full driving automation (level 5) clarifying the role of the (human) driver and/or the automated control system. This leads to the definition of the automated driving system (ADS) that is defined as “the hardware and software that are collectively capable of performing the entire DDT on a sustained basis, regardless of whether it is limited to a specific operational design domain (ODD).” This is used to describe the higher driving automation system levels [28]. According to the SAE J3016 Table 2.1. levels of driving automation, level 1 and 2 are defined as partial autonomy, which requires the driver to execute or supervise the longitudinal and the lateral vehicle motion control at all times. Table 2.1 shows SAE 0 through 2 DDT, OEDR and ODD detail.

Table 2.1. Summary of levels 2 and below of driving automation [10].

Level	Name	Narrative Definition	DDT		DDT Fall back	ODD
			Sustained lateral and long. Vehicle motion control	OEDR		
Driver performs part or all of the DDT						
0	No Driving Automation	The performance by the driver of the entire DDT, even when enhanced by active safety systems.	Driver	Driver	Driver	n/a
1	Driver Assistance	The sustained and ODD-specific execution by a driving automation system of either the lateral or the longitudinal vehicle motion control subtask of the DDT (but not both simultaneously) with the expectation that the driver performs the remainder of the DDT.	Driver and System	Driver	Driver	Limited
2	Partial Driving Automation	The sustained and ODD-specific execution by a driving automation system of both the lateral and longitudinal vehicle motion control subtasks of the DDT with the expectation that the driver completes the OEDR subtask and supervises the driving automation system.	System	Driver	Driver	Limited

The conditional driving automation of levels 3 and above are shown in table 2.2. is where the driver and the system can exchange the vehicle control with the fallback feature if the automated system fails. Level 4 is referred to as high driving automation, where the automated driving system performs all driving operations under specific driving modes and the fallback system is able to can appropriately perform without any expectation of the driver to intervene.

Full driving automation or level 5 is defined as sustained and unconditional performance by the automated driving system of the entire DDT from point A to point B

Table 2.2. Summary of levels 3 and above of driving automation [10, 28].

Level	Name	Narrative Definition	DDT		DDT Fall back	ODD
			Sustained lateral and long. Vehicle motion control	OEDR		
ADS ("System") performs the entire DDT (while engaged)						
3	Conditional Driving Automation	The sustained and ODD-specific performance by an ADS of the entire DDT with the expectation that the DDT fallback-ready user is receptive to ADS-issued requests to intervene, as well as to DDT performance-relevant system failures in other vehicle systems, and will respond appropriately	System	System	Fallback-ready user (becomes the driver during fallback)	Limited
4	High Driving Automation	The sustained and ODD-specific performance by an ADS of the entire DDT and DDT fallback without any expectation that a user will respond to a request to intervene.	System	System	System	Limited
5	Full Driving Automation	The sustained and unconditional (i.e., not ODD-specific) performance by an ADS of the entire DDT and DDT fallback without any expectation that a user will respond to a request to intervene.	System	System	System	**Unlimited**

(Also known as door to door). Thus, the driver, if present, may perform other tasks while a dedicated control system controls the vehicle or even there is no need for the driver in the vehicle at all [29]. The control vehicle motion (CVM), which is the system operative part of the object event detection and response (OEDR), needs to be integrated in the ADS to provide status and capabilities of feasible maneuver and follow the planned trajectory. These subtasks are necessary in order to perform the DDT and to assure that the vehicle can be safely operated in higher automation mode such as SAE level 3, 4 or 5 [10 ,28]. The introduction of the on-board automated CVM increases the risks of hazards due to E/E malfunction, hence the complexity of vehicle control architecture increases as well. The deployment of the automated CVM requires the capability to be integrated with the sense vehicle motion (SVM) to detect the environment, locate its position, and operate the vehicle to get to the specified destination safely without human input. This includes the perception system sensors such as: camera, radars, LIDARs, GPS, and ultrasonic applications and additional actuators such as active steering, electronic braking and active suspensions systems. Vehicles equipped with these intelligent systems (SVM, CVM and actuation) are able to identify obstacles on the road such as pedestrians or other moving vehicles. Also, they can detect the lane markers and keep the vehicle in the center of the lane by applying steering actuation to avoid lane departures which is also known as lane keep assist (LKA).

Shih-Chieh Lin et al explained the architectural implications of autonomous driving systems in detail from the perception perspective. However, it lacked any controller information because the perception system was linked to a planner and an

action block [30]. A model-based safety analysis (MBSA) was performed for the autonomous driving system for ACC controls longitudinal speed and LKA controls lateral trajectory [31]. It was concluded that the yaw rate and the longitudinal speed of the ego vehicle are critical elements (because they appear in order 1 cutsets) of the simulated sequence events. However, the main objective of the study was to study the traffic jam chauffeur using AltaRica language and Simfia software [31]. Figure 2.1 shows the dynamic driving task flow.

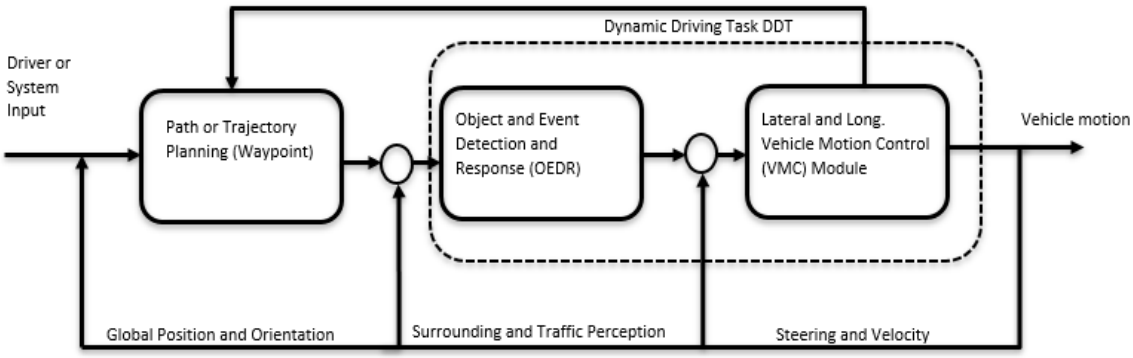

Figure 2.1. Schematic view of the driving task (adapted from [29]).

The Co-operative Systems are the most promising technology within the ITS framework. The word “co-operative” indicates that vehicles are collaborating with each other and with the infrastructure, exploiting wireless communications. The vehicle on-board active safety systems are integrated with the Co-operative Systems architecture to mitigate any potential risk or hazards due to mishap or malfunction of the control systems as shown in figure 2.2 [32].

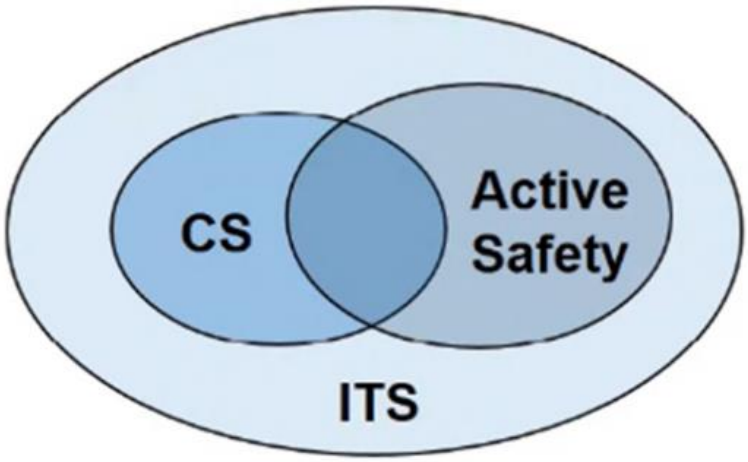

Figure 2.2. Intelligent Transportation Systems consistent of cooperative systems and active safety systems integrated with each other to support the drivers in automated vehicles [32].

The adaptive MPC technology is an effective control strategy that can be systematically taken into consideration the future prediction, patterns and the system operation constrain in design and operation stages [33]. The capabilities of the adaptive MPC for controlling multivariable plants (vehicle actuators) and parameters using the initial state of the plant within every application-imposed constraint i.e., minimum, and maximum values of speed, acceleration, steering positions, make it a suitable choice for autonomous driving applications, where the system faces dynamically changing environment and must satisfy crucial safety constraints. The current control action is obtained by solving on one at each sampling instant using an optimizer unit, starting with the initial state to generate a finite horizon open loop. The optimization yields an optimal control sequence and the first control in this sequence is applied to the plant. This is the main difference from the conventional control strategy, which utilizes a pre-computed

control law [34]. In classical controls, it is challenging to achieve closed-loop stability with (non-parametric) uncertainties. Since adaptive MPCs are online and real-time updated and are based on the long range but finite horizon concept, they establish the control sequence so as to guarantee the closed-loop stability. Figure 2.3 shows the adaptive MPC past and future attributes and control action within the length of the control horizon to solve the optimization problem at each time step.

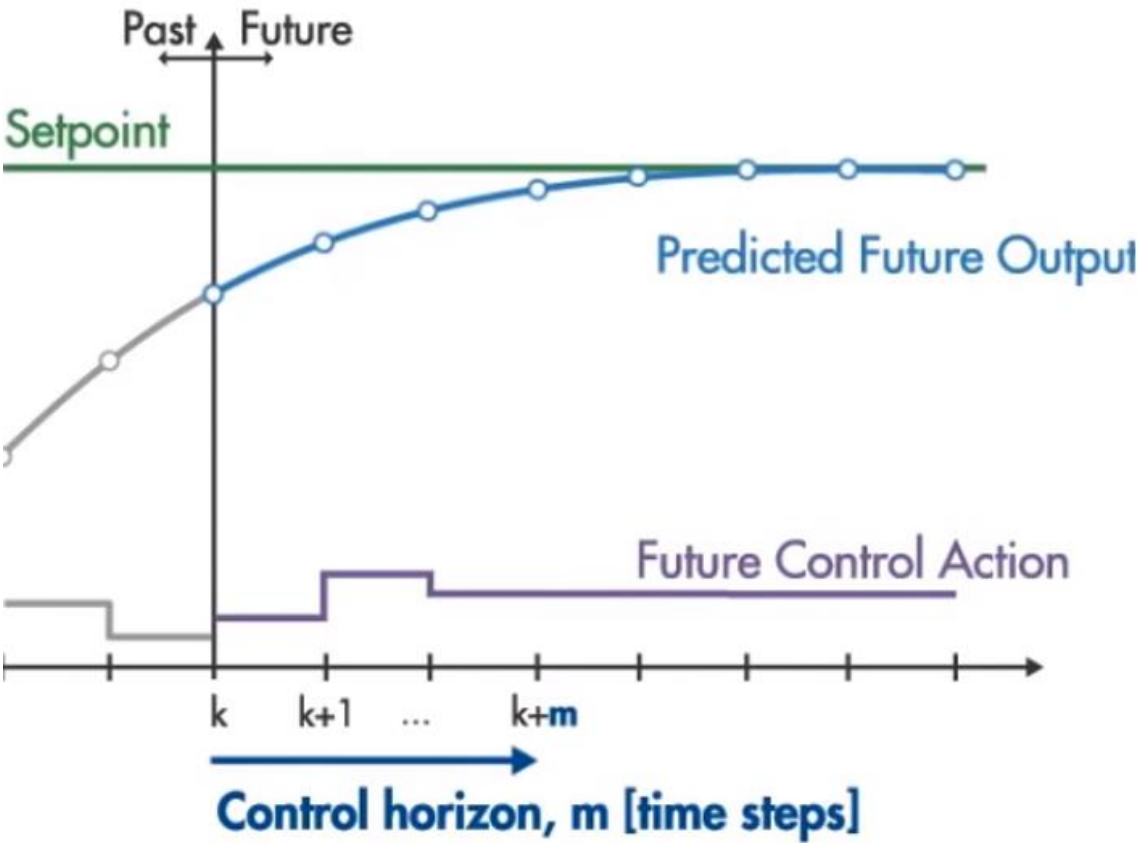

Figure 2.3. Adaptive MPC past and future attributes and control action [34].

The first of such optimal moves is the control action applied to the plant at time At time t +1, a new optimization is solved over a predefined and shifted prediction horizon [35]. Therefore, it operates in a receding horizon fashion, meaning that at each time step, new measurements of the system and new predictions into the future are made by solving multi input datasets applied to the system which allows to predict the future system states based on the current states and control input [36].

The controls strategy of the front wheel angle of steer by wire vehicles was researched by Jiang-Yun et al using a fuzzy neural network [37]. Their results showed that the overall steering ratio curve is just similar to 'S' shape with a certain degree of delay between the hand wheel angle and the front wheel angle. Ikbal Eski et al studied the active steering system design based on the neural network [38]. According to their study, the neural network predictive controller (NNPC)approach gave the bestresults based on random signal input. However, no vehicle data was used in the evaluation process. Jie Duan et al have used a five layers neural network in agricultural tractors as shown in figure 2.4 [39].

The first layer is the input layer of the magnitude and direction of the front wheel angle. The fifth layer is the output layer which predicts the angle of the target front wheel. The in between layers are explained in detail in [39, 40]. Seungjin, Park et al reported that the lane change recognition (LCR) accuracy was enhanced by 25% using the Support Vector Machine (SVM) and the Hidden Markov Model (HMM) [40]. They were able to reduce the sensor noise and uncertainty using covariance of Gaussian distrusted observation data. Another control approach of proportional–integral–derivative

controller (PID) based on radial basis function (RBF) neural network was used by Zeyu, Li et al [41].

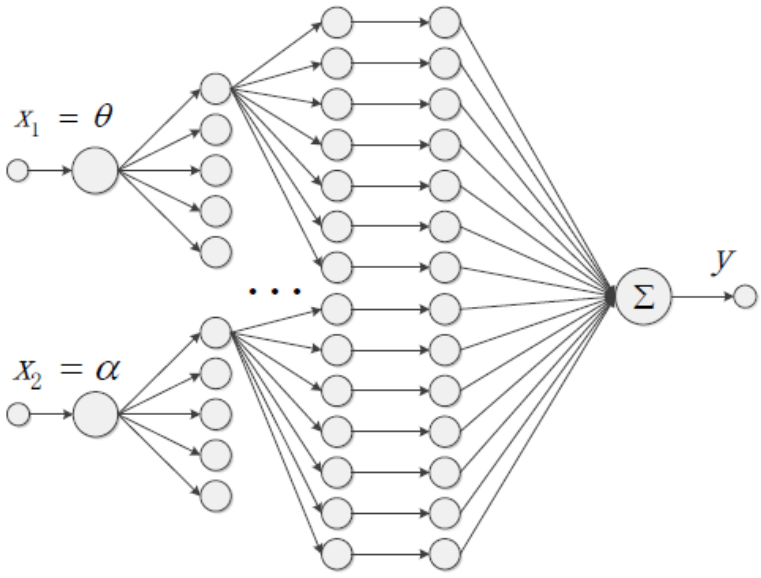

Figure 2.4. Fuzzy neural network structure diagram [39].

The intelligent PID which combines PID controller and neural network was run inMATLAB with reference data and it shows that a self-learning function of the neural network can reduce the impact of the external disturbance and adapt to the input of desired reference signal change. Their work can be applied to the ship's automatic tracking course change. The adaptive neuro-fuzzy inference system (ANFIS) simulation result was studied by Ana Farhat et al. Levenberg-Marquart algorithm (LMA) and least square estimation (LSE) hybrid methods were used for training ANFIS using MATLAB to lower the cost function and increase the model accuracy [42]. A neural network optimized by adaptive particle swarm optimization approach was applied in the fault

diagnostic of the automobile steering system by Yanan et al [43]. It showed that the neural network approach effectively improves the accuracy of the fault recognition. The introduction of the AI and ANN in the safety critical systems of the vehicle can effectively increase the performance in terms of the system reliability and durability such as steering and braking systems control of high automated vehicles. Yet, to the best knowledge of the researcher, no real sensors data connected to the ECU and the actuators and EPS of steering systems have been trained or studied in literature.

2.1 Research Objectives

The main research objective of the dissertation is to address the emerging technology challenges of the higher automated and electric and autonomous vehicles steering systems architecture integrated with the framework of functional safety of ISO 26262. Due to the increasing vehicle curb weight trend that will continue through 2030 that will put more load on the steering tires or wheels, there are emerging challenges for steering systems with higher rack forces for steering needed to turn the road front wheels. Consequently, with any SLOA in the EPS system, the driver has to perform manual steering with suddenly significant and increasing wheel torque that can reach up to many times the maximum human capability to steer the steering wheel. This research studied the effect of the increasing vehicle curb weight on the driver manual torque in case of SLOA and performed experiments to measure the controllability of the steering wheel and related the findings to the ISO 26262 ASIL matrix computation parameters and framework. Whether the driver of the automated driving system control the vehicle, the EPS architecture design is very crucial to provide high availability to control the

vehicle as it interacts with both the driver and the automated system as shown in figure 2.5.

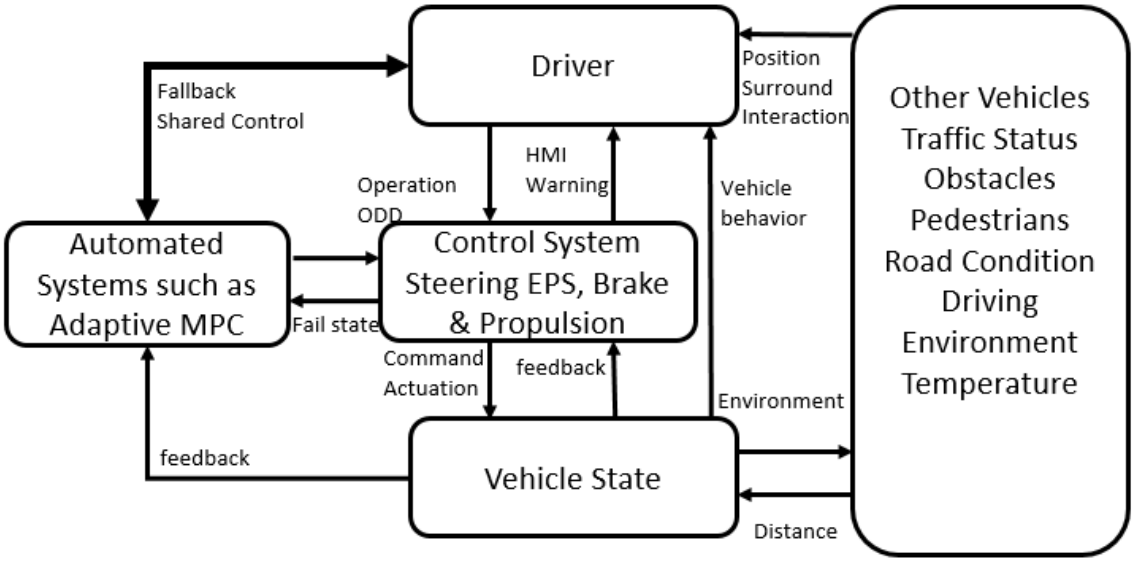

Figure 2.5. EPS systems interaction with the driver and the automated driving system.

The specific objectives of this dissertation are as follows:

- Develop and compute a safe and highly available architecture for EPS systems in compliance with the ISO 26262 standard given the fact that more battery electric vehicles (BEV) are replacing conventional engine vehicles (CEV) and the continuous trend of the average vehicle curb weight increasing in the next 10 years.
- Develop an adaptive MPC model to simulate the longitudinal and the lateral motion of the vehicle and follow a predefined trajectory using the MPC optimizer and prediction capabilities. Due to the complexity level of the vehicle dynamic

system motion, the multi-input, multi-output (MIMO) control system represented by the adaptive MPC block was chosen in this study to satisfy the manipulated parameters out of the adaptive MPC controller such as: ego speed, steering wheel angle, and brake signal, etc. within the predefined constraints and limits that represent the traffic policy, the driving situation and trajectory and the minimum and maximum control parameters. The stability analysis of the vehicle dynamic is a major problem in automotive technology that requires sophisticated control systems, optimizers and tuning capabilities with efficient implementation scheme and formation. Therefore, the steering system of higher automated vehicles has more safety challenges as the role of the driver (human) in vehicle control has been decreasing. Figure 2.6 shows the developed model schematic that will explained in detail in chapter 4.

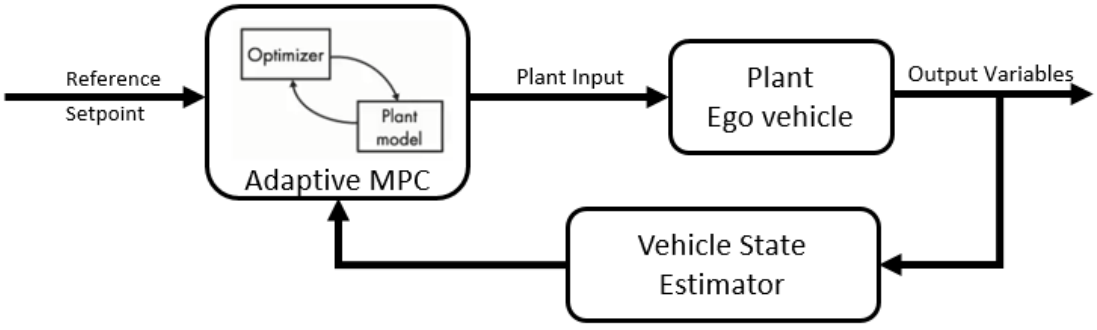

Figure 2.6. Adaptive MPC MIMO control system.

- Train and predict the steering wheel torque commands and pattern using dataset of steering system parameters such as: steering wheel angle (SWA), steering

wheel speed (SWS) or rate, yaw rate and vehicle velocity. The performance of the artificial neural network to predict the steering command based on the SWA, SWS and ego speed was validated with a regression value of ~ 98.5 % versus the measured SWA dataset.

The deployment of higher automated and connected vehicles accompanied with active safety and ADAS systems in public roads aims to reduce the driver workload and fatigue. This enhances the driving experience and increases the traffic safety but at the same time transfers more tasks to the automated control system of the vehicles. Consequently, the driver and the automated control system are working interchangeably as a team as they intervene and escalate to each other to handle the driving tasks and subtasks. The driver can perform or undertake other activities while the system is controlling the vehicle which was previously impossible while driving SAE level 2 or below. The control systems are replacing the drivers by making the decision based on the perception of the surrounding and planning the trajectory based on the predefined algorithms reside in the controller units. Interestingly, the society and the public were supportive of the systems in which the driver supervises automated driving than of systems in which the driver has a lesser role and can do something else other than the driving tasks. Additionally, some participants wanted to have automation during long, boring drives (i.e., for increased comfort and reduce fatigue), while others wanted it to help cope with difficult driving situations (i.e., for increased safety) [44]. Thus, the society and drivers acceptance and trust in the control system are necessary to support the automated vehicles to take these advantages. The intelligent transportation associated with the e-mobility are developing

quickly due to the need for new, safe and sustainable technology for people and goods to move. The passenger or personal air vehicles (PAV) is advancing the future of on-demand transportation and air vehicles that potentially will change humanity transportation systems. All these innovations and transportation ecosystems are all made possible by safe and reliable control systems that will reshape the future of propulsion systems within the functional safety of the ISO 26262 Standard.

2.2 Thesis Layout

The proceeding chapters of the dissertation are as follows:

- Chapter three describes the new challenges of the increasing steering rack forces due to the continuous trend of curb weight increase of EV and AV in the upcoming ten years. It was found that new challenges have emerged recently for the EPS system such as higher forces at the steering rack and more ADAS functionalities; Consequently, The ASIL computation has shifted for the EPS system because any SLOA may lead to catastrophic accidents that the driver would not be able to steer the vehicle manually. Concludes were made that the definition of controllability in ISO 26262 is not fully mature and needs some modification in the light of the above given facts and findings of the functional safety of an EPS system. The study performed experiments on the human steering wheel torque capability and proposed a new metric to relate a range of torque magnitudes to the controllability class C0 – C3 in table B.6 part 3 ISO 26262 Standard. Consequently, the EPS system architecture was analyzed and the new assigned ASIL C mitigation or risk reduction was achieved by incorporating a

dual core microcontroller integrated with a power management and safety-monitoring unit. The proper implementation of this logic control path of dual core µc integrated with power management and safety monitoring makes the EPS system simpler, faster, reliable and more cost effective.

- Chapter four describes the model-based development of the ADS using the adaptive MPC block deployed in MATLAB-Simulink environment. The automated driving system was validated in straight and lane change trajectories' scenarios. The study also redefined the controllability classes or categories C0 – C3 of high automated vehicles based on the vehicle global position related to the lane marker lines to accommodate for the machine in the loop controlling the DDT in autonomous vehicle maneuvering. The findings of this model reveal that there are human factors challenges in SAE level 3, 4 and 5 and the interaction between the driver and the automated control system of the vehicle that require HMI modalities as explained in table 4.2 of chapter four. The driver – automated control system engagement in the steering system of the vehicles is one of the crucial control complex scenarios that add uncertainty and potential risk when handing over the steering control between the driver and-or the automated control system. Even when the driver is in full control of the steering system, the ESP is still responsible for approximately (~ 80%) of the SWT required to steer the vehicle. Therefore, the steering system design and functional safety metric require specific architecture redundancies in SW, HW and system level for high availability and risk mitigation mechanisms. This research highlighted the need to

define the driver intervention in high-automated vehicle of SAE level 3, 4 and 5 in order to sustain the traffic safety and keep the vehicle in the intended trajectory. This can be addressed by HMI and the human factor implementation in ISO 26262 to standardize the driver-machine relation with the DDT in real time and interactive environment. Both manual and automated driving modes demand the functional safety implementation of the steering system to mitigate any system malfunction or failure. Therefore, the fault injection concept supports the safety mechanism implementation and correctness of the system architectural design with respect to faults and failures during the runtime. This improves the test coverage of developing safe control system to operate as designed and meet the safety requirements in compliance with the OEMs and government regulations. Another aspect to consider in the future work is to utilize the HMI in ASIL D systems in ISO 26262 in more detail and include the HMI in the safety mechanisms of the vehicle's control system.

- Chapter five describes the use of the artificial neural network and machine learning in the steering wheel commands prediction pattern and recognition. Dataset of steering system from vehicle level hardware-in-the-loop simulator of the high fidelity dSPACE bench was collected and analyzed to build the ANN for training, validation and deployment of the steering column torque commands using the MATLAB and Simulink environments. Then, the ANN results were compared against the bench data of the steering wheel column torque using regression analysis.

CHAPTER THREE

COMPUTATION OF SAFETY ARCHITECTURE FOR ELECTRIC POWER STEERING SYSTEM AND COMPLIANCE WITH ISO 26262

3.1 Abstract

Technological advancement in the automotive industry necessitates a closer focus on the functional safety for higher automated driving levels. The automotive industry is transforming from conventional driving technology, where the driver or the human is a part of the control loop, to partially or fully autonomous development and self-driving mode. The Society of Automotive Engineers defines the level 4 of autonomy: "Automated driving feature will not require the driver to take over driving control." Thus, more and more safety related electronic control units (ECUs) are deployed in the control module to support the vehicle. As a result, more complexity of system architecture, software, and hardware are interacting and interfacing in the control system, which increases the risk of both systematic and random hardware failures. In order to reduce these risks and minimize any potential failure or loss of control, ISO 26262 Standard provides guidance to the automotive OEMs and suppliers (tier 1 and 2) to ensure an adequate and acceptable level of safety procedures is implemented in the vehicle control modules. This chapter focuses on the electric power steering system and its ASILs assignment. It was found that new challenges have emerged recently for the EPS system such as higher forces at the steering rack and more ADAS functionalities; Consequently, The ASIL computation has shifted for the EPS system because any SLOA may lead to catastrophic accidents. The definition of controllability in ISO 26262 is not fully mature

and needs some modification in the light of the above given facts of the functional safety of an EPS system. The study proposed a new metric to relate a range of required torque magnitudes to the controllability classes C0 – C3 in table B.6 part 3 ISO 26262 Standard.

3.2 Introduction

This chapter begins with a brief description of the steering system and the architecture system of the main components of the steering systems followed by a brief description of the safety goals and mechanisms implementation. After which, failure classification, ASIL decomposition of the steering system was explained by the failure classification, ASIL decomposition of the steering system, and the ASIL matrix were explained in detail. The challenges of the ADAS functions in the steering system were addressed and their impact on the ASIL calculation of the steering system in the case of SLOA in the EPS is investigated leading to an ASIL level C to be calculated based on the fault metric in compliance with ISO 26262. The study proposed logic control system paths for readily available EPS systems based on SW or HW redundancy to maintain safe calculation and decision making for the steering systems at a lower cost, higher reliability of simpler design with the focus of SLOA scenarios in the EPS and its ASIL calculations.

3.3 Scope of Study

This section developed and investigated a case study of the vehicle steering system control module functionalities. Development and analysis of the safety strategies and mechanisms were investigated based on the state of the art of the current ISO 26262 guidelines and the levels of SAE autonomy. The steering system represents a standard functionality on every vehicle to control the lateral direction of the vehicle. Also, provide

enhanced stability for the vehicle [45]. The needs for more fuel efficiency and more user friendlysteering wheel to reduce driver fatigue have increased the role of the E/E components in the steering systems, such as electric power steering, electro-hydraulic power steering (EHPS) and steer by wire (SbW) systems with dedicated steering ECUs and algorithms. Therefore, the steering system has more safety challenges due to the complex nature of the control module of the electrically driven motor or hydraulically assisted power steering systems and their critical role in the control of the vehicle's lateral motion. In SAE level 2, the role of the driver in vehicle guidance is decreasing as the automated driving system has the longitudinal and lateral control. Therefore, this requires a smart or intelligent steering system linked and connected to the ADAS applications e.g. cameras, radars, LIDAR or GPS [46]. These integrated systems and applications require environmental perception or recognition based on the processed data, communication protocols, and fusion processes of the data. Therefore, the steering control module or steering ECU, which represents the decision maker to activate or actuate motors that act on the rack, needs to perform complex calculations at a sufficient rate to meet the safety requirements of lateral control of the vehicle's motion, sampled at 1-20 msec [48, 49] Consequently, highly computational and intensive support of E/E components is needed in the steering system. This leads to more challenges in the reliability and safety concepts of the E/E components and the ADAS applications of the steering systems. The block diagram of possible steering control architecture of SAE level 2 and the interface components is shown in figure 3.1.

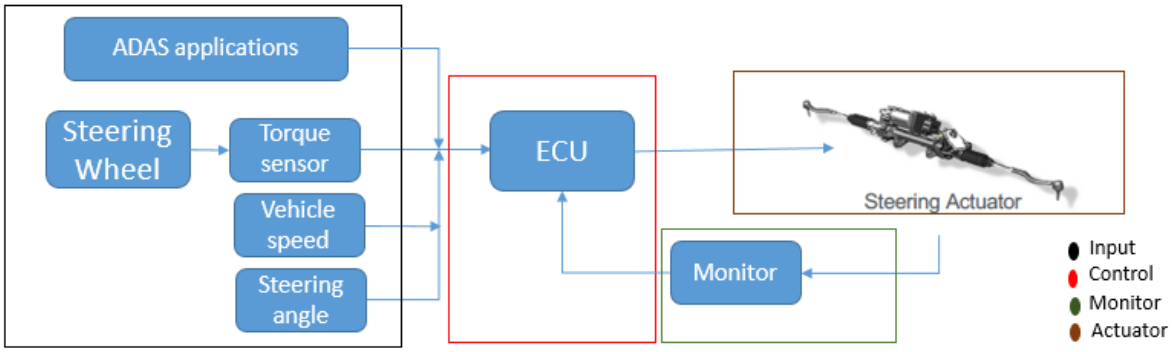

Figure 3.1. Electric power steering basic interface components.

From the generic hardware components schematic of figure 3.1, there are four main areas or interfaces of the system architecture of the steering control module described as following [50]:

1- Input from sensors: vision or perception sub-system such as camera, radar, LIDAR, ultrasonic, steering wheel angle, vehicle speed and GPS, aka SVM.

2- Electronic control unit or ECU: The decision maker unit or processing the received data of the ADAS, calculating how much assistance to add to support the driver and keep the vehicle in the planned trajectory; e.g. LKA in active steering systems where the system is designed to automatically keep the vehicle in the lane or lane departure warning (LDW) in passive steering systems to warn the driver to take action and correct the vehicle trajectory manually.

3- Actuators: these sub-system devices translate the computational or processed data in the ECU and HMI into mechanical actions to act on the steering rack and front wheels as desired such as the electric motor of the EPS.

4- Monitoring system: Safe steering systems and ADAS applications require monitoring systems to perform real-time acceptance tests to validate the system behavior during the start-up and the running time.

The steering system control module requires torque, position, steering wheel angle, yaw rate, speed, lateral and longitudinal acceleration, and electric motor angular position sensors data to calculate the amount of the appropriate duty cycle or the pulse width modulation (PWM) to actuate the electric motor based on predefined values and look-up tables. When actuating the steering system, it is of critical importance that the commanded assistance from the ECU should match the received assistance at the actuators input to make sure that the intended assistance is not violated during the computation and the communication. If the actuators misbehave, the monitor should turn the actuator off as a fail-safe or aka fail silent when the remedial action is to halt all the communications and serial data. In case of a fail-operational unit, the monitoring system will switch the control to the fallback system with degraded mode to reduce any risk of losing the vehicle control [51].

3.4 Safety Mechanism of Steering System

Due to the potential malfunction of the E/E components of the steering control module and linked ADAS applications such as cameras, sensors and actuators and other subsystems, a hazard could be presented due to unintended locking of the steering or unintended lateral steering while driving, which could lead to the loss of lateral vehicle control. Therefore, the ASIL classification of the steering system is very critical to prevent any intended path violation. Steering system designers spend extended time and

efforts to determine the proper ASIL for steering systems in different scenarios and maneuvers. This requires the OEMs and steering system suppliers to develop a rigorous safety mechanism and strategy to avoid any loss of vehicle control. Therefore, the safety goals of the steering system are: to avoid unintended locking, SLOA, and uncontrollable steering assistance while driving or parking the vehicle, which could drive the vehicle out of the intended driving lane or trajectory. With the advancement of the steering system functionalities that require position recognition, faster update rates, and environment perception added complexity and reliability issues are applied to the steering system. These advancements impose more of the functional safety goals and mechanisms and require the introduction of the concept of the fault tolerance according to ISO 26262 [52]. This is necessary to provide and guarantee an acceptable reliability level for the design of the E/E components. Part 4 of the ISO 26262 section 6.4.2.1 defines the safety mechanism that detects faults and prevents or mitigates the failure presented at the output of the system that violates the functional requirements. The functional safety requirements include five main concepts on the system level as shown in table 3.1 [53].

Table 3.1. Safety mechanism coverage of ISO 26262 Part 4 [53].

No	Safety Mechanism	Purpose
1	A safety mechanism related to the detection, indication and control of faults in the system itself.	A- Self-monitoring to detect random HW faults and systematic faults. B- To detect and control of channel failures e.g. data interface and communication buses. C- Specific w.r.t. the appropriate level within the system architecture.
2	A safety mechanism related to the detection and control of faults in other external elements that interact with the system.	ECUs, Power supply and communication devices.
3	A safety mechanism that contributes to the system achieving or maintaining the safe state	In case of multiple control requests from the safety mechanism
4	Define and implement the warning and degradation strategy	To escalate to the driver via the HMI to control over the vehicle
5	A safety mechanism that prevents faults from being latent	Self-test that occurs during power-up, operation mode, and during power down as a part of maintenance

3.5 Failure Classification and Hardware Random Failure Metrics

ISO 26262-Part 5 classifies the malfunction of the E/E component into two main types of failures [54]:

1-Systematic failures: Which can be caused by missing requirements during the design, development phases and can be addressed by change requests (CR) before releasing the product or the start of the production (SOP). System testers can capture it during the verification and validation (V&V) processes.

2-Random Failures: Due to physical causes such as aging, wearing out and tearing down of the E/E hardware component during the system's lifetime, different levels of random failures may appear in the E/E components. Due to their random nature, statistical information can be produced from testing and historical data about this type of fault. Thus, the average probability, and hence the risk, associated with the occurrence of a random fault can be calculated.

The random faults can be further divided into two categories: permanent faults such as 'stuck at' faults, and transient faults, such as soft errors that can not violate the safety goals if it is presented in the system. It is difficult to forecast the likelihood of random failure of the E/E components during the 'lifetime' of the hardware service. Therefore, the random faults require the system designer to include and develop a safety mechanism to continuously monitor, capture (detect) any random failure and react (control) the malfunction to reduce any risk or hazard by taking remedial actions. Hence, this minimizes any safety violation and maintains a safe state when random faults occur.

3.6 Methodology

3.6.1 ASIL (Automotive Safety Integrity Level) Matrix

ISO 26262 standard, part 3 defines automotive risk levels as QM, ASIL A, B, C and D with the consideration that ASIL D represents the highest degree of safety integrity and ASIL A represents the lowest one [54, 55]. The quality management (QM) represents any hazard that does not impose any safety requirements. The QM classification indicates that the quality processes are sufficient to manage and handle the risk. The steps to determine the ASIL of the steering system, at the vehicle level, within hazard analysis and risk assessment (HARA) in ISO 26262 Standard is shown in figure 3.2. The objectives of HARA are to:

1- Identify the hazard events of SLOA caused by the malfunction of an item, which is the steering system control module in this case. According to the NHTSA, EPS assist may be lost momentarily, followed by a sudden return of EPS assist or jitter assist. Therefore, the driver may have difficulty steering the vehicle especially at low speeds, increasing the risk of crash and lost the intended path. For examples, General Motors (GM) recalled more than 1 million trucks and sport utility vehicles (SUVs) in 2018 due to SLOA [56].

2- To formulate the safety goals with their corresponding ASILs in order to mitigate any hazard events and avoid any unreasonable risks.

3- The HARA and ASIL determination do not require the design details of the steering system because the purpose is to identify and evaluate the potential hazardous events, which relate to the functional behavior of the steering system.

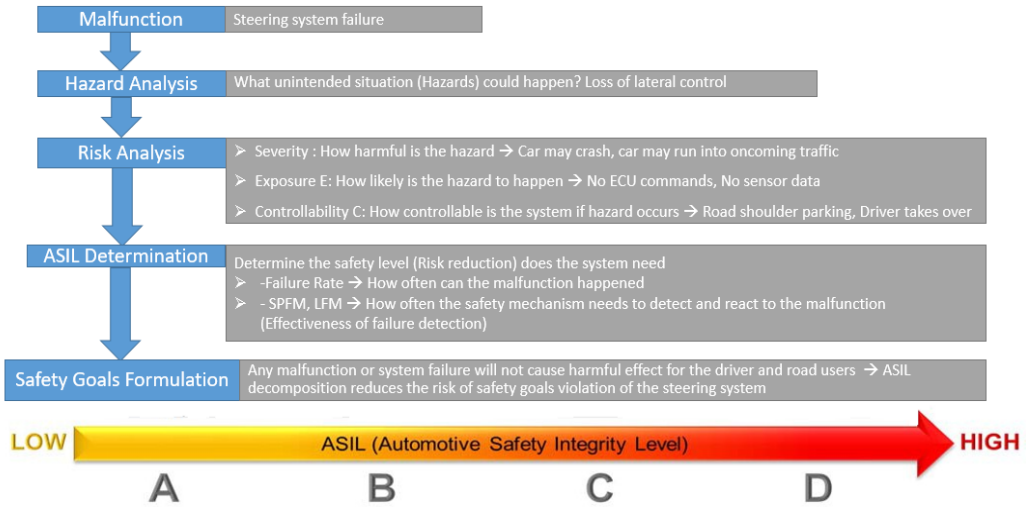

Figure 3.2. ASIL determination steps of the steering systems.

The ASIL is determined by considering severity, exposure and controllability [54, 55]. A brief definition of each is given below:

1- Severity (S): Defines the severity or intensity of the damage or consequences to live persons (drivers, passengers, pedestrians and other road users) at risk of potential harm for each hazardous event. The severity order (class) description is given in table 3.2:

Table 3.2. Severity classes and description [55].

	Class			
	S0	S1	S2	S3
Description	No injuries (Material damage)	Light, moderate injuries	Severe and life-threatening injuries (Survival probable)	Life-threatening injuries (Fatal injuries)

2- Exposure (E): Measures the possibility or likelihood for being in a situation, e.g. Highway and urban driving, curve driving, parking, and road ramps, etc. The exposure levels are given in table 3.3.

Table 3.3. Exposure classes and discerption [54].

	Class				
	E0	E1	E2	E3	E4
Description	Incredible (Rare)	Very low probability	Low probability	Medium probability	High probability

3- Controllability C: Measures the ability (Capacity) of the driver involved in the operational situation to control the hazardous event due to failure or malfunction. Various levels of Controllability are assigned as shown in table 3.4:

Table 3.4. Controllability classes and description [54].

	Class			
	C0	C1	C2	C3
Description	Controllable (Easy)	Simply Controllable	Normally controllable	Uncontrollable (Difficult)

The resulting hazards for the EPS system are evaluated based on the Severity (S), Exposure (E) and Controllability (C) scales that are provided by ISO 26262 to determine the ASIL level as shown in table 3.5.

System designers and manufacturers employ a variety of techniques and safety mechanisms to reduce the risk and achieve a tolerable system for target numbers of faults, such as: ASIL decomposition, driver warning lamp fault detection mechanism, plausibility check, Built-In self-test (BIST), and redundancy. Consequently, the desired ASIL is achieved to mitigate undelaying safety risks. All these technologies are introduced in the system architecture at different levels of abstractions to detect and correct the malfunctions in order to ensure that the safety goals that were determined in the HARA phase are not violated.

Table 3.5. ASIL matrix [54, 55].

		C1	C2	C3
S1	E1	QM	QM	QM
	E2	QM	QM	QM
	E3	QM	QM	ASIL A
	E4	QM	ASIL A	ASIL B
S2	E1	QM	QM	QM
	E2	QM	QM	ASIL A
	E3	QM	ASIL A	ASIL B
	E4	ASIL A	ASIL B	ASIL C
S3	E1	QM	QM	ASIL A
	E2	QM	ASIL A	ASIL B
	E3	ASIL A	ASIL B	ASIL C
	E4	ASIL B	ASIL C	ASIL D

No ASIL assignment is required for S0, E0 or C0.

3.6.2 Effectiveness of Safety Mechanisms

ISO 26262 – Part 5 introduces the metrics used to detect and control random failures based on the hardware architectural design as the following [54]:

A- Single Point Fault Metric (SPFM): Measures the effectiveness of the safety mechanism architecture to the single (Individual) point faults. It can be calculated according to equation (3.1) considering that the single point faults λ_{SPF} and the residual faults λ_{RF} are directly violating the safety goals in case they are not covered (detected) by the safety mechanism of the system.

$$SPFM = 1 - \frac{\sum(\lambda_{SPF} + \lambda_{RF})}{\sum\lambda} \tag{3.1}$$

B- Latent Fault Metric (LFM): Measures the robustness of the safety mechanism architecture to latent faults either by design (safe faults), fault coverage via safety procedure or by the driver's recognition via the HMI of the fault's existence before the infraction of the safety goals. It can be calculated based on equation (3.2) considering that latent multi-point fault rate $\lambda_{MPF,L}$ is not directly violating that safety goal, if a subsequent fault occurs, it may be exacerbated by the first undetected fault to violate the safety requirements. As can be seen in equation (3.2), the single point fault and the residual fault rates are subtracted from the overall fault rate λ.

$$LFM = 1 - \frac{\sum(\lambda_{MPF\,L})}{\sum(\lambda - \lambda_{SPF} - \lambda_{RF})} \tag{3.2}$$

The faults classification and their symbols are given in table 3.6:

Table 3.6. Failure rates and description.

Class	Symbol (Rate)	Explanation
All faults	λ	Total failure rate of a safety related hardware element. λ can be calculated according to equation 3.3.
Single Point Fault	λ_{SPF}	Single point faults directly cause a violation of the safety goal because the safety mechanism is not implemented to detect this fault.
Residual Faults	λ_{RF}	The residual faults are the faults that are not covered by any implemented safety mechanisms
Latent Multi Point Fault	$\lambda_{MPF,L}$	Latent multi point faults are faults that do not directly violate the safety goals but overlapping two independent faults will violate the safety goal.
Perceived Multi Point Fault	$\lambda_{MPF,DP}$	There are multi-point faults that are perceived or detected by the driver.
Safe Fault	λ_S	Safe faults do not cause any violation to the safety goals.

The overall fault rate λ can be calculated according to the following equation (3.3):

$$\lambda = \lambda_{SPF} + \lambda_{RF} + \lambda_{MPF,L} + \lambda_{MPFD,P} + \lambda_S \quad (3.3)$$

From (3.1), (3.2) and (3.3), the $SPFM$ and the LFM can be re written as:

$$SPFM = \frac{\sum(\lambda_{MPF,L} + \lambda_S)}{\sum\lambda} \quad (3.4)$$

$$LFM = \frac{\sum(\lambda_{MPF,DP} + \lambda_S)}{\sum(\lambda - \lambda_{SPF} - \lambda_{RF})} \quad (3.5)$$

C- Probabilistic Metrics for Hardware Failures (PMHF): Provides the rational that the residual risk of the safety goal violation due to random hardware failures is sufficiently low and acceptable. Evidence that the hardware safety architecture adequately prevents/controls random failure in accordance to ISO 26262 section 5-8 (evaluation of hardware architecture metrics should be fulfilled) [54, 55].

ISO 26262 – Part 5 section 8.4.5 determines the requirements that apply for ASIL B, C and D in terms of fault metrics as shown in table 3.7:

Table 3.7. ASILs and failure rates.

ASIL	Failure Rate	SPFM	LFM
A	<1000 FIT (<10^{-6}) h^{-1}	Not Applicable	Not Applicable
B	<100 FIT (<10^{-7}) h^{-1}	≥ 90%	≥ 60%
C	<100 FIT (<10^{-7}) h^{-1}	≥ 97%	≥ 80%
D	< 10 FIT (<10^{-8}) h^{-1}	≥ 99%	≥ 80%

The Failure in Time (FIT) is defined as the number of failures in time of a component expected in one billion hours interval of operation and it is calculated accumulatively. FIT measures the reliability of the component of interest in 10^9 hours of operation. Therefore, a FIT of 1 means that the Mean Time to Failures (MTTF) is 1 billion hours and can be written as (10^{-9} h^{-1}) for E\E components.

λ is the failure rate in h^{-1} which represents the number of failures in one hour. Proven in use concept of ISO 26262 requires real numbers of failures from the deployed HW in use

in the field [57]. Other common methods to calculate failure rates of semiconductor used in automotive applications ECU and printed circuited boards (PCB) include IEC/TR62380, SN29500 and FIDES guide.

3.7. Steering Systems Analysis

3.7.1 ADAS Functions on the Steering Systems

The autonomy levels introduced by the SAE J3016 released in June 2020 and the NHTSA defined level 1 autonomy such that the driver is continuously exercising lateral control while the system controls the longitudinal control, such as adaptive cruise control [10]. However, in level 2 autonomy, the system controls both longitudinal and lateral motion of the vehicle. Level 2 is also called partial automation, with ADAS playing a crucial role in the chassis control of the vehicle i.e. brake and steering control modules for some driving modes. However, the driver always has to monitor and supervise the system. So even with feet and hands off, the driver's eyes must be on the road and the machine interface i.e. steering wheel or the brake pedal. More ADAS functions pose new challenges for steering hazards, such as longer reaction time of the driver in case of sudden events. In addition, the different responsibilities shared between the driver and the controllers of the steering systems for some driving modes. Therefore, electronic back-up is crucial for vehicle controllability in driving autonomy level 2 and above. Any sudden failure in the electronic control module such as the µc of the EPS system will lead to SLOA if the architecture does not have a back-up control path. Consequently, this SLOA in the electric power steering systems will drastically increase the required torque to steer the vehicle by the driver, especially at lower speeds. The ASIL of electrical power-

assisted steering system was given ASIL level B in table 3.3 for the loss of the direction commands [58]. This assignment is questionable and might not satisfy the new challenges emerging in the EPS system of modern vehicles, such as BEVs, SUVs and pick-up vehicles.

3.7.2 Steering Systems Case Study and Data Collection

The functional safety analysis of the vehicle steering systems was performed assuming that the steering system is an EPS assist system. The approach of the safety analysis was developed in complaint with the ISO 26262 standard and the ASIL classifications explained in the previous section. Under the assumption of use (AoU) that the driver will be presented in the vehicle all the time and can control the vehicle's path even if the EPS system failed due to malfunction or failure. This means that in case of any SLOA of EPS assist in the steering system, the driver should be able to retain the full control and perform the required steering torque manually to claim the absent of the unreasonable risk of the EPS malfunction. The loss of the vehicle's direction commands was assigned to ASIL B in the literature [59]. A safety analysis was conducted in this study case to investigate the severity, controllability and the exposure of the ASIL determination in the published literature.

By definition, E3 is normal probability and C2 normally controllable and their combination with S3 (fatal injuries) was assigned ASIL B for the case of the SLOA of the EPS assistance that most the steering systems suppliers and developers claimed [58, 59]. The generic definition of normal controllability C2 explained in table B.6 part 3 ISO 26262 states that between 90% and 99% of the average drivers or other road users are

able to avoid harm in case of malfunction [54]. The part 3 of the ISO 262626 section B.6 gives examples, scenarios, and their controllability assignment. However, given the fact that the vehicle torque demand could be five times of the human maximum torque capability, the controllability section B.4 part 3 ISO 26262 should provide a scale or a range of the torque magnitudes or values for each controllability class rather than rely on the drivers percentages. Therefore, the human torque capability and torque magnitude is needed to determine the accurate controllability in the ASIL calculations for the SLOA.

In order to measure vehicle steering and human construability and torque capability, the Research Office at Oakland University was contacted by the researcher to get the institutional review board (IRB) approval (IRB-FY2021-183) to conduct the experiment at the Engineering Center (EC), School of Engineering and Computer Science (SECS). The purposes of the experiment were to measure the human controllability, capability and comfortability to steer the steering wheel with a range of torque values in both clockwise and anticlockwise directions. The steering wheel torque experiment was performed while the vehicle was stationary in at the neutral point of the steering wheel (Stationary steering torque). In order to have accurate steering torque measurement, the torsion bar was removed from the connected joint, and the steering column replaced with a rigid shift to measure the torque more accurately. First, the front axle wheels were lifted from the ground and secured so no friction between the tires and the ground can happen, which dissipates energy and causes error reading the torque applied to the steering wheel. Then, the torque cell was connected to the main shaft of the steering column to sense the torque that the participants perform in the steering wheel. The torque sensor used in the

experiment meets the American Society of Mechanical Engineers Standard ASME B107.14-2004, ISO 6789 standards with matching certificate of calibration traceable to the National Institute of Standards and Technology (NIST) as shown in figure 3.3. Twenty participants (ten male and ten females) aged between 28 and 44 years were asked sit comfortability in and hold the steering wheel while in neutral position and adjust the driver seat to feel more comfortable and mimic the driving scenario and look to the headway direction.

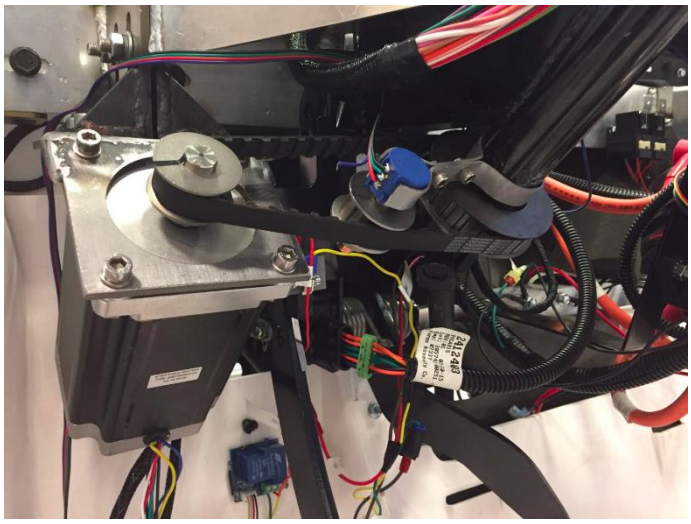

Figure 3.3. Torque and steering wheel angle sensors and their interfaces hardware placed in the steering column below the steering wheel.

The participation criteria of this experiment were published ahead of the time to make sure that the subjects have at least two years of driving experience and do not have any previous arm injury that effects their steering controllability or grip strength.

Then the participant was asked to perform the maximum steering torque with the clockwise direction for three times and the steering torque magnitudes were recorded.

Then the participant was asked to rest for five minutes and the same procedure was repeated in the anticlockwise direction to reduce bias and give time to rest the participant's muscles. Then, the collected steering results were analyzed and the average of the three readings were taken to represent the steering torque of the participant. No personal information was collected in the experiment in complaint with the IRB personal confidentiality for the participants and present any personal data exposure.

3.8 Results and Discussion

3.8.1 Human Controllability and torque measurement results

The selection criteria of the subjects were published ahead of the experiment time to make sure that the participants read and understand the research procedure and objectives. The average age of the participants was 35.5 years for males and 35 for females. This participants sample was necessary to represent the licensed drivers in the United States that age of 35 years representing the highest percentage according to the US Department of Transportation (DoT) and the Federal Highway (FDHW) statistic as shown in figure 3.4 [60].

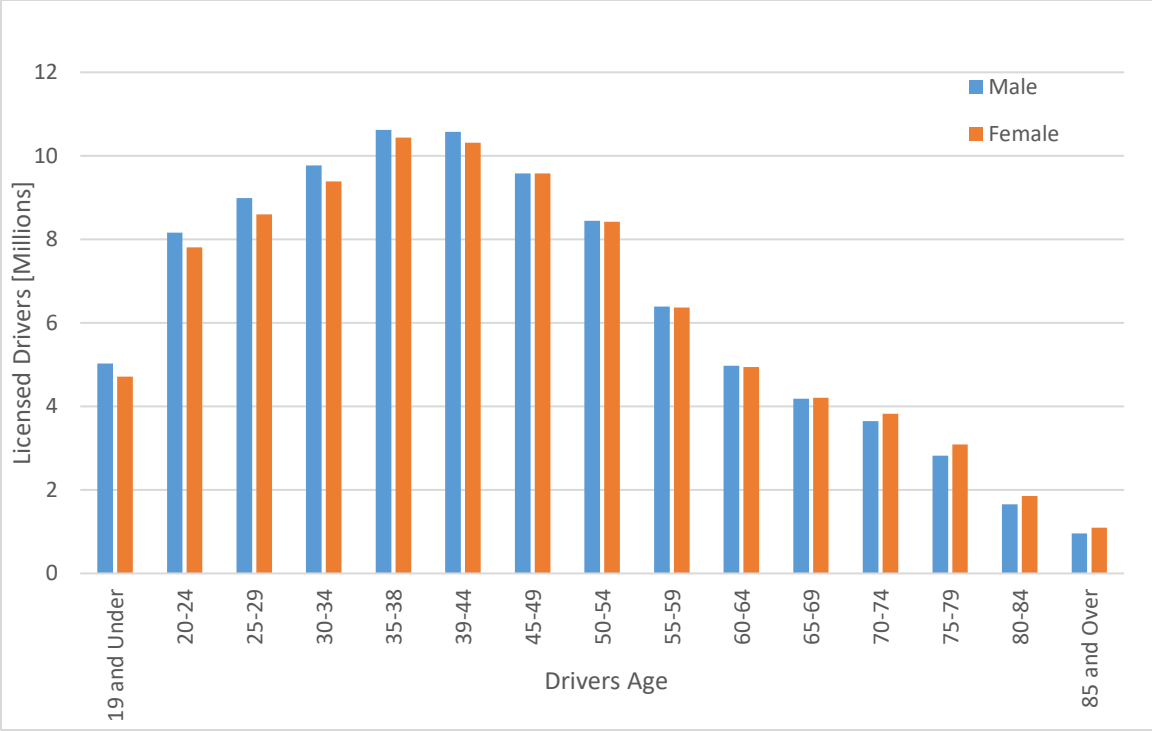

Figure 3.4. Licensed Drivers by Age and Sex reported by FDHW in 2020 [60].

NHTSA now recommends the technique known as "9 and 3"by placing the left hand of the driver on the left portion of the steering wheel in a location approximate to where the nine would be if the wheel was a clock and the right hand should be placed on the right portion of the wheel where the three would be located [61]. All participants performed the steering wheel torque measurement and hand placements following the “9 and 3" position. All participants answered that they feel their arms are comfortably aligned with their shoulders in the nine and three position before the experiment starts.

Interestingly, it was found that all participants performed a little bit higher steering torque in the ACW direction than the CW for both males and females. This is due to the fact that in the ACW direction, the right hand pushes up and the left hand

pushes down to rotate the steering in the ACW and 90% of the participants were right hand dominant. The turning of the steering wheel is a result of the hand push and the other hand pull method. Another remarkable finding was that all participants right's hand grip strength was high than the left side except the one left hand dominant participant.

Another interesting result of the experiment that the average steering torque that the male participants performed was ~18.775 N.m. However, the average steering torque that the female participants performed was ~17.925 N.m. these values represent the maximum steering wheel torque that the human can manually perform and put in the vehicle steering wheel system for the average age of ~35 years. Table 3.8. shows the participants breakdown and the average values recorded from the experiment.

Table 3.8. Hand grip strength and steering wheel torque Experiment results.

	Age	Weight [KG]	Height [cm]	Dominant arm	Driving years	Hand Grip R [kg]	Hand Grip L[kg]	Steering torque CW [N.m]	Steering torque ACW [N.m]
Male	35.5	77.9	171.6	90% R 10% L	10.8	36.64	33.16	18.44	19.11
						(avg.) 34.9		(avg.) 18.775	
Female	35	62.8	162.8	100% R	8.4	31.81	30.61	17.74	18.11
						(avg.) 31.21		(avg.) 17.925	

It is crucial to baseline the controllability classes' calculation and categorization relative to these numbers and values that were experimentally found in this dissertation

and consider the gender at the same time for precisely calculation of the steering system ASIL. Consequently, this new criterion proposed in this research calculates the controllability class of the ASIL matrix of ISO 26262 based on the maximum torque that the human can perform in the vehicle steering wheel that was found in this study as shown in table 3.9.

Table 3.9. Controllability class based on the human torque capability.

Controllability	C0	C1	C2	C3
Description in table B.6 part 3 ISO 26262	Controllable in general	More than 99% of the average drivers are able to control	Between 90 and 99% of the average drivers are able to control	Less than 90% of the average drivers are able to control
Steering wheel torque (N.m)	All drivers	99% of drivers	90% of drivers	Less than 90% of drivers
Male	18.775	18.775+0.0187	18.775+0.187	< 18.775+0.187
Female	17.925	17.925+0.0179	17.925+0.179	< 17.925+0.179

The new challenges of more ADAS functionalities and higher forces in the steering rack of modern vehicles impose more stringent safety requirements in case of SLOA for EPS systems is in the next section.

3.8.2 New Challenges for the EPS Systems

A comprehensive test and features comparison of electric versus hydraulic power steering assist was published in 2018 [62]. Currently 90 % of all new vehicles are being produced and manufactured with an EPS system to assist the driver and support the ADAS application and features [63]. In additional to higher automated driving system that requires EPS system, another motivation of switching from hydraulic power assist steering systems to electric power assist steering systems is to reduce parasitic losses and increase the fuel efficiency. This is due to the fact that EPS only has a significant draw of electrical current when the driver is turning the vehicle' steering wheel, while the Hydraulic power Assisted Steering (HPAS) is always "on" whether the vehicle is turning or not. About 4 % of fuel efficiency was achieved by switching from HPAS to EPS systems [6364]. Additionally, the development of the electric motor technology, the control advancements and the hybrid and electric vehicles advancement are enabling the use of the EPS systems in heavier vehicles where it could not be applied previously, e.g., the Ford and GM sport utility vehicles and pickups. Also, the development of hybrid and battery electric vehicles (BEV) requires the EPS installation [65].

The average curb weight (Net weight) of the new vehicles has increased in the last decade as shown in Figure 3.5 [66]. From 2004 to 2021, there was a 13.6% increase in the weight of SUVs and multi-purpose vehicles (MPV). This growth of the curb mass is expected to continue increasing given the fact that more BEV are replacing conventional engine vehicles. Battery electric vehicles are equipped with heavy batteries and electric engines that are placed in the front part of the chassis.

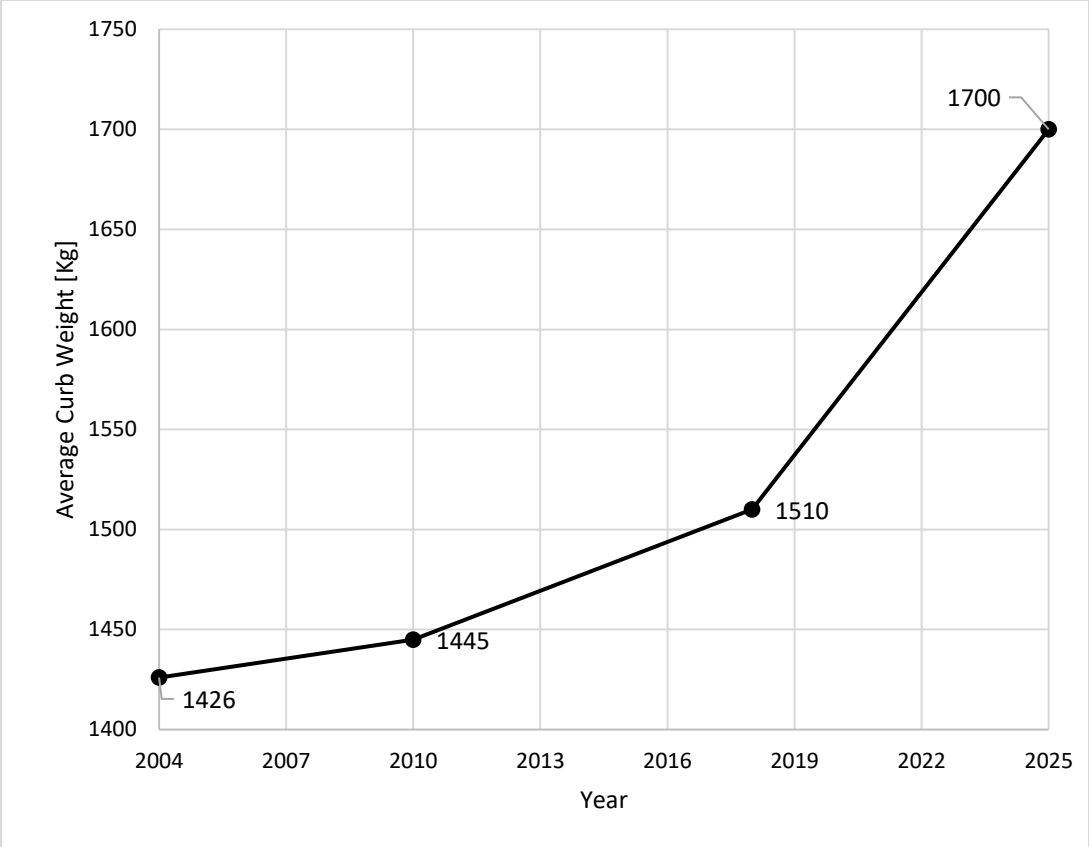

Figure 3.5. Vehicle Average Curb Weight Increase Trend [66].

The lateral force (F_y) at the front axle, is the product of the proportional mass of the vehicle at the front axle (m) and the lateral acceleration (a_y) as shown in equation (3.6) [67].

$$F_y = m \,.\, a_y \tag{3.6}$$

The vehicle weight can be calculated from equation (3.7).

$$Vehicle\ Weigh = m \,.\, g \tag{3.7}$$

The steering torque around the steering axle (M_z) can be calculated using equation (3.8):

$$M_z = F_y . (r_\tau + r_P) \tag{3.8}$$

Z is the perpendicular axis on the front steering axel as shown in Figure 3.6. To maintain the vehicle in the curved path, M_z needs to cover the full range of rotating motion which can be measured as the steering wheel angle.

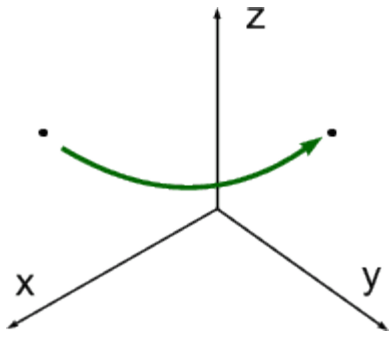

Figure 3.6. Steering torque at the front axle rotation about the z axis.

The driver has to apply a SWT reduced by the kinematic steering ratio and the steering assistance ratio see equation (3.9):

$$SWT = \frac{M_z}{i_s . A_s} = \frac{F_y . (r_\tau + r_P)}{i_s . A_s} \tag{3.9}$$

i_s = the kinematic steering ratio and A_s = the steering assistance ratio. Equation (3.9) shows that the SWT is proportional with the weight of the vehicle at the front axle. The constructive trail r_τ and the pneumatic trail r_p can be found from figure 3.7.

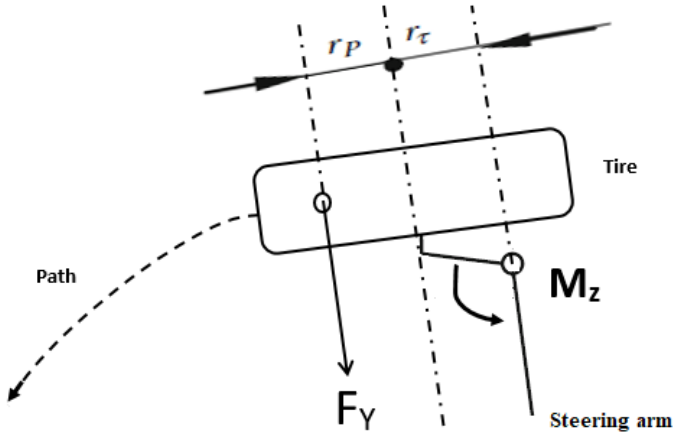

Figure 3.7. Steering torque at the front wheel (Vehicle turns to the left side).

This trend of increased net vehicle weight has introduced a new challenge for the EPS system. A higher force at the steering rack is required to steer the vehicle and control the motion laterally to keep the vehicle in the intended trajectory.

3.8.3 GT Model Vehicle Weights Case Study

A steering system was developed utilizing 3D vehicle model in Gamma Technologies (GT) Suite software in which the vehicle tires were simulated using the "Tireconn3D" objects available in GT Suite version 2021 representing the full 3D environment. The vehicle follows a series of real-world driving cycles based on data acquired from a GPS system available in the driving library of the GT model. A multi-case parameterization study was created in the model to run the simulation with five vehicle weights of 1000, 1250, 1500, 1750 and 2000 kg respectively to study the impact of the vehicle weights increase in the front tires lateral forces and overturning torques

required to turn the front axle wheels. The GT Suite built-in tire maps and Pacejka high fidelity model were used for tire reaction loads [68]. All other vehicle operating conditions and roads were kept the same through the multi-case simulations except the vehicle weights parametrizations in which normal driving and road surface conditions were assumed. The front tire lateral forces were obtained from the GT Post results by selecting the respective object such as the front right and front left tires. The front tire lateral forces increase as the vehicle weights increase as shown in figure 3.8.

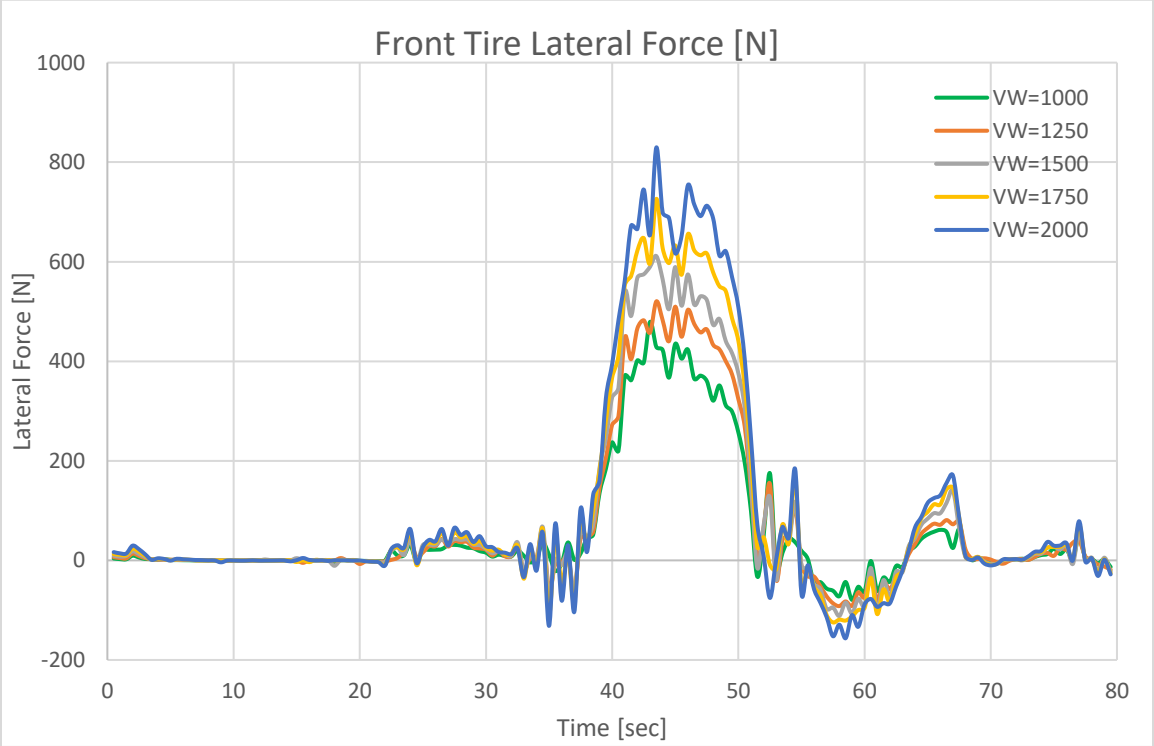

Figure 3.8. Front tire lateral force for different vehicle weights.

It is clear that the front tire lateral force doubled in magnitude when the vehicle weights increased from 1000 to 2000 kg. However, the front tire overturning torque increased by 50% from ~133 to ~ 200 Nm for the same vehicle weights increase cases as shown in figure 3.9 due to the non-linear behavior change of the dimensions r_τ *and* r_P with the vehicle weight increases as shown in (eq. 3.8).

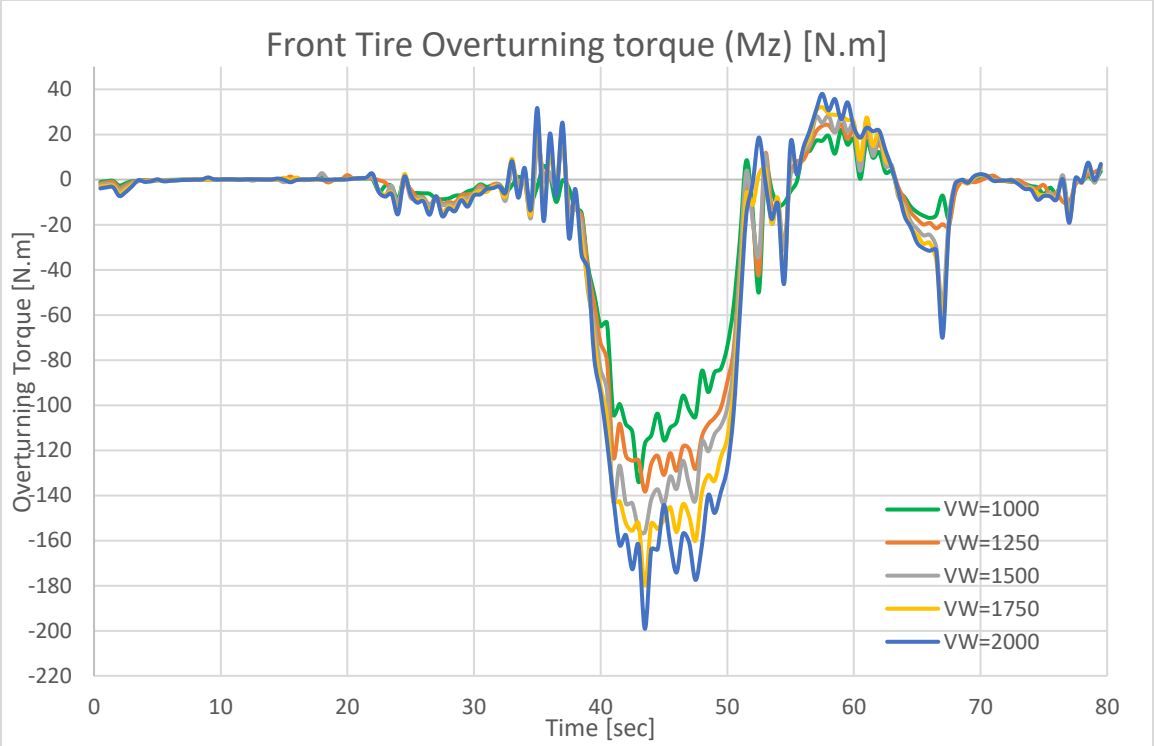

Figure 3.9. Front tire overturning torque for different vehicle weights.

In addition, it is clear that the vehicle weight case of 2000 kg, it requires 200 [N.m] overturning torque to turn the front tire and follow the desired trajectory and this is more than 10 times of the human capability of controlling and turning the steering wheel according to table 3.9. Therefore, in case of SLOA from the EPS systems, the driver has

to perform a fully manual (without electric motor assistance) steering with a sudden, significantly increased steering wheel torque of ~ 200 [N.m] required to compensate for the SLOA within a 1-20 msec time frame [69, 70].

Another interesting finding of the vehicle weight increase is that the wheel camber or inclination angle (γ) increased during the vehicle curvature maneuver which means that the front wheel is tilted inward (Negative pointing inward) at the top of the wheel as shown in figure 3.10.

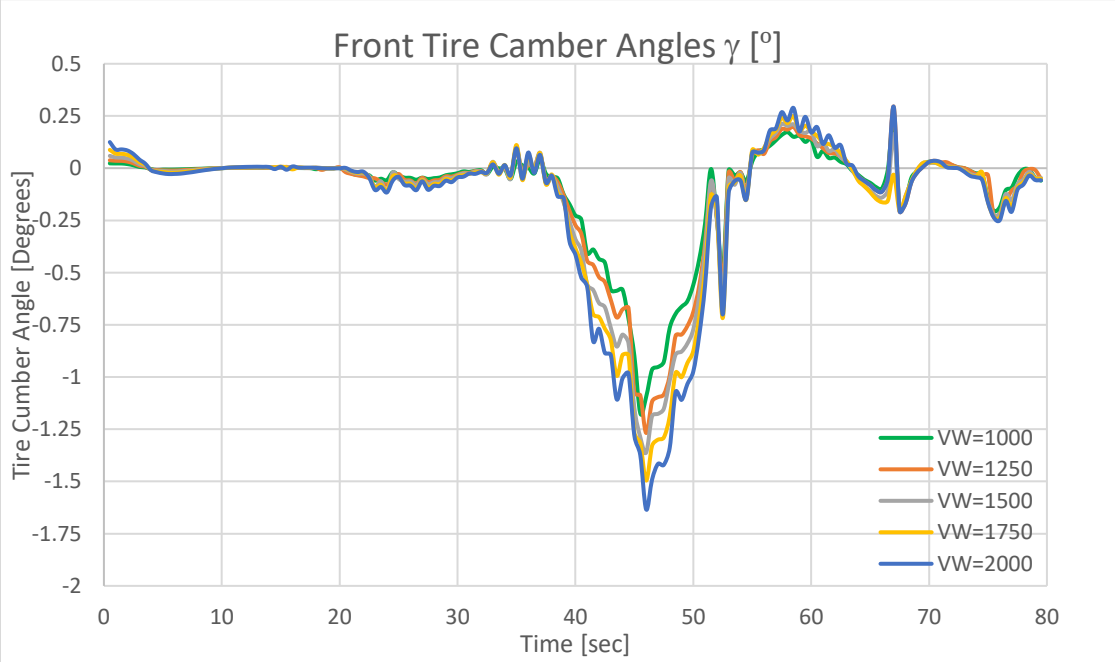

Figure 3.10. Front tire camber angles for different vehicle weights.

This explains the increase in the required overturning torque of the front axle wheels associated with the higher VW because the higher γ values will result in distortion of the contact region of the tire and the road surface, consequently, this introduces more

dissipated torque for the lateral deformation with respect to the contact flat plane in the contact region of the tire and the surface.

The controllability class C needs to be changed from C2 to C3 in case of SLOA for EPS systems and consequently the assigned ASIL has increased from B to C as shown in table 3.10.

Table 3.10. New ASIL assignment for ADAS and higher forces on the steering racks.

Proposed severity class	Exposure	Controllability		
		C1	C2	C3
S3	E1	QM	QM	A
	E2	QM	A	B
	E3	A	B	C
	E4	B	C	D

ASIL D was already assigned for failure modes where the EPS loses the vehicle control such as self-steering (the steering wheel rotates without any input by the driver or the system) and steering-lock where the steering wheel freezes. In this case, the EPS system with the redundant control path complaint with ASIL D switches the state machine of the EPS to the fail-operational architecture with a degraded mode to maintain the steering system so the driver can take action manually. This is out of the study scope as the research here focuses more on the SLOA associated with the increased weight of the new vehicles, such as SUV and BEV, which puts more load in the front axle and this requires more force in the steering rack to apply the commands on the road wheels as shown in equations (3.7) and (3.9). In addition, the introduction of more ADAS functions for the steering systems has affected the ASIL classifications in the presence of more

sensors and actuators. For example, if the camera fails to perceive the road lane markers, a diagnostic trouble code (DTC) will be activated, which causes the ECU of the EPS system to enter error, reset, fail-silent mode that leads to SLOA and escalate to the driver to take immediate action and take the vehicle's control by performing the required SWT manually.

3.8.4 SPFM and LFM of the EPS Systems

According to ISO 26262 and as shown in table 3.7, the SPFM and the LFM for ASIL B and ASIL C are very different. In addition, the probabilistic metric for random hardware failures requires more risk reduction for ASIL C than ASIL B. ASIL C requires mandatory reduction of the risk and higher-level matrices of safety concepts as shown in table 3.11:

Table 3.11. Handling of safety matrices of ASILs [54-55].

	QM	ASIL A	ASIL B	ASIL C	ASIL D
Safety Handling	Rigorous design and test to avoid potential failures			Control potential failure	
SPFM	No	No	≥ 90%	≥ 97%	≥ 99%
LFM	No	No	≥ 60%	≥ 80%	≥ 90%
PMHF	No	No	<100 FIT	< 100 FIT	< 10 FIT
FTA	No	No	No	Yes	Yes
DFA	No	No	No	Yes	Yes
FMEA	No	No	Yes	Yes	Yes

It is clear from Table 3.11 that ASIL C requires higher safety measures or mechanisms to fulfill the SPFM ≥ 97% and the LFM ≥ 80%. ASIL B, however, requires lower measures of SPFM ≥ 90% and LFM ≥ 60%. Thus, ASIL C requires a change in the system architecture to satisfy these targets of SPFM and LFM. ASIL C is a mandatory assignment for the EPS system for modern vehicles to reduce any potential SLOA in the EPS or sudden return of assistance. This ensures high availability of the ADAS functionality and provides the required assistance of the EPS system for the driver of heavier vehicles.

3.8.5 Architecture for Highly Available EPS Systems

A single logic or control system for ASIL C is not enough to mitigate or reduce any potential risk of SLOA because ASIL C requires tolerance up to 3% of single point element failure and 20% of the latent failure as explained in the ISO 262626 standard [53 - 55]. This forcefully introduces the concept of redundancy for the control and logic gates of the EPS system to ensure high availability in case of SLOA. The redundant systems can be classified to:

1- Homogenous redundant systems: where multiple elements of a single type or component are used to achieve redundancy, such as the use of dual ECUs, multicore microcontrollers, two power supplies for the steering motor and dual sensors (multi channels). In general, it is simpler to implement and maintain, however, it is susceptible to systematic faults.

2- Heterogeneous redundant systems: also known as diverse redundancy; where multiple components of different types are used to back up the EPS system, such

as steering by differential brakes. The heterogeneous redundancy is more resistant to systematic faults that are caused by design or manufacture flaws [71].

The implantation of redundancy has introduced the concept of fault tolerance for random faults. If the system fails for any reason, it shall switch to a backup system to take over and at the same disable the failed system. Therefore, SLOA or any consequence of hazards can be avoided, which keeps and maintains the safety goals from being violated. This ensures high availability of the EPS system and reduces the risk of SLOA in the EPS. A higher level of autonomous vehicle requires redundant steering systems to fulfill much higher availability for the steering systems than previously.

ISO 26262 standard- part 5 Annex E explains in detail an example of calculating the SPFM and the LFM for each safety goal of an item (EPS in this study) [5455]. In part section 5 specifies the use of-11 semiconductors such as microcontrollers, system on chip (SoC), and application specific integrated circuits (ASICs). These hardware elements. The functional safety requirements are applicable to both non-programmable and programmable elements, such as ASICs, field programmable gate array (FPGA), and programmable logic device (PLD). In addition, a microcontroller, an ASIC, a gate drive unit (GDU), or similar SoC can be treated as separate hardware parts [72]. The FIT . rates of the EPS logic gate elements are different based on the system architectures and the implemented safety mechanisms. The FIT contribution of the logic gate elements found in the literature showed that the main FIT contributor is the microcontroller with a range of PMHF from 41 % to 45% by considering the SPFM [73]. Therefore, if the main microcontroller fails with SPFM ~ 41 %, which is more than the safe allowance of the

3% of ASIL C, this will violate the safety goals of the EPS controller. To mitigate this potential risk of the SLOA due to microcontroller failure, redundant logic is the key solution for ASIL C assigned for the EPS systems for SLOA.

3.8.6 Redundancy of the EPS Architecture

The newly proposed ASIL C assignment for the EPS systems requires ASIL decomposition to reduce the risk in case of SLOA. Redundancy is one of the successful techniques or measures contained in ISO 26262:

1- Software diversified redundancy (One hardware channel): The aim of the SW redundancy is to detect as early as possible failure in the processing unit by dynamic software comparison [54, 72]. Either it uses the same or different hardware resources e.g RAM, ROM memory ranges. In the case that the ,deployed primary path fails, the second implementation referred to as the redundant path, is responsible for verifying the primary path's calculation and taking action if a failure is detected. This can be done using separate algorithm designs and code to provide software diversity. Figure 3.11 shows the redundant SW comparison in the same processing unit.

2- Reciprocal comparison by software in separate processing units: The aim is to detect as early as possible failures in the processing unit by dynamic software comparison. Two processing units exchange data and compare the data using SW in each unit to detect differences which might cause failure on a real time basis. This approach allows for HW and SW diversity if different processor types are used as well as separate algorithm designs, code and compilers. Logic paths can

be implementedusing separate cores of dual or tri core processors as shown in figure 3.12.

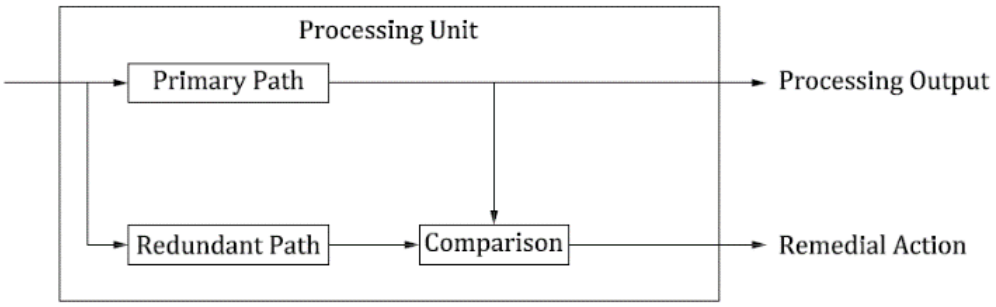

Figure 3.11. Redundant SW comparison in the same processing unit.

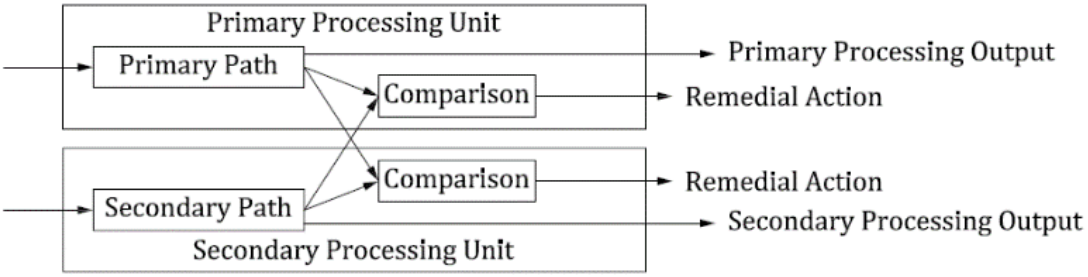

Figure 3.12. Redundant SW comparison using different processing units.

3.8.7 ASIL C Solutions and the Influence of Safety Architecture

Depending on the combination of the hardware and the software interaction used to meet ASIL C requirements of the EPS systems, several approaches or system architectures developed in this dissertation are possible as the followings:

1- The use of two separate microcontrollers to conduct an external comparison of safety outputs; main microcontroller and safety microcontroller. Each microcontroller has a single core. This approach relies on the physical or HW

duplication of safety and non-safety related functions and features. However, this increases the complexity of the configuration because more components are required on the printed circuit board assembly PCBA, which reduces reliability and increases costs [74]. This architecture configuration is shown in figure 3.13.

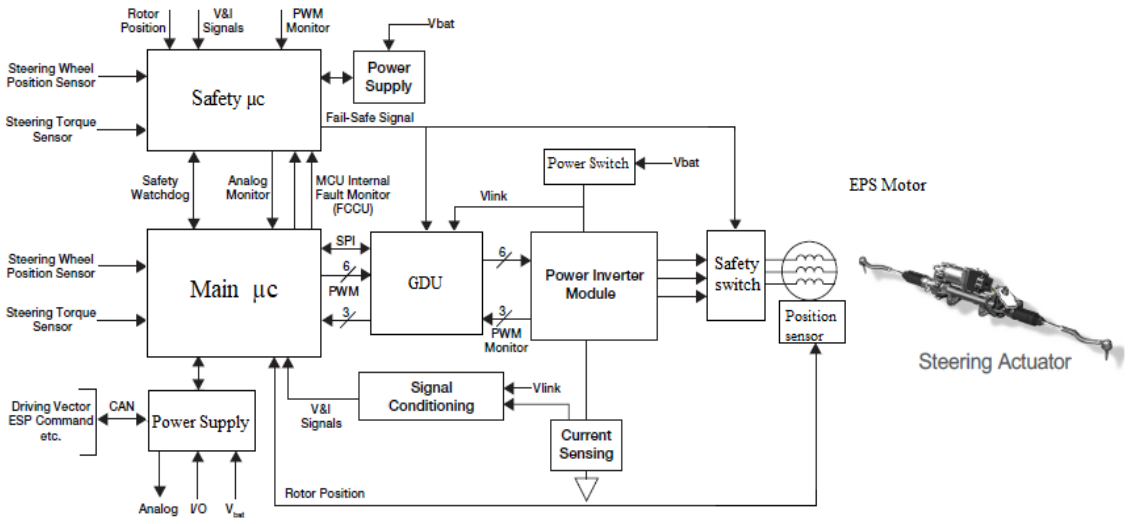

Figure 3.13. EPS control logic path based on a single core and safety µc.

2- The use of multi-core microcontroller (dual or tri-core) is a recent development in the EPS system. This design combines an internal built in self-test (BIST) and lock step mode central processing units (CPU) in the arithmetic logic unit (ALU). The power supply management also combined in one module to monitor the microcontroller and control the safety switch of the EPS motor as shown in figure 3.14.

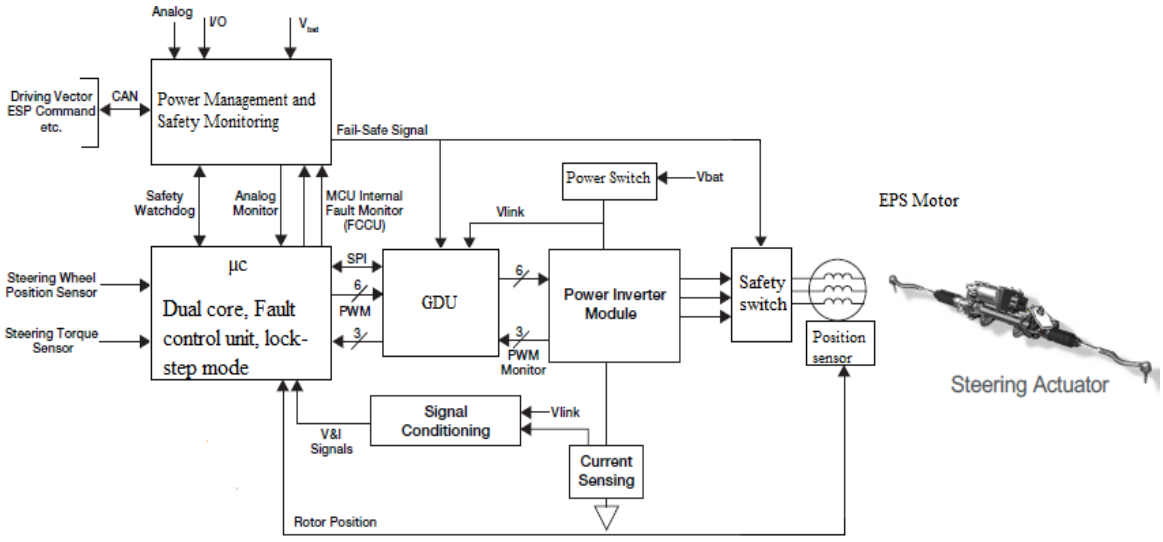

Figure 3.14. EPS control path based on a dual core µc integrated with power management and safety monitoring.

The multicore system architecture provides a higher level of safety to control the EPS motor. It utilizes the backup channel in multicore microcontrollers, which reduces the complexity of the system and improves the availability of the control module. Therefore, the FIT decreases tremendously to the level that satisfies ASIL C assignment (PMHF < 100 FIT). In case of any sudden failure of the main logic path of the microcontroller, the redundant logic path can back-up the control module to mitigate or reduce any violation of the safety goals of the EPS systems. This architecture provides high availability and controllability for the EPS systems to decompose ASIL C determination of the EPS system in case of loss of assistance. Therefore, ASIL C mandates the use of multichannel logic control paths to fulfill the safety metrics. Table 3.12 shows the ASIL target metrics and the logic path architecture of the EPS system.

Table 3.12. Safety and ASIL target metrics and logic requirements.

	QM	ASIL A	ASIL B	ASIL C	ASIL D
Safety Handling	Rigorous design and test to avoid potential failures			Control potential failure	
SPFM	No	No	≥ 90%	≥ 97%	≥ 99%
LFM	No	No	≥ 60%	≥ 80%	≥ 90%
PMHF	No	No	<100 FIT	< 100 FIT	< 10 FIT
FTA	No	No	No	Yes	Yes
DFA	No	No	No	Yes	Yes
FMEA	No	No	Yes	Yes	Yes
Path Architecture	Single logic path is sufficient			Dual-core or tri-core logic path satisfies and fulfils all above metrics	

3.9 Discussion

There are three main key elements in the EPS system control module and ECU as the power supply unit, the microcontroller and the gate driver unit GDU. The functional safety requirements of these units are driven from the safety goals and the ASIL determination of the EPS systems. The use of more ADAS applications in the EPS and the continuous increase of the curb weight of modern vehicles have created new challenges for the EPS system. Any potential SLOA due to E/E failure of the EPS systems have introduced new challenges to the controllability (C) class of the steering systems due to the increase of the required force at the steering rack. This chapter evaluated the ASIL determination of SLOA of the EPS and developed a new methodology for the assessment of a highly available EPS system control logic path. The

safety architecture of the EPS systems can be made of four parts; safe acquisition, safe calculation and safe actuation and the serial data communications. The focus of this work was on the safe calculation of the decision logic to actuate the EPS motor by providing redundant logic paths to ensure that the microcontroller is working correctly. The proposed ASIL C for EPS systems requires dual logic paths, which can be achieved by redundant physical microcontrollers or by dual and tri-core microcontrollers integrated with a power supply management unit. The dual logic path is a mandatory requirement for ASIL C to fulfill the safety metrics according to the ISO 26262 standard as shown in table 3.12. Considering the safety of use and the controllability of the EPS systems, the results indicate that any potential SLOA for the steering torque with more ADAS deployment or higher forces required at the steering rack increases the risk of loss of vehicle trajectory control, which may endanger the driver and the surrounding traffic, if presented. Whereas the SLOA can be reduced by highly available architecture EPS systems logic control design and using redundant logic paths. Therefore, redundancy is critical and required for high availability EPS systems to avoid any loss of assistance or lose the lateral control of the vehicle. This enables the driver in the loop to manage the vehicle's trajectory without any negative impact on the driver performance in case of SLOA. The highly available EPS system is operated under a failed-operational state when a fault or failure is present in the EPS system. Redundancy increases safety and availability, but at the same time has negative effects on the system complexity and the costs. A reliable EPS system means the ability of the EPS system to control the lateral direction of the vehicle under the assistance of the steering electric motor conditions

within a given time. Figure 3.15 shows the conflict zone of functional safety, the availability, and the costs.

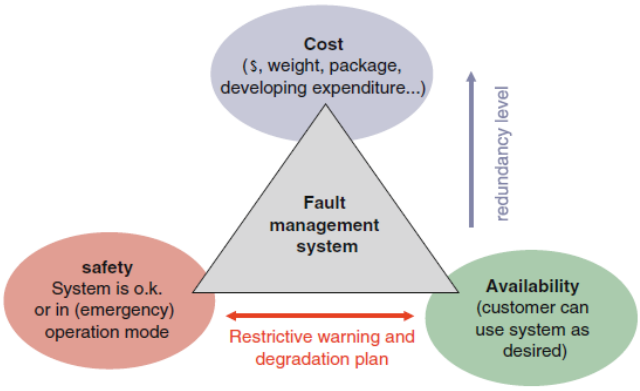

Figure 3.15. Conflict zones of safety, availability and costs.

CHAPTER FOUR

FAULT INJECTION IN MODEL-BASED SYSTEM FAILURE ANALYSIS OF HIGHLY AUTOMATED VEHICLES

4.1 Abstract

The active safety control systems of highly automated vehicles for SAE level 3 and higher are still not fully developed and facing some unresolved issues. The deployment of automated driving systems and the functional safety development present challenges in driver – machine control relationship when there is a system failure or malfunction. The current definition of the product development and controllability classes of the road vehicles functional safety (ISO26262) are not feasible in highly automated vehicles. This chapter developed an overview of fault or disturbance injection on the EPS system of highly automated model to study the impact of steering system sensors malfunction. The approach was to study the fault propagation using a model-based engineering development in a virtual environment of MATLAB. Subsequently, the steering control system of automated vehicle was developed using an adaptive MPC structure to study the control system sensors failures on a system-feature level of the vehicle. It was concluded that the steering wheel angle sensor failure has a significant impact on the planned trajectory of the vehicle and thus it was classified as an ASIL D, which represents the highest critical safety component and requires comprehensive safety mechanisms to meet the safety goals of the system. The study also introduced a new criterion for controllability classes suitable for highly automated systems based on the global vehicle position relative of the lane marker lines, to deal with the active safety systems and risk

handling strategies. The drivers – vehicle control systems are changing significantly in SAE level 3 automated vehicle and above that driving functions are controlled by the vehicle control systems. This presents human factors challenge in this interactive system with moving to SAE levels 4 and 5. Hence, several human machine interfaces and scenario-based testing were introduced to mitigate any risk or safety uncertainty resulting from control handing-over between the driver and the vehicle control system.

4.2 Introduction

The main objective of this chapter is to address the emerging technology challenges of the higher automated and electric vehicles steering system architecture integrated with the framework of the road vehicles functional safety standard ISO 26262 in the presence of the human machine interface. This requires special means in system design and validation during the run time of the automated vehicle control system. Therefore, the current work developed an adaptive MPC model to simulate the longitudinal and the lateral motion of the vehicle and follow a trajectory path using the adaptive MPC optimizer and prediction capabilities complaint with the ISO 26262 standard- Part 4 (Product development at the system level) implementation of the safety related function and behavior.

In this chapter, the research methodology was presented in this work and the high level of the adaptive MPC was explained. Two driving scenarios were generated and validated in a fully virtual environment and the model was deemed to be ready to perform the fault injection tests both in velocity and the steering wheel angle sensors. A new controllability criterion was introduced and defined based on the higher automated

driving systems when the driver might not be part of the control loop in section 4.5. In conclusion, the human machine interaction in the highly automated driving system represents new challenges in these interactive systems of the HAV.

4.3 Methodology

With the deployment of the new technology of the ADAS and AV controlling systems during the last decade, the concept of sensor infusion has been used in the higher automated vehicles, in which multiple channels and sources of surrounding information are connected and processed together to give more confidence in the SVM system that feeds other subsystems such as localization, planning and controlling subsystems [14, 17]. It enables the vehicle control modules to anticipate future events beforehand based on pattern recognition and dataset training using the adaptive MPC block, fuzzy logic, and recurrent neural network (RNN) strategy [75, 76]. Consequently, it alerts the driver before performing any maneuver or action to avoid any potential danger or risk. In the higher automated driving level such as SAE level 3 or above, the electronic control units can make a controlling decision based on the perception input that feeds the programmed algorithm, which resides in their microcontrollers and systems on the chip to make a control decision and send it to the actuators. This is where AI and ML have effectively played a key role to build a vehicular sensory platform with sensor fusion, decision making and actuation streams and pipelines in real time basis. This requires super-fast data computing and processing systems, more memory resources, low latency communication to support the self-driving cars with zero tolerance for error in the driving control system.

The parallel advancement and innovation in theory and hardware computing systems (HCS) have enabled a range of applications such as adaptive MPC and AI to be executed in real-time basis in automotive applications such intelligent steering and electronic braking systems using Ethernet protocols in machine to machine communications. Using the state-of-the-art of math optimization solvers and rapid prototyping, systems have enabled the control modules to perform complex calculations at a sufficient rate to meet the safety requirements of highly automated vehicles with 360 º surrounding coverage.

To deal with the change of the vehicle dynamics in the HAV with SAE level 3 or above, the adaptive MPC provides a new linear planar model at each time step as the operating conditions change; therefore, it makes more accurate prediction for the new operating conditions of the vehicle trajectory maneuver. The adaptive MPC can then control:

1- The longitudinal velocity as the driver sets it in the ACC automated system.
2- The lateral position of the vehicle by following a predefined trajectory or LKA or lane centering systems.

In figure 4.1, the adaptive MPC computes the longitudinal velocity and the steering angle position and rate and provides them as commands to the plant. Then, the real-time vehicle state parameters such as longitudinal velocity, lateral position and yaw rate are the real-time states representing the plant or the vehicle on the road while moving or maneuvering.

Another advantage of deploying the adaptive MPC in the controller is that the plant model connected to an embedded optimizer can be updated in each time step in the runtime for the current operation conditions.

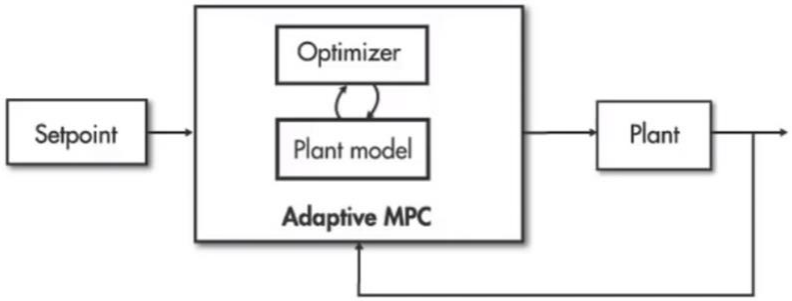

Figure 4.1. A high-level schematic of using the adaptive MPC in the automotive longitudinal velocity and lateral position in the real time simultaneously and it shows the plant model connected with an embedded optimizer to update the operation conditions for the current time step and predict the next time step.

4.3.1 Adaptive MPC design in MATLAB control Toolbox

The traditional or classical MPC control toolbox uses a constant internal plant model, which limits its capability for real time updating and optimization. However, the adaptive MPC that was used and deployed in the research work utilizes the new version of the MATLAB control toolbox (Version 2021) that has an embedded optimizer that linked to the internal plant model, which updates every time step when executed in real time basis. This makes the adaptive MPC effective and suitable for the HAV steering systems to change the lane and follow a planned trajectory by controlling the steering angle input to the plant. At each time step, the Adaptive MPC updates the internal plant model with the same structure of the optimization problem across different operating

points according to the programmed numbers of states and constraints. Therefore, the adaptive MPC is computationally complex because it solves an optimization problem at each time step in real-time basis of the vehicle maneuver. In addition, the adaptive MPC computation gets more complicated with the increase of states constraints and the length of the control horizon and prediction horizons.

To build and simulate the virtual driving environment, the driving scenario designer of automotive application in MATLAB was used to generate roads, lanes and define maneuvers and the driving scenarios and other traffic predefined operating conditions. A passenger car was added to the driving scenario and two maneuvers were generated as follows.

1- Straight trajectory in which the adaptive MPC was deployed to control the longitudinal trajectory and the vehicle velocity of the vehicle as shown in figure 4.2 A. This is represented by the X axis in the global Cartesian positioning system.
2- Lane change trajectory in which the adaptive MPC was deployed to control the lateral global position or trajectory and velocity of the vehicle as shown in figure 4.2 B. This is represented by the Y axis in the global Cartesian positioning system.

The passenger car was set as an ego vehicle in the model. The sub model of the driving scenarios with all the data of the straight and lane-change maneuvering was saved and converted to a MATLAB function and exported to the workspace of the main MATLAB command window in the form of .mat extension file. This is an effective

approach for utilizing vehicle dynamic models in a model based engineering, which has emerged recently in the automotive industry for the ADAS applications development, V&V demonstration purposes in the early phase of the vehicle development to confirm the feasibility and applicability of the design and reduce the change requests later. It moves the vehicle product development engineering towards the left side of the V model, which reduces time, cost, and utilizes control toolbox more efficiently.

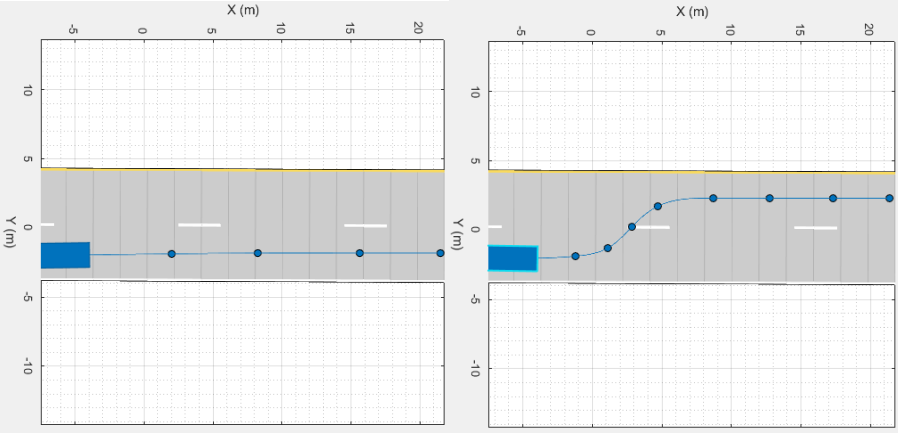

A B

Figure 4.2. The driving environment, roads, lanes and maneuvers scenario were generated virtually using the Driving Scenario Designers in the automotive applications of MATLAB. A (left) is straight maneuver and B (right) is left lane change maneuver.

The plant (ego vehicle) was developed as a state space model representing the lateral, longitudinal vehicle dynamic. The input to the plant is the vehicle longitudinal speed and the steering wheel angle. However, the plant outputs are the lateral position and the yaw angle. In figure 4.3, the horizontal axis denoted as X-axis [m] to represent the longitudinal distance of the headway of the ego vehicle while the vertical Y-axis

represents the driving lane width [m]. There are the referenced X_{ref} and Y_{ref} that will be used in the model. In addition, $\boldsymbol{x}$ $(\boldsymbol{t})$ and $\boldsymbol{y}$ $(\boldsymbol{t})$ are the global parameters that represent the real-time instantaneous vehicle position as the ego vehicle moves in the headway road based on the X_{ref} and Y_{ref}. This predefined trajectory will be the referenced path that the vehicle shall follow with the deployed adaptive MPC in the time domain t. Which controls the vehicle longitudinally and laterally as will be explained in more detail in the next section. The referenced values of the lateral position and the yaw angle are calculated with respect to the referenced horizontal X_{ref} axis as shown in figure 4.3.

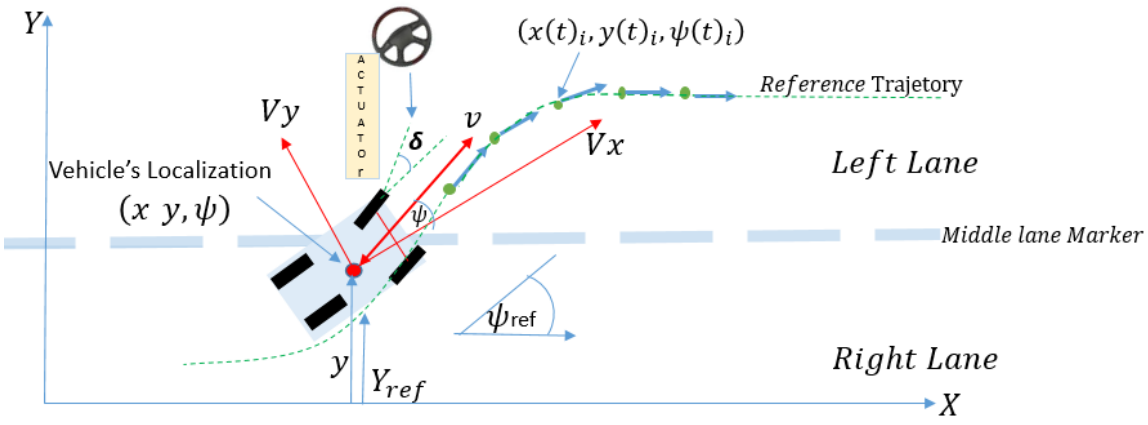

Figure 4.3. Left lane change reference trajectory and vehicle parameters and the reference axis (Longitudinal dimension to the vehicle motion direction).

4.3.2 Adaptive MPC topology Integration

MATLAB Simulink package library was utilized to create the adaptive MPC block and connected to the plant (ego vehicle) as shown in figure 4.4.

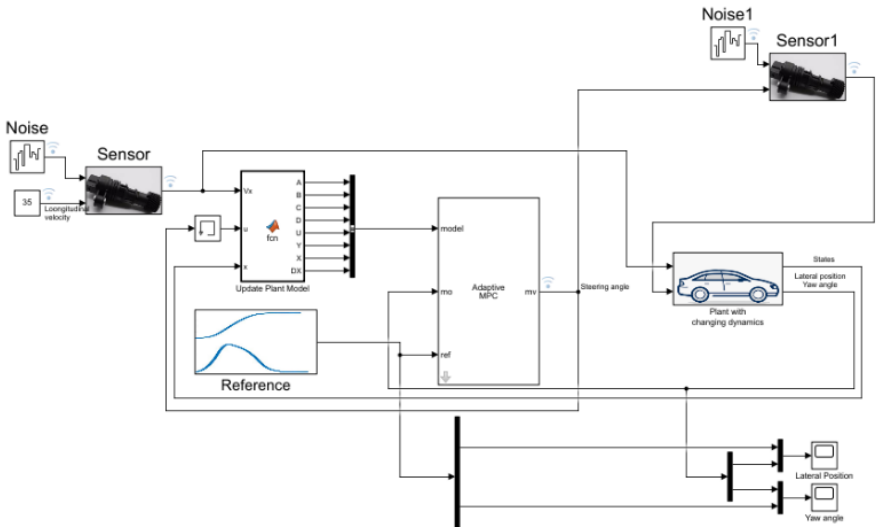

Figure 4.4. The adaptive MPC block and the vehicle model connected to the referenced library that generates the predefined trajectory.

Two lanes with widths of 4 meter each were defined in the driving scenario designer. The plant (ego vehicle) was developed as a state space model representing the lateral vehicle dynamic using the bicycle model as the following equations 1 and 2 which are used in the first step to calculate the state space matrices of the vehicle velocity V_x and the vehicle position $\boldsymbol{y}$. Then it computes the discrete model to update the nominal conditions of the discrete time plant of the current operation conditions in the same order that was created inside the MATLAB function through the signals bus that was connected to the adaptive MPC block.

$$\frac{d}{dt}\begin{bmatrix} y \\ \psi \\ \dot{\psi} \end{bmatrix} = \begin{bmatrix} -\frac{2C_{\alpha f} + 2C_{\alpha r}}{mV_x} & 0 & -V_x - \frac{2C_{\alpha f}\, l_f - 2C_{\alpha r}\, l_r}{mV_x} \\ 0 & 0 & 0 \\ -\frac{2l_f\, C_{\alpha f} - 2l_r\, C_{\alpha r}}{I_z V_x} & 0 & -\frac{2\, {l_f}^2 C_{\alpha f} + 2{l_r}^2\, C_{\alpha r}}{I_z V_x} \end{bmatrix} \begin{bmatrix} y \\ \psi \\ \psi' \end{bmatrix} + \begin{bmatrix} \frac{2C_{\alpha f}}{m} \\ 0 \\ \frac{2l_f\, C_{\alpha f}}{I_z} \end{bmatrix} \boldsymbol{\delta} \quad (4.1)$$

Global $\boldsymbol{y}$ position

$$\boldsymbol{y} = V_x \psi + V_y \tag{4.2}$$

$$\dot{x} = V_x \cos\psi - V_y \sin\psi \tag{4.3}$$

$$\dot{y} = V_x \sin\psi + V_y \cos\psi \tag{4.4}$$

$$\dot{v}_y = -V_x \dot{\psi} + \frac{F_{y,f} + F_{y,r}}{m} - g\Phi \tag{4.5}$$

$$\dot{v}_x = \dot{\psi} \cdot V_y + a_x + g\Theta \tag{4.6}$$

Where;

$\boldsymbol{y}$ is the global vehicle lateral position at a time t measured from the reference.

V_x is the longitudinal velocity at center of gravity of vehicle

m is the total mass of vehicle

I_z is the yaw moment of the vehicle inertia

l_f is the longitudinal distance from the center of the gravity to front tires

l_r is the longitudinal distance from the center of the gravity to rear tires

C_α is the cornering stiffness of tire

$\boldsymbol{\delta}$ is the front steering angle

ψ is the yaw angle

Φ is the road banking angle

Θ is the road grade angle

$F_{y,f} + F_{y,r}$ Lateral forces of the front and the rear tires

Both road banking and grades effects were added to the Adaptive MPC model to account for the uncertainties and instabilities effects of the road profile as shown in equations (4.5) and (4.6). The adaptive MPC block receives the predefined trajectory that was already defined in the driving scenario designer from the reference block that was embedded in the adaptive MPC block in figure 4.4. The predefined trajectory represents the lateral position of the vehicle maneuver. Another input is the current or the real position of the vehicle, which feedback from the plant (ego vehicle) as lateral position and yaw angle that will change as the vehicle dynamic changes so that the adaptive MPC controls the vehicle trajectory as close as the desired trajectory and at the same time, controls the longitudinal velocity as close as to the set point velocity that was already defined as an input to the model to represent the ACC. The advantage of the adaptive MPC is that it is a multivariable controller that controls the outputs simultaneously by considering all the interactions between system variables within the predefined constrains and ranges of these variables. Constrains such as steering wheel rate, velocity increase step, are important because constrain violations can lead to undesired consequences. Therefore, the adaptive MPC can handle multi-input multi-out (MIMO) systems and therefore, this makes it suitable for high-level automation and autonomous vehicle applications. In addition, another feature of the adaptive MPC is its preview capability, which is similar to feedforward control technique to control upcoming events accurately.

Another output variable from the plant (ego vehicle) is the state of the vehicle, which represents the actual longitudinal velocity, and lateral position of the vehicle. The

state estimator is part of the feedback loop to the adaptive MPC to measure the vehicle velocity and position incrementally in each time step and adjust the output accordingly.

The adaptive MPC updates the plant (ego vehicle) each time step T with the below operation conditions and parameters values used to design the adaptive MPC setting in this work are shown in table 4.1. The adaptive MPC uses an internal plant model to make predictions and optimization iterations to find the optimal control actions utilizing fixed and variable horizon optimizers. In order to calculate the next step decision, the controller operates in two phases:

1- Estimate the current state which includes the true values of the controlled vehicle parameters such as the longitudinal vehicle speed and the steering wheel angle. This is very crucial to make an intelligent move in the future step based on the current and past measurements of the data buffers. The state estimator in this study was a default Kalman Filter.

2- Optimize the values of the set points, measured disturbance and constraints specified over the finite horizon of the future sampling instants T+1, T+2, ….. The adaptive MPC control action at time T is obtained by solving the optimization problem and the cost function as explained in the MATLAB user guide of the adaptive MPC Toolbox [77].

Table 4.1. Adaptive MPC Parameters.

Parameters	Explanation
T_s	Execution time step update = 0.1 sec
T	Simulation duration =15 sec
Prediction Horizon	Controller prediction of the sample time = 1
Constraints	Represent the physical limitation of vehicle
	Steering wheel turns at of 15 degree/sec
Weights	Set the input and output parameters to value
	Such yaw angle to 0.1 and position to 1
Response	Ramp input
Plant Input	The long. speed V_x and the front steering angle $\boldsymbol{\delta}$
Plant Measured output	Lateral position $\boldsymbol{y}$
	Yaw angle ψ
State Estimator	Default Kalman Filter
Vehicle mass	1575 kg

4.3.3 Adaptive MPC design parameters selection

The selection of magnitudes and values of the adaptive MPC is important as they affect not only the controller performance but also the computational complexity of the adaptive MPC algorithm that solves an online optimization problem at each time step. In automotive applications, the sample time (T_s) of the adaptive MPC determines the rate at which the controller executes the control algorithm and commands the actuators based on

the predefined algorithm and calculation. In the same time, too small T_s requires excessive computational load on the system resources and memories that add more design complexity, constrains and cost. The adaptive MPC computations get more complex and resource demanded with the increasing number of vehicle states, constraints, length of control, and the prediction horizon. The vehicle dynamic optimization processes and solving the cost function need to be solved within small sampling intervals in the order of milliseconds (msec) execution time to converge results through iteration.

4.3.4 ISO 26262 Active Safety Requirements

This framework for the fault injection test methodology at the ego vehicle level for the vehicle motion controller was developed considering the ISO 26262 standard – Part 4 product development at the system level. It requires evidence for the correct implementation of the safety related functions and behavior on the system level (HW & SW) combination as shown in table 4.2. However, it does not specify whether the tests need to be done in virtual environment or real scenarios and maneuvers. ASILs B, C and D require fault injection test in the run time while the control system is deployed. It is considered one of the effective methods to test the robustness of the active safety control system after integrating the HW and the SW components of the system [53- 55]. Consequently, this provides an evidence that system elements interact correctly with an adequate level of confidence that unintended behaviors (that could violate a safety goal), are absent from the current integration design of the vehicle motion controller system.

Table 4.2. ISO 26262 Active safety implementation of fault injection.

Methods	ASIL			
	A	B	C	D
Requirements-Based Test	+	++	++	++
Fault Injection Test	+	++	++	++
Back-to-Back Test	+	+	++	++

Note: ++ indicates that the method is highly recommended for the identified ASIL
+ Indicates that the method is recommended for the identified ASIL

A fault injection test uses corrupted, interrupted and false data and means to introduce faults into the steering system during the run time of the vehicle. The fault injection was performed on the developed MATLAB model. Most of the suppliers and testers are moving towards the virtual hardware in the loop (VHIL) technology for V&V of the ADAS applications and their active safety mechanisms to meet the designed safety goals under these conditions. Therefore, the fault injection test can be done in a fully virtual environment of a model based to study the behavior of the active safety system in the early development phase of the developed products and address any issues easily and costly effective before the prototype implementation and execution.

Faults were generated in the model of the steering system and injected in the interface of the adaptive MPC. Following this new approach developed in this dissertation introduces the concept of the fault injection test coverage in a fully virtual environment of the steering sensors and adaptive MPC block. The injected faults in form of noise needs to cover the data corruption, timing, program flow and sequences. The SW

architecture design goal is to be able to monitor, detect, isolate and recover from the faults and maintain a safe and highly available architecture. Table 4.3 shows examples of fault models and types.

Table 4.3. Fault Models.

Type	Examples
Data errors	Data integrity, Data processing, Data exchange
Timing errors	Violation of specific timing behavior of the executed SW
Program flow errors	Erroneous sequence or execution order
HW errors	Faulty hardware parts in the system

The error can be defined as the incorrect state of the subsystem that is caused by the fault can lead to failure mode. The failure is the termination of the ability of the system or the function unit. This loss of function can appear as abnormal behavior such as an unintended vehicle path and loss of assist. Consequently, hazardous events could lead to an accident with negative potential inherited from this set of conditions. Personal injuries and property damage can be caused and experienced which depend on the severity of the hazard and the environment of the drivers, passengers and other road users and surrounding infrastructures.

4.4 Results

4.4.1 Adaptive MPC model results

The MATLAB-Simulink model was executed with two driving scenarios; the first scenario was a left lane change from the host lane and continues the maneuver in left

adjacent lane. The second scenario was driving the ego vehicle in same host lane straightforward both with longitudinal velocity of 35 m/sec, which was fed in the reference trajectory. The adaptive MPC of the ego vehicle followed the reference trajectory lane change very closely as shown in figure 4.5 orange dotted line. The implementation of the adaptive MPC in the ego vehicle integrated in the Simulink explains the combination of controlling of the longitudinal speed, which is known a full range speed adaptive cruise control (FRSACC) across a wide range of different speeds. In addition, following the lateral reference trajectory vehicle position, which fulfils the third level of the SAE automation level where the vehicle control system can drive the vehicle longitudinally and laterally simultaneously and follows a defined path from point A to point B. The deployment of the adaptive MPC model achieves level SAE 3 automation in this research work. Consequently, the adaptive MPC application can be considered as a suitable fit in HAV's CVM integrated with other localization, positioning and mapping applications that can be optimized for the reference path utilizing artificial intelligence and machine learning platforms and constitute layers covering vehicle control [78]. The model was deemed fully validated against the driving scenarios that were generated virtually using the driving scenario designer of automotive application in MATLAB

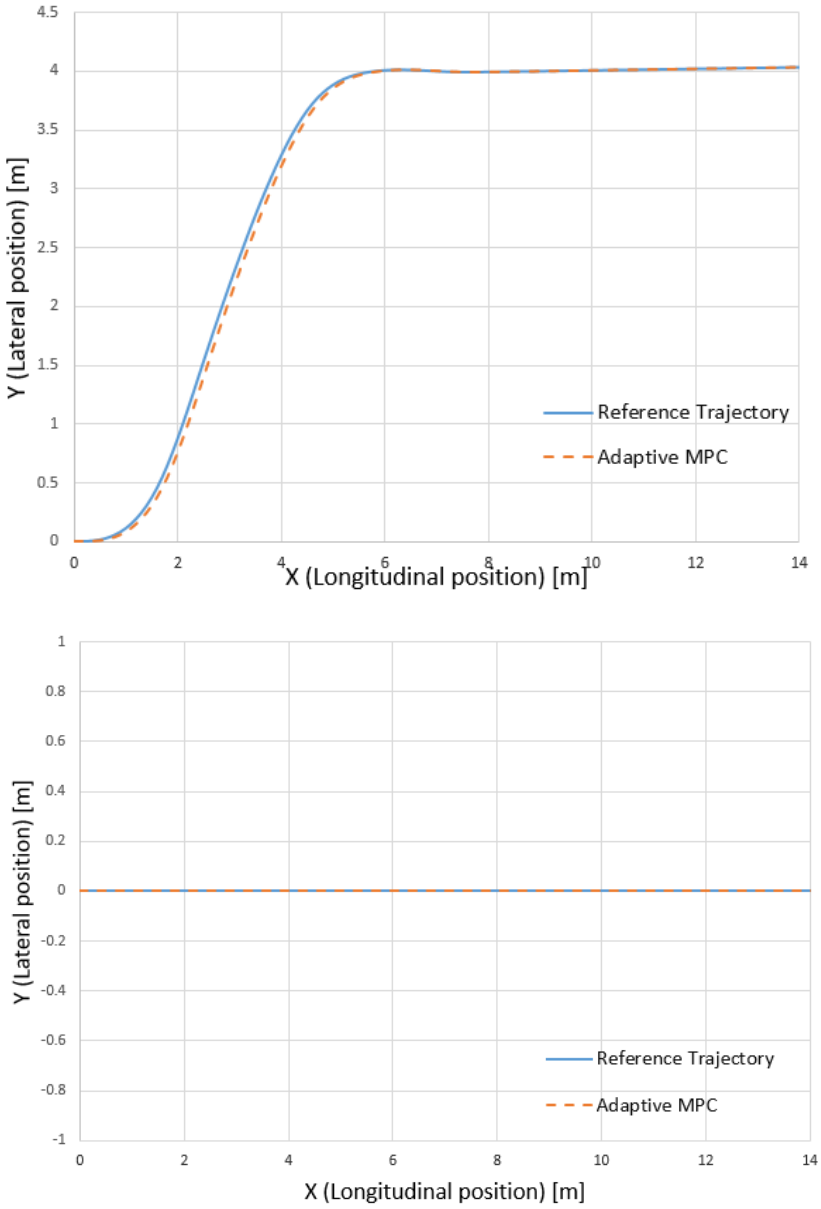

Figure 4.5. The MATLAB-Simulink model of the adaptive MPC ego vehicle results following the reference trajectory of left lane change (Top) and stay in the same straight maneuver (Bottom).

4.4.2 Controllability of adaptive MPC and system failures

After validating the adaptive MPC of the ego vehicle by matching the reference and vehicles paths as shown in figure 4.5, the longitudinal velocity and steering hand wheel angle sensors failures or degradation events were performed in the Simulink model by injecting a predefined percentage of noise or disturbance (faults) on the signals to evaluate the fault injection metric of the ISO26262 in a virtual environment. In addition, this represents an end-to-end (E2E) performance test coverage of the adaptive MPC block that represents the vehicle's CVM. The chosen evaluation of the noise or disturbance impact considers the longitudinal and lateral vehicle motion and position. The ACC, LKA and the automatic lane change assist (LCA) are the features on the system level that can be impacted by any functional failure or signal disturbance in these sensors due to the injected faults. Two noise or disturbance blocks or sources were linked to the longitudinal velocity sensor and the steering hand wheel angle sensor as shown in figure 4.4. The band-limited white noise block generates normally distributed random numbers that are suitable for use in continuous or hybrid systems with sample time of 0.1 sec to represent malfunction or degradation of the sensors or the transmitted signal from the sensor to the adaptive MPC module block.

The first case involved tracing the longitudinal velocity sensor output without any noise as shown in blue color in figure 4.6, which is clear that the longitudinal signal sensor is fully functional without any noise, and the signal is stable at 35 m/sec. The orange trace in the same figure shows manipulated velocity with a random noise of 10%

of the original longitudinal velocity, which represents a fault or sensor degradation that cause the transmitted velocity signal to be unstable as shown in figure 4.6.

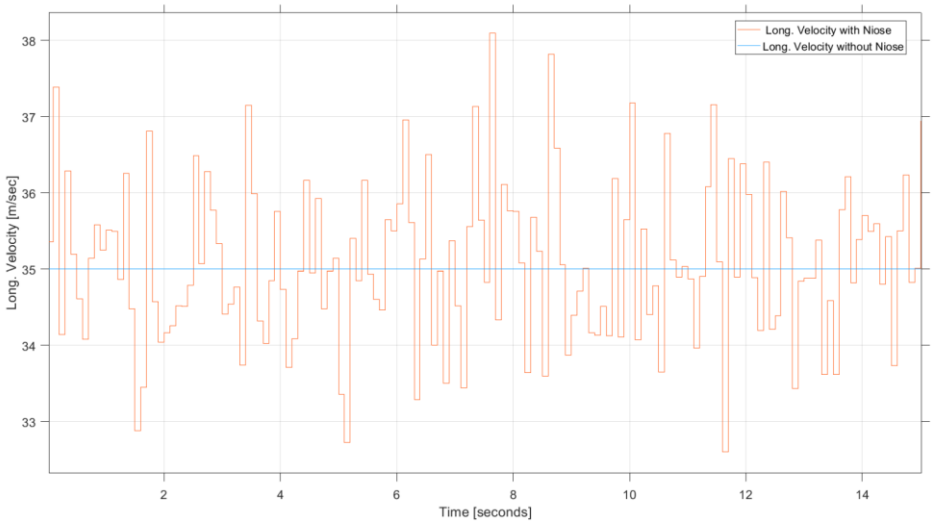

Figure 4.6. Longitudinal velocity sensor signal without any noise or disturbance (blue color) and with 10% noise (orange color).

It was found that the injection of 10% of noise or disturbance on the vehicle velocity does not impact the adaptive MPC model following the reference trajectory because the velocity sensor path or trace in the model is totally separated from the lateral position control path. According to the ISO 26262, the functional safety of the road vehicles, the malfunction of the longitudinal velocity sensor due to faulty signals would not be considered as a high risk because the absence of the unreasonable risk when the velocity sensor fails. In addition, it is known as safe faults or latent faults, which is unable to violate the safety goal of the system because the safe faults cannot propagate to the relevant paths of the lateral control logic gates or the internal registers. Consequently,

it is unable to affect the design function so the system is tolerant for this type of faults. It might be still uncomfortable maneuver or experience for the driver or the road users, but still not a high-risk failure in the E/E system of the vehicle velocity sensor.

The second case involved tracing the SWA sensor output signal with 1% noise or disturbance as shown in orange color with respect to the original steering hand wheel angle signal without noise as shown in blue color in figure 4.7. The steering wheel angle unit used in the model was chosen in radians (1 rad. = 57.29 degrees) and this is the reason that a noise magnitude of 1 % was selected in the research to investigate the small increment of the SWA failure in the order of 0.5729 degrees and evaluate its impact on the adaptive MPC model following the reference trajectory. Again, the orange trace shows a random noise distribution across the run time of the simulation of real time run of the ego vehicle.

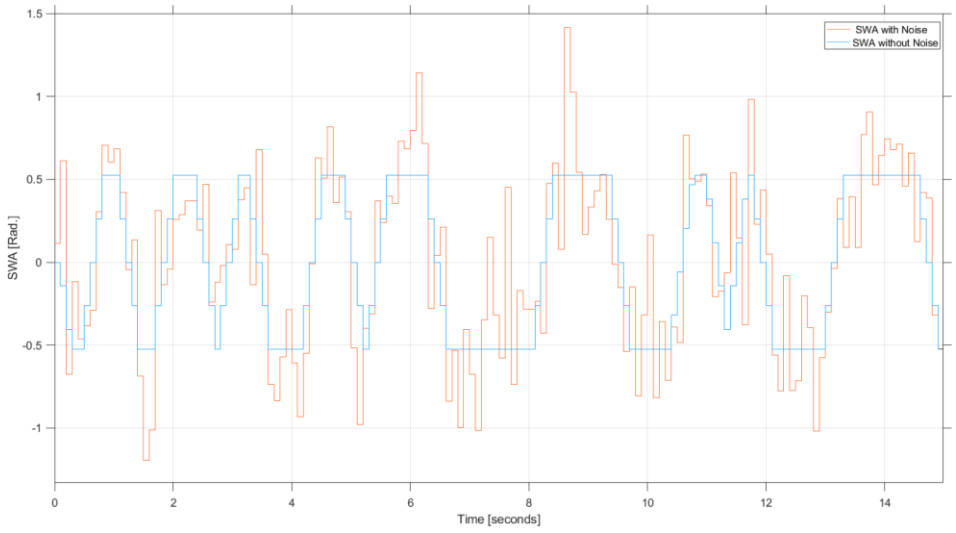

Figure 4.7. Steering wheel angle sensor signal without any noise or disturbance (blue color) and with 10% noise (orange color).

The added noise or disturbance representing faults was injected on the trace of the SWA sensor to study SWA failure scenario that can degrade the function of the sensor and sending faulty signals. Consequently, this faulty signal propagates through the plant or the vehicle CVM causing it to jitter in the right and left directions, which drives the ego vehicle out of the intended trajectory as shown in figure 4.8 even before the vehicle starts the lane change. The ego vehicle in this scenario can be described as non-controllable vehicle due to SWA sensor failure in the host lane, lane change and the target lane. This means that the ego vehicle needs the SWA input to keep the vehicle in the same lane for the straightforward scenario. This is the reason that the SWA sensor is categorized as a safety critical component with an ASIL D classification that ISO 26262 highly recommends fault injection test as shown in table 4.2. This is an example of a single point or primary fault that can propagate through the CVM controller and violate

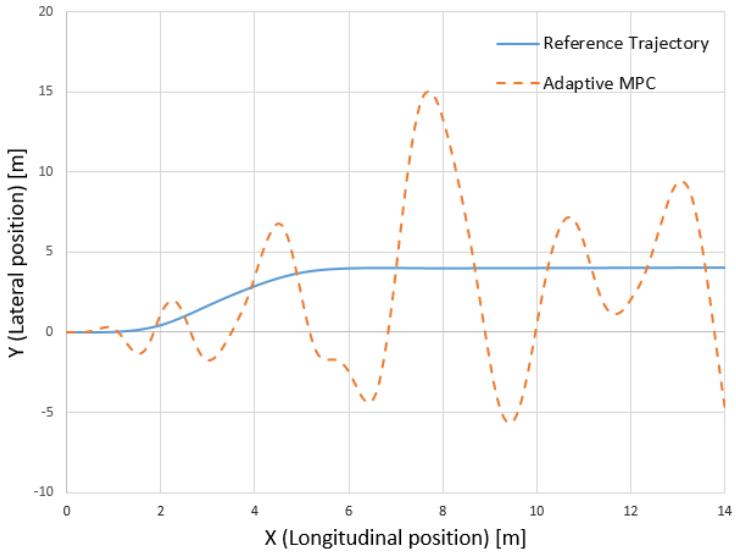

Figure 4.8. Adaptive MPC model result with 1% noise added to the steering wheel angle sensor [rad.]

the safety goals such that the safety mechanism cannot observe, mitigate or remediate it. Therefore, ISO 26262 recommends to perform a fault propagation analysis (FPA) to test the safety mechanisms and the diagnostic coverage of single fault point metric to satisfy the SPFM and ASIL B, C and D targets as shown in table 4.4 [55]

Table 4.4. ISO26262 Single point fault metric and ASIL B, C and D targets.

Methods	ASIL			
	A	B	C	D
Single-Point Fault Metric	–	$\geq 90\%$	$\geq 97\%$	$\geq 99\%$

In addition, the highest spike of the noisy signal causes the vehicle to deviate further from the reference trajectory or path around the running time of 8 sec as shown in figures 4.7 and 4.8. This presents the evidence that the lateral vehicle motion was influenced by the quality of the SWA signals to keep the ego vehicle in the intended path. The SWA signal oscillation that is caused by the added noise maneuvers the ego vehicle out of the intended path and the host lane until it reaches to the furthest point of 15 m off the road.

Then, the negative spike of the SWA signal drives the vehicle towards the intended path again and departs the intended path in the other side or direction. This requires developing a safety goal and safety mechanisms associated with a diagnostic coverage to monitor, detect and mitigate any potential faulty noise that causes failure in the SWA sensor. Examples of safety mechanisms are such as HW redundancy, fail safe

or silent, and cyclic redundancy check (CRC), checksum counters and alive rolling counters (ARC) in the serial data communication [79].

4.4.3 Disturbance Rating Scale

The SWA faults that were injected in the automated steering system by adding noise or disturbance on the sensor output signal can be rated by their impact on the vehicle intended trajectory deviation as shown in figure 4.8. The continuous injection process of faults causes the adaptive MPC vehicle to bounce in sinusoidal behavior, which can be seen as jitters or spikes anomalies from the intended path in both directions. Most of the ADAS and active safety applications sensors run in a synchronous mode with the CVM controllers. This means that the oscillators that generate the signals in a defined pattern and frequency in the sensors need to match the ECU input requirements to keep the synchronous operation mode running normally as designed. The system level scale that measures the SWA disturbance is characterized by a unique defined tolerance limit of the vehicle lateral position with respect to the lane marker lines. Rating on the vehicle lateral dynamic position is strongly influenced by the steering control system sensors, ECUs and actuators functionalities and safety goals in case of any malfunction while being deployed in the field. In addition, the vehicle lateral acceleration plays a key role in this scale. In order to give a common sense of the proposed scale in this dissertation, the concept of vehicle steering system controllability should be redefined, described and what is the threshold to say whether the vehicle is controllable or non-controllable with respect to the intended path in the host lane. This way, the vehicle is integrated with the environment through the global position of the vehicle in respect to the lane marker.

As explained in chapter three and based on the ISO 26262, the current controllability is categorized into four classes C0-C3 with the main difference in the probability from one C class to the next class in the order of magnitude, i.e., C1 is associated with 99%, C2 with 90-90%, C3 with less than 90% of the drivers can control the malfunction and avoid the accident or the crash. This definition does not hold true in case of complex automated driving system being deployed in controlling the vehicle maneuver due to the extreme difference between the human and the computer or machine systems nature such as response time and influence by other driving ecosystem components. This difference can be understood as the comparison between human machine interaction and computer machine interaction (CMI). The human or the driver can distinguish more clearly between controllable and non-controllable scales such as unnoticeable, noticeable, disturbing and even dangerous as shown in figure 4.9.

Figure 4.9. Rating scale of controllability and uncontrollability and human feeling categorization and response to disturbance and steering system malfunction.

For the steering system and the lateral vehicle control that the driver or the human is in the control loop, the controllability is defined as the estimated probability of the driver to gain the lateral vehicle control by rotating the steering wheel to keep the vehicle in the intended path. The system allows the driver to steer the vehicle very easily and

comfortably under all driving conditions by providing up to 80% of the required SWT. So, the driver is expected to provide the remaining 20% of the required SWT [6]. Therefore, there are two scenarios:

1- In case of SLOA due to EPS control unit malfunction or failure, the driver needs to compensate for the EPS assistance loss and perform the required SWT manually [6]. Otherwise, the vehicle will not be laterally controllable and lose the intended or safe trajectory and cause harm or accident. This is the reason that the vehicle steering control system is considered as a very critical safety component and requires a high availability system architecture design to mitigate any failure or malfunction. In addition, this includes avoiding risks and harm to other traffic participants such other vehicles' drivers, passengers, and pedestrians. The solutions were proposed in chapter 3 in this dissertation [80 - 83].
2- In case of the human driver who is in charge of the DDT does not perform the steering commands before the time to collision (TTC) in upcoming safety critical situation to maintain vehicle path and headway due to distraction, fatigue and alcohol impairment [84]. Even if the EPS functions normally and the steering assist is presented, the driver did not trigger or command the steering wheel to turn and keep the vehicle in the intended path so the malfunction here is because of the driver did not trigger the system to follow the intended path.

When the vehicle is equipped with the automated control system that deploys the computer platform to take the lateral control of the vehicle and follow the intended trajectory, here is a special case that the current ISO 26262 standard controllability class

would not hold true anymore when it comes to controllability classification and categorization. The reason is that the human driver is not the active part of the control loop of the vehicle and therefore it is very difficult to measure the controllability of HAD systems based on the computer control system. In an alternative controllability class definition and categorization in the system level of HAD can be considered as shown in table 4.5. Figure 4.10 shows the controllability classes redefinition metric developed in this dissertation.

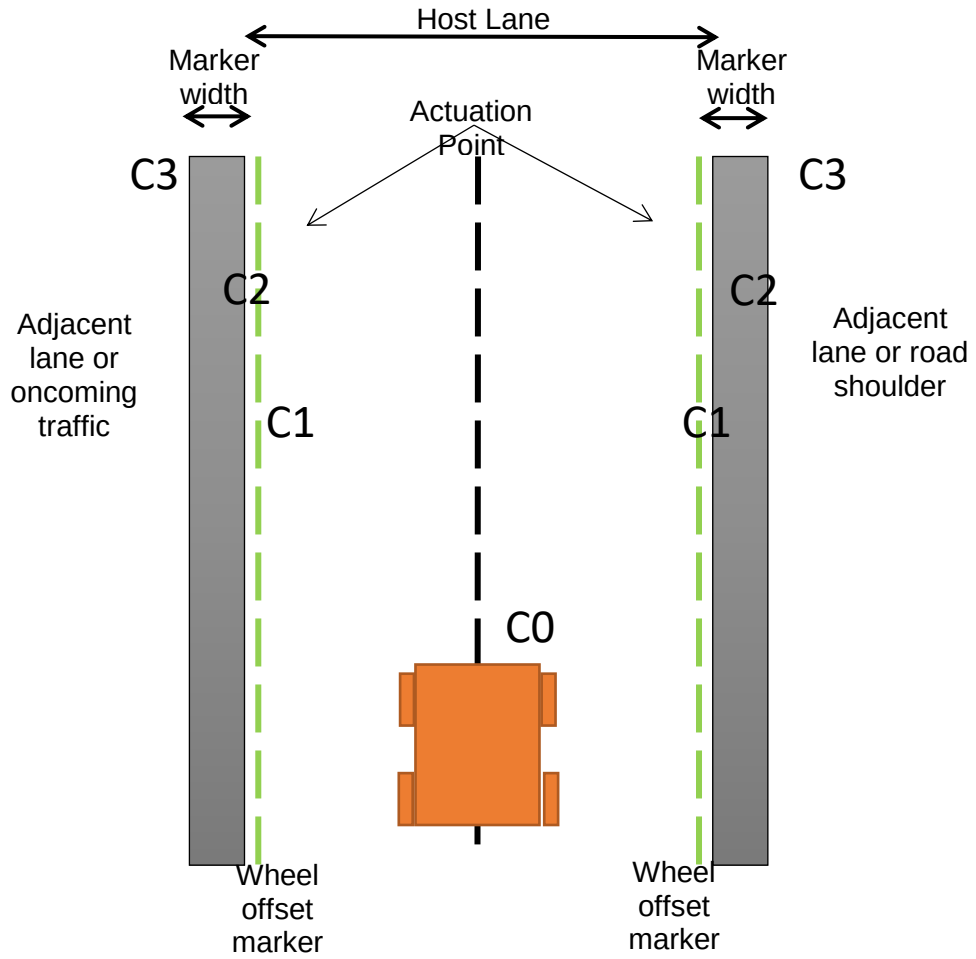

Figure 4.10. Controllability classes redefinition for the vehicle global position.

Table 4.5. Controllability class definition for SAE 3 with higher automation and deployment driving level.

C0 (100%)	C1(99%)	C2(90-99)%	C3(< 90%)
Controllable (Unnoticeable)	Simply Controllable (Noticeable)	Normally Controllable (Disturbing)	Uncontrollable (Dangerous)
Maintain the intended driving path at all times (Vehicle is in the center of the lane and does not cross the wheel offset marker)	Vehicle is still inside the intended lane and the front wheel end does cross wheel offset marker line but does cross the inside end of the lane marker (Wheel offset marker is 10-15 cm)	Vehicle front wheel crosses internal end of the lane marker but does cross out of the lane marker.	Loss of lateral control of the vehicle (Vehicle is uncontrollable and lost driving path) and it is outside of the intended lane (Oncoming traffic lane) or road shoulder. The front wheel crosses the outside end of the lane marker. .
No Accident or harm	Avoidable accident and no harm	Partially avoidable accident with minor harm	Non avoidable accident and it causes severe harm
No risk	Minimal risk	Reasonable risk	Unreasonable risk
Recoverable by the vehicle controller	Recoverable by the vehicle controller	Partially recoverable by the driver vehicle controller	NON recoverable
Intervention is not needed	Intervention is partially needed	Intervention is required	Intervention is required
Unnoticeable	Noticeable	Disturbing	Dangerous

This is a new concept developed in this dissertation to accommodate for the HAD systems when the CMI controls the vehicle. Figure 4.9 and table 4.5 are in alignment for the highest level of uncontrollable steering system, which marks it as dangerous and life threating accident when the unreasonable risk is presented. Consequently, the control system is considered unrecoverable, and the accident is non-avoidable due to the fact that the non-return point was reached. In addition, it can be concluded from figures 4.9, 4.10 and table 4.5 that from the controllability standpoint, the disturbing class failures whose effects are usually controllable by sensible human response and system reaction that could cause minor harm. It represents the conversion point where the system becomes out of control, which makes it dangerous because the system failure results in a safety critical situation. This represents the moment that the vehicle's front axle wheel or tire departs the outside edge of the lane marker line and continues towards oncoming traffic or same direction traffic. If the driver or the control system cannot return the vehicle inside the host lane within 1-3 seconds. At this moment, the vehicle is C3 and out of control. Then, backup systems such as the braking and evasive steering are the two options that the driver can rely on to avoid collision or accidents. The development of evasion systems is a challenge when it comes to HMI and the time-critical scenarios that require highly dynamic steering action within 200 msec [85-87].

4.4.3 Human Machine Interface and Steering Safety Metrics

The high system level hazard definition of steering system failure metric is the unintended steering motion or activation regardless of the vehicle propulsion system status (i.e., parked, neutral or any drive gear position). This happens when the steering

system provides unexpected assist in the form of torque due to failure in the electronic control unit of the steering system or the transmitted signals and commands. Consequently, the vehicle loses the intended lateral path due to uncontrollable or excessive assist from the steering system while driving the vehicle. The vehicle is unable to be steered due to the operator being unable to overcome the steering wheel forces necessary to rotate the steering wheel. Interestingly, in SAE level 3 when the vehicle control system is deployed to drive the vehicle, the driver must be able to take over the control at any time during the maneuver and be able to control the vehicle while the automated steering feature is active such as LKA, LCA and advanced parking assist. The loss of vehicle stability while moving due to steering malfunction may result in loss of control or vehicle roll over. Therefore, the below two metrics shall not be violated for the unintended steering wheel motion:

1- The unintended steering wheel torque assistance that comes from the EPS shall not exceed more than 4 to 5 [N.m] at any time during the maneuver or parking scenarios.
2- The unintended steering wheel movement rate shall not exceed a defined threshold by the manufacturers (depends on the vehicle weight, center of gravity height and dynamic properties) [88]

The steering safety metrics are applicable for all vehicle-operating conditions with the vehicle speed ranges from zero to maximum speed. If the steering safety metrics are violated for any reason, the operator will experience difficulty controlling the vehicle and remaining in the intended path of the host lane. For example, if the unintended steering

wheel torque assist exceeds (4-5) [N.m], consequently, the operator might lose the steering control causing to the intended trajectory loss and vehicle can be described as uncontrollable. The steering torque assistance that the EPS provides is calculated based on the vehicle speeds in the predefined programmable look-up tables of the EPS controlling unit. With the higher vehicle speeds (i.e. 35 m/sec), the assist decreased due to the friction reduction between the front axle wheels and the road surface. This case of high importance and critical safety designation because even with minimal amount of unintended torque assistance with the high vehicle speed scenario, the vehicle is highly susceptible to lose the intended path faster due to the vehicle high lateral acceleration that deviated the vehicle quickly out of the intended lane. This is the reason that active safety systems in higher automation SAE level 3 and above use different intervention strategies in case of failure of the control system to trigger the driver's response to take the vehicle control over from the automated control system. The interventions can be delivered to the driver via the HMI located in the cockpit such as displays, haptic devices, sound alert and flashing lights. The human drivers are still responsible for most of the road crashes even in SAE level 1 and 2 automated vehicles because these active safety-controlling systems are designed to hand the control over to the driver using the intervention HMI in case of malfunction or failure [89, 90]. This is the reason that the drivers – vehicle control systems are changing significantly in SAE level 3 automated vehicle and above that. Driving functions are controlled by the vehicle control systems and this presents human factors challenges in this interactive system with moving to level 4 and 5. HMI modalities can be divided into three main categories as shown in table 4.6.

Table 4.6. HMI Modalities.

Visual	Auditory	Haptic
Color	Sound type (Speech, tone, auditory icon)	Vibration – Frequency
Symbol	Loudness (Absolute and relative to masking threshold)	Location
Text	Muting or partial muting of other sounds	Intensity
Size	Onset of offset	Direction
Brightness	Duration (pulse & interval)	Rhythm
Contrast	Musicality	-
Flashing	Frequency	-
Duration	Spatial location	-

The visual HMI warnings are appropriate for primary warning information and lower priority attention. However, the auditory HMI warnings are suitable for high priority alerts and indicate the onset of system malfunction or limitation. In addition, the haptic HMI can be used to provide information that the auditory HMI is unlikely to be effective. The driver can get a specific information from the HMI about the required action such as braking, swerving or acceleration rather than just getting warning alerts. The HMI can be integrated in the steering wheel itself such as light bar or haptic steering to get the driver's attention quicker to maintain the vehicle's control between the driver and the automated system interchangeably.

CHAPTER FIVE

INTELLIGENT PERFORMANCE ANALYSIS OF AUTOMATED STEERING SYSTEMS FOR AUTONOMOUS VEHICLES

5.1 Abstract

Intelligent ground vehicles (IGV) require automated steering control systems. The complexity of the automated steering systems has increased as the concurrent data receiving, processing, decision-making and monitoring all happen simultaneously in super-fast sampling rates. This chapter focuses on the neural network training and machine learning approaches for an automated steering system of IGV. The essential information of the steering controller was trained using artificial neural network and pattern recognition algorithm approaches. The objective is to investigate the design of ANN training, deep machine learning and AI on collected data from sensors of steering wheel angular position, speed, steering column torque, and ego vehicle speed and generating acceptable steering commands for the vehicle. The results of the research showed that the proposed ANN control system had trained and validated more than ~96.4% steering system behavior patterns and adapted large random disturbances of the steering controller commands. It is, therefore, necessary to develop ANN and AI methodologies in automated steering systems of autonomous vehicles with neural networks representing the main topology blocks of the control system architecture and utilize ANN abstraction in the control system of autonomous vehicle steering control systems.

5.2 Introduction

In this chapter, the concept of ANN and ML in the intelligent steering system was introduced and discussed in section 5.3. Then, the dataset methodology used to obtain the steering system input and output signals was explained in section 5.4. Also, the artificial neural network model building, training and validation processes are discussed. Results are presented in section 5.5. Finally, section 5.6. presented the safety of ANN and ML algorithms and its relation to the V model and the ISO 262626 standard.

5.3 Machine Learning in Steering System

5.3.1 Electric Power Steering System

The need for safer and high reliable steering systems to meet the government regulations and comply with standards associated with the development of ADAS have increased the complexity of the steering system architecture. More sensors, actuators, safety monitors which are purely electrical and electronic E/E components have enabled the steering systems to be smarter and more intelligent. Consequently, ASIL rating of the critical control systems have increased due to potential SLOA or loss of features (LOF) [6, 91]. The correct behavior of autonomous vehicles is only possible if a complex connected subsystems of perception, localization, planning, CVM, actuation and monitoring are accurately made on the correct time, magnitude and direction. This requires a proper tuning of pertaining parameters and receiving the correct data from connected sensors to infuse them in the control module. Then, producing commands to the actuators to achieve the required action of the controller module leading to feature service level such as LKA or trajectory follow up etc. The challenge is to collect all the

required data from the sensors in real time and monitor the actuators whether the correct action has been performed or not. This is the reason that intelligent steering systems are fault tolerant systems as the complexity and multi-dimensions levels and layers topology involve the steering systems. Therefore, manual efforts and conventional control approaches are unlikely to yield the desired level of execution and robust performance in such complex steering systems [92]. This has introduced the concept of forward-backward control systems, ANN, ML, and the artificial intellegence models, in which training examples are used to control the system and derive the model.

5.3.2 Artificial neural network (ANN)

The dynamic and kinematic behaviors of the steering systems make it non-linear and non-unique steering commands with higher number of degrees of freedom (DoF) on the vehicle level. Therefore, the ANN approach is preferable for steering systems due to the ability to learn with high-speed performance, parallel input and output data topology, and generalize the nonlinearity behavior. ANN has been shown to be a good classifier for unrelated data which is the case of the intelligent steering system in this study. The input data to the steering controller such as steering wheel angle, steering wheel speed (SWS), ego vehicle speed, and driver torque applied to the steering wheel are different categories encoded data. The representations of these data are fed to the electric power steering control module as either analog signal i.e. 0 – 5 direct current (DC) volts or on the controller area network (CAN) bus as entire frame message with end to end cyclic redundancy check and checksum protection.

Figure 5.1 left side shows the conventional or traditional control systems architecture and topology. The microcontroller is the central decision maker which receives, processes, computes and actuates outputs. Currently, the critical safety control systems use tri-core CPUs with higher computational capabilities and memories to provide sufficient puffer and signal processing. Whether it is consisted of application specific integrated circuits or field programmable gate array the main functions of the microcontroller relies on the operating software or algorithm in which a programmable math model controls the logic gates of the output based on the input signals. The right side of figure 5.1 shows the artificial neural network where the topology consists of input layer, hidden layers and output layer. The board support package (BSP) and system on the chip hosts these layers in which the training and predicting processes are performed.

The machine learning algorithm hosted by the SoC and neural network processors (NSP) offers the diversity of architectural implementation and redundancy because of the training and predictability with the feed forward or forward-backward control systems. This can be used in highly automated control systems of autonomous vehicles when higher architecture complexity and non-linearity models are deployed supported by system accelerators to process the payload data of the intelligent steering system.

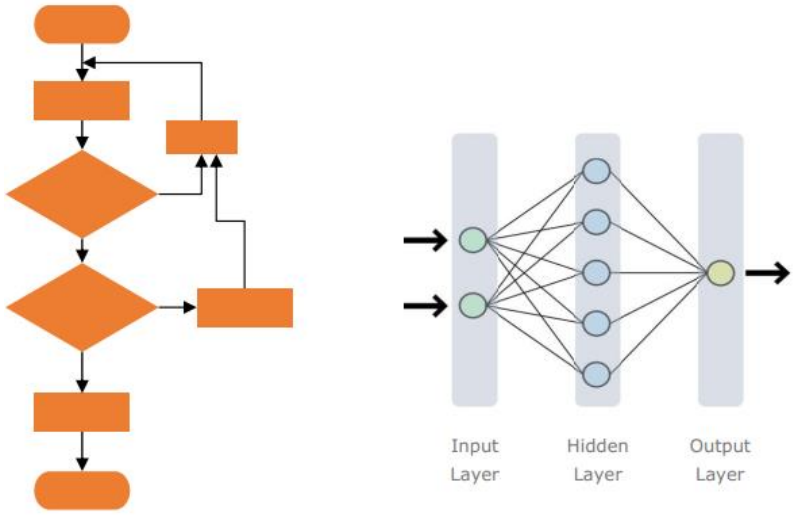

Figure 5.1. Conventional (traditional) control system (left) VS Artificial Neural Network System (right).

5.4 Methodology

5.4.1 Model Build and Simulation Tool Suite

In order to test and ANN in the EPS system, the driving environment and ecosystems along driving scenarios and vehicle maneuvers were identified and created in the model of the Simulink. Then, the model was run in the Simulink itself to make sure it is bug-free model. Upon successfully running the model, the code was compiled using the target link and the source code and generated S-functions were imported in the high fidelity dSPACE model desk. Interestingly, the dSPACE motion desk generates 3 dimensions model which runs in real time during the vehicle maneuvering and can be looked at from the driver and aerial views. All the simulations and tool suite that were running in this experiment are real time to mimic the real driving and maneuvering interactions and capture the vehicle dynamics parameters. The simulation is a realistic representation of the real-life events of the vehicle maneuvering. Consequently, this

method is very efficient to develop and validate vehicle models and collect data for analysis and post processing especially in the early vehicle and engineering product development processes.

5.4.2 Dataset and logs Collection

The experiment and maneuvers were performed on the high fidelity dSPACE SCALEXIO hardware-in-the-loop (HIL) bench and the vehicle dynamic model of the automotive simulation model (ASM) from the built-in Simulink model open source available in the library of the MATLAB. First, the Simulink model was compiled, and C code was generated and flashed in the dSAPCE built-in controller units to run the vehicle and create the virtual environment and mock-up functions. Then, the ego vehicle maneuver, traffic and road definition were defined and saved in the Model desk package of the dSPACE application which runs by python script. After that, the Model desk was downloaded in the Motion Desk and the graphical user interface (GUI) was ready to be used in the Control Desk package to drive the ego vehicle in a fully virtual environment. Figure 5.2 shows the layout of the dSPACE bench topology and application connections of this experiment. The ASM tool suite supports virtual test drives in complex traffic environments with high degree of fidelity so that sensor data can be generated for development in the early design phases of ADAS features and control units. The dSPACE manuals were used to set up the fully virtual environment and the virtual electronic control units [92].

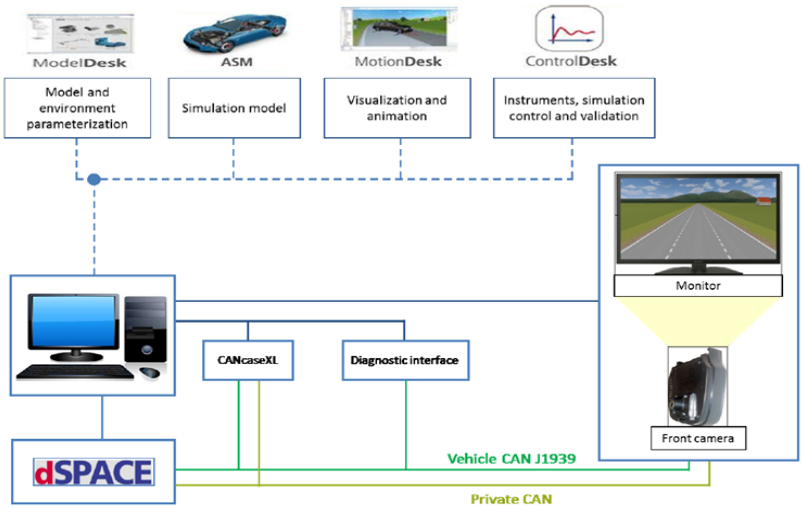

Figure 5.2. The generic layout of the dSPACE bench topology.

The real-time interface CAN multimessage blockset was used to generate and collect data from the CAN bus network. The bench setup allows to control the vehicle manually via external steering wheel joystick in real-time basis response as shown in figure 5.3.

Figure 5.3. The hardware-in-the-loop bench setup with the steering wheel to manually drive the ego vehicle on real time basis.

The dataset was collected in extensions of binary log file (BLF) from the bus logger and measurement data format (MDF). Then, the selected signals related to the

steering system were exported and stored in tabular data as csv extension to be used later to create the artificial neural network and post process data purposes. Table 5.1 shows the collected data, sampling rate and sources according to IEEE754 standard.

As a result of dataset recording and exporting, a log was formed and saved with the above parameters from the model. In total, about 11,100 time synchronized data points for the above parameters were obtained. Using the global cruiser of the CAN bus logger, the synchronization of all parameters was executed in the same updated time step.

Table 5.1. Dataset collected from the HIL bench.

Data [unit]	Sample rate	Data Type	Source
Time [sec]	2 msec	Int32	Simulink model
Vehicle speed [m/sec]	50 msec	Float32	Front wheels speed sensor
Steering wheel angle [deg]	2 msec	Float32	Simulated steering wheel sensor
Steering wheel speed [deg/sec]	2 msec	Float32	Simulated steering wheel sensor
Steering column torque [N.m]	10 msec	Float32	Torque sensor in the Logitech joystick steering wheel

5.4.3 Data Post Processing and Analysis

Using MATLAB R2021a version that supports all automotive toolboxes and sets, the collected dataset was imported to the workspace of MATLAB and the extension was

converted to .mat file to be compatible with the workspace of the neural network toolbox. Then, the artificial neural network was constructed using the Neural Network Training (nntraintool) toolbox of MATLAB. The input was four parameters as (time, SWA, SWS, and the ego vehicle velocity). The output or the target was loaded with the steering column torque dataset. The number of hidden neurons was adjusted to 20 to increase the training performance and decrease the mean square error (MSE). The MSE represents the average square difference between the outputs and the targets. Figure 5.4. shows the interfaces and the boundary layers of the neural network constructed in the work.

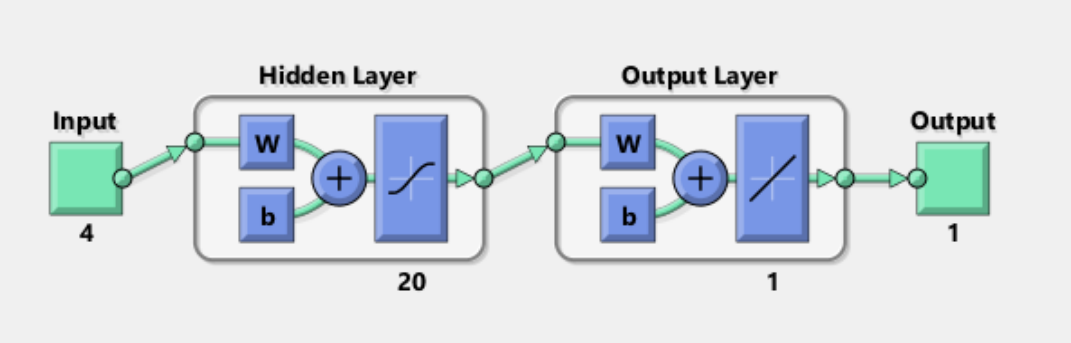

Figure 5.4. Neural network structure toolbox.

The ANN concept of work is that it is ultimately trying to mimic the human brain to solve different tasks. The artificial neuron gets several input data as a vector as shown in equation (5.1):

$$x = (x_1, x_2, \ldots\ldots, x_m) \tag{5.1}$$

Where m is the number of inputs. It weights each input x_i with a pre-determined weight w_i and sums up all the weighted input. A bias b is added to the sum and the result is

provided to an activation function λ, which is non-linear [94]. The output of the artificial neuron can be written as:

$$Output\ from\ Neuron = \lambda\ (\sum_{i=1}^{m} w_i\ x_i + \ b\ ) \tag{5.2}$$

The training algorithm was chosen as Levenberg-Marquardt (LM) following the work of Farhat, A. et al approach [95]. This algorithm requires more memory, but less time as reported in the MATLAB toolbox guideline [96]. The MSE is the average squared difference between the output and the trained target: lower values of the MSE are better . The regression (R) measures the correlation between outputs and the trained target. A value of R of 1 means a close relationship between the outputs and the targets. However, a value of 0 means a random relationship [97]. The neural fitting tool automatically divides the ANN samples to 70 % training, 15% validation and the rest of 15 % to testing [98]. The validation portion is used to validate the network and stop the training before overfitting. However, the test part is used as a completely independent test of the network generalization becasue the test part does use the labeled data that had been already used in the training and validation. This means that the test yields the data .similar to the input data formatThen, the ANN was trained to predict the steering column torque based on four input dataset of time, SWA, SWS and ego vehicle speed. The neural network toolbox runs 138 iterations and stops automatically to give as less as possible of MSE and as high as possible of R.

5.5 Results

5.5.1 Model Performance and Validation

In order to evaluate the performance of the validation and training of the proposed ANN of the steering system dataset, the trained ANN output was validated against the dataset of the input dataset parameter based on the steering column torque and the SWA. Two methods were developed in this dissertation based on the trained dataset used for the training and the target dataset as the followings:

1- The target data is the steering column torque based on all other trained dataset.

2- The target data is the SWA based on all other trained dataset.

5.5.1.1 Steering Column Torque Dataset as Target

The first method was to train all the dataset and set the steering column torque dataset as the target. The steering column torque values from the torque sensor was in the input dataset of the ANN for training. Then, it was set as a target in the ANN output in which it will be validated against the input dataset using the regression method. Plots of training, validation, test and all are generated from the ANN. The training output is shown in figure 5.5.

Figure 5.5. Training of the steering wheel torque output vs. the input dataset.

The x-axis in the plot represents the original steering column torque measure from the torque sensor in the experiments which is the target of the ANN training. However, the y-axis represents the predicted or trained torque output from the trained ANN based on other input parameters (time, vehicle speed, SWA and SWS). This output compared with the original steering column torque as shown in figure 5.5. It's clear that the deviation between the measured and predicted steering column torque values increase toward right and the left extremes because the non-linearity correlations between the inputs and steering torque commands and vehicle dynamic nature are associated with three degree of freedom systems or more.

The validation and the test of the output vs the input is shown in figure 5.6 and figure 5.7.

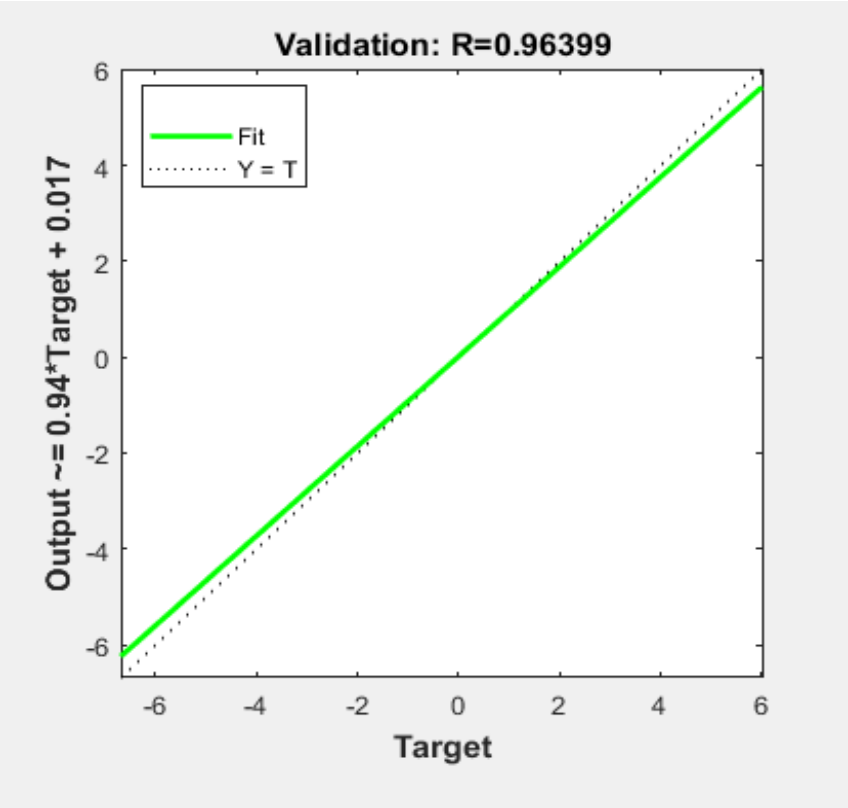

Figure 5.6. Validation of the steering wheel torque output vs. the input dataset.

The built ANN in this study is a two-layer feedforward network with tansigmoid transfer function in both the hidden and the output layer with 20 input neurons and 1 output neuron which is equal to the number of parameters in the target vector of the steering column torque. The regression of 96.25% was achieved for all, which means that

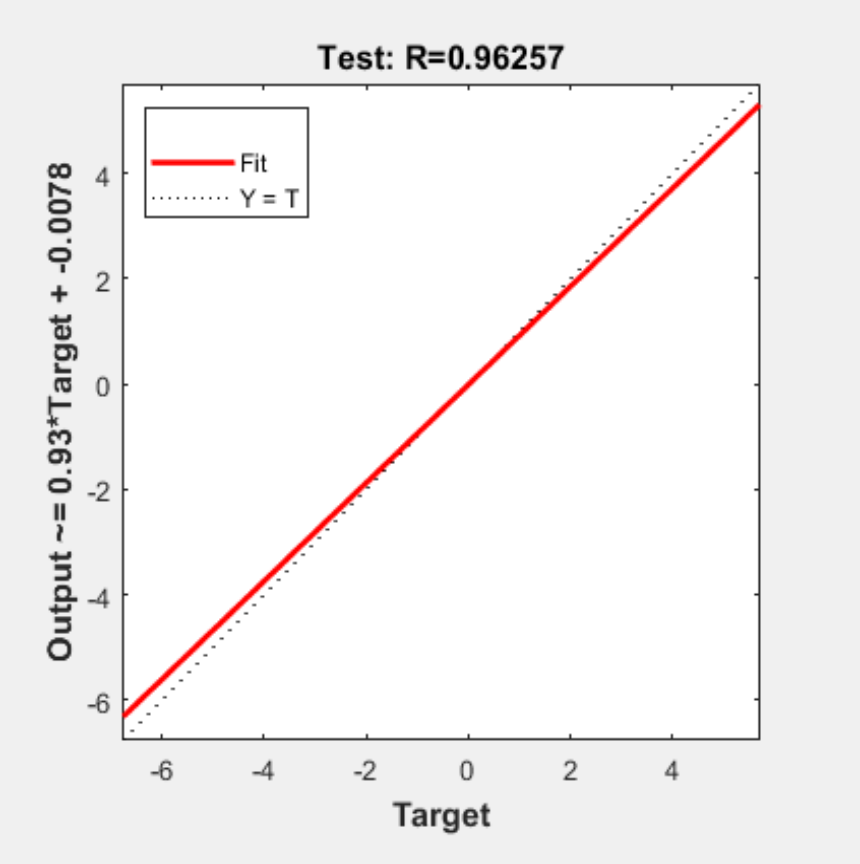

Figure 5.7. Overall test regression (R) of the steering wheel torque output vs. the input dataset.

there is ~ 3.75 % of deviation between the input and the trained output steering column torque. The shows that built ANN considering the main parameters of SWA, SWS and ego vehicle speed with their temporal rate was successfully trained towards predicting the steering column torque with ~ 3.75 % deviation mostly at the extreme edge of the steering torque commands. A calibration or correction factor can be added to the physical component of coil driver to address this deviation. The best validation performance was computed by the neural fitting tools to be 0.19717 at epoch 132 with the MSE and R as shown in table 5.2.

Table 5.2. Training, validation and test results for the SWT target.

Results	Samples	MSE[-]	R[-]
Training	7775	2.13399e-1	9.58652e-1
Validation	1666	2.32399e-1	9.53627e-1
Testing	1666	2.45282e-1	9.52188e-1

This requires 138 iteration cycles that last for almost 1 minute. Since the output dataset that has been trained, validated and tested with ~ 3.75 % deviation as shown in figure 5.8.

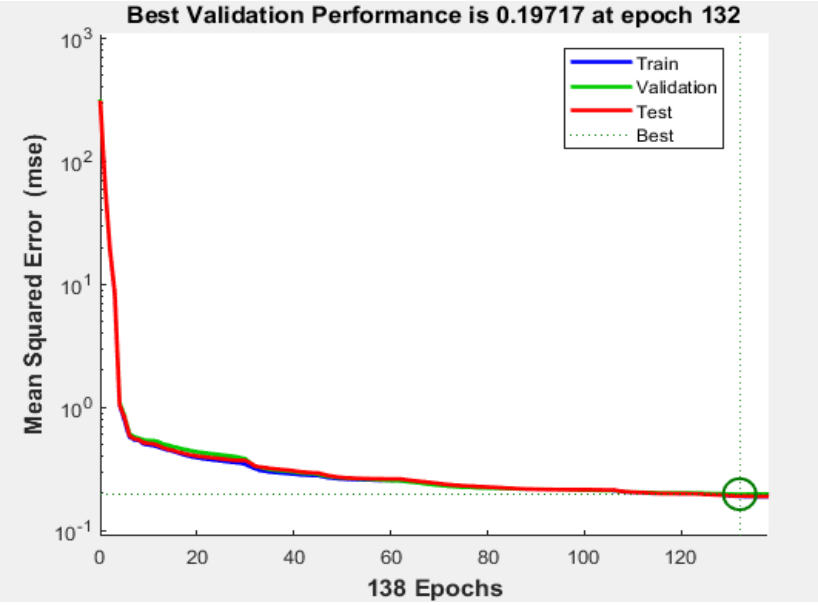

Figure 5.8. Best training, validation and test performance and MSE.

5.5.1.2 Steering Wheel Angle Dataset as Target

The second method developed in this dissertation was following the same approach of the previous section and switching the steering column torque with the

steering wheel angle dataset in the target so the ANN model will train and validate to predict the SWA dataset using the same dataset input of the previous section.

Interestingly, the training of the steering wheel angle dataset yields better results for all aspects of training, validation and test as shown in figures 5.9 through 5.11. with

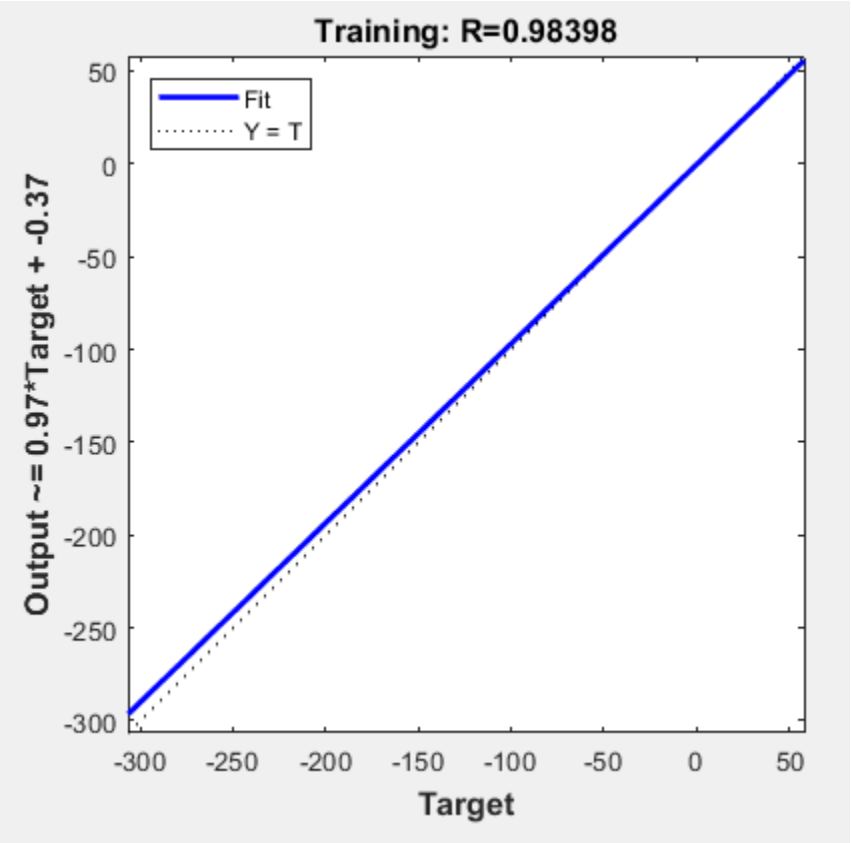

Figure 5.9. Training of the steering wheel angle output vs. the input dataset.

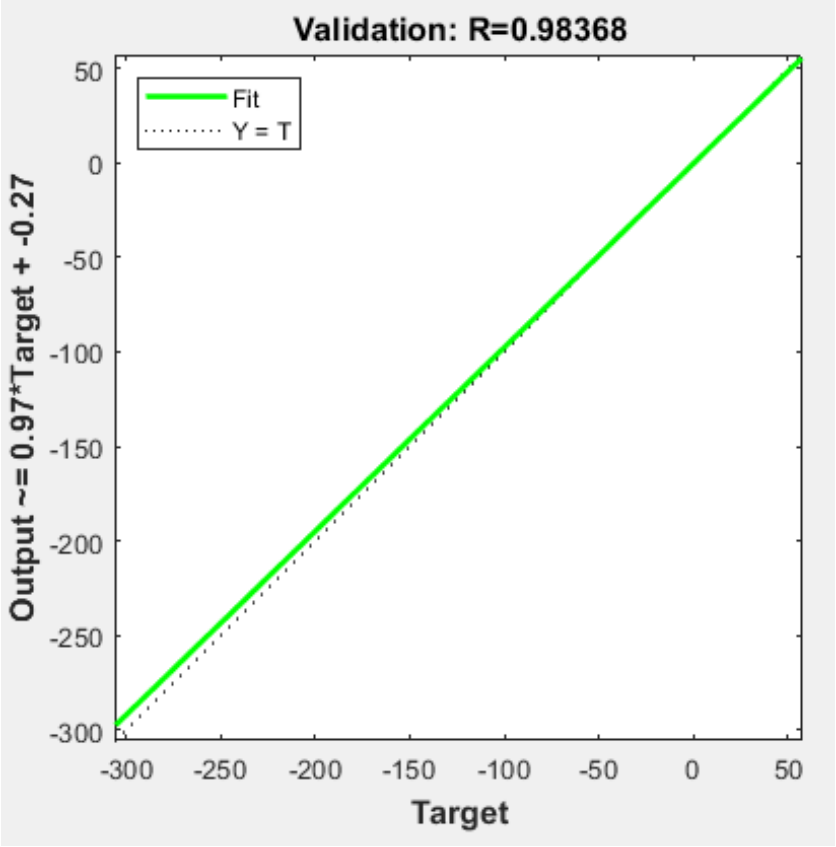

Figure 5.10. Validation of the steering wheel angle output vs. the input dataset.

R= ~ 98.36% vs. the previous section R = ~ 96.25%. The reason that the SWA yields better training results is that the steering wheel speed dataset is directly related to the SWA in the same time domain and using the same sensor of the steering wheel angle sensor. Also, another reason is that the steering wheel angle dataset samples increments were lower than the steering torque dataset due to the SWA sensor capacities to update that data every 2 msec as shown in table 5.1. for both SWA and SWS. Therefore, more SWA dataset means the ANN can better train and fit the output data with the input dataset. Another remarkable finding is that the SWA magnitudes range from 50 to -300 º

because the data acquisitions captures the SWA in degrees. The increase in the range and the difference between the min. and the max values with lower sampling increments provide the ANN model and layers with abundant data to train and

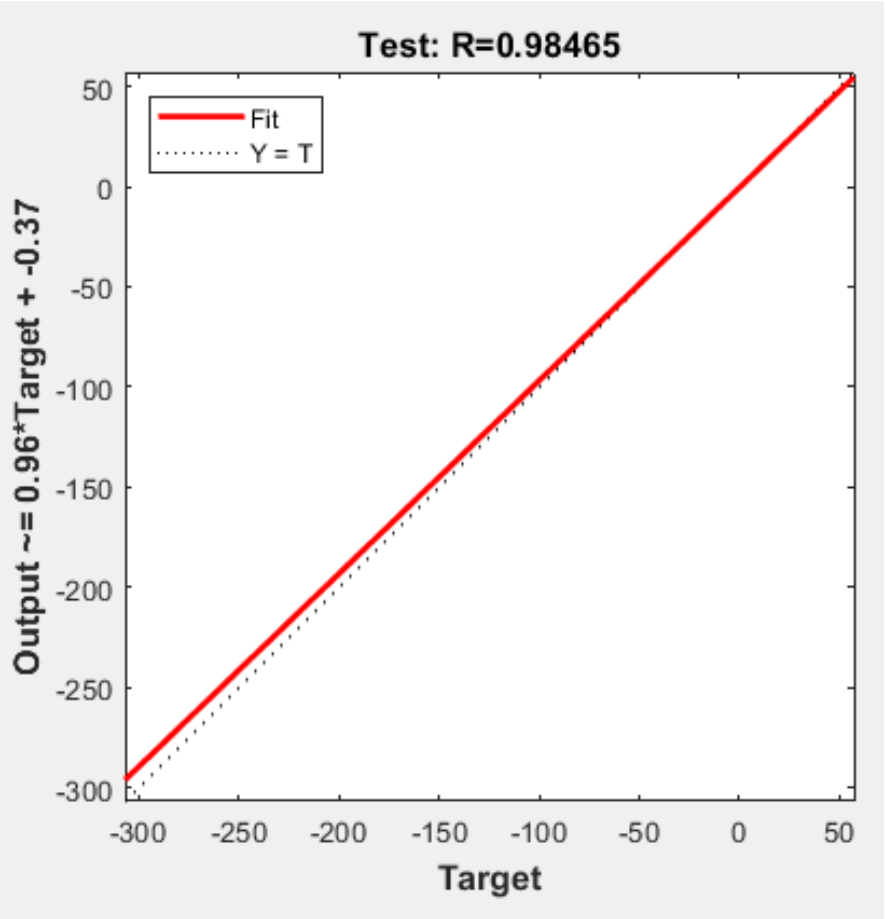

Figure 5.11. Overall test regression (R) of the steering wheel angle output vs. the input dataset.

reach the best fit in 47 epochs with the best validation performance of 81.8. This means that the training processes in the hidden layers took less time to converge the data and reach a pattern for the SWA target. Therefore, EPS systems should be developed to work

and response based on the SWA associated with the ANN and ML for better resolution, higher accuracy and pattern recognition. This feasible approach allows for autonomous vehicles designers to use ANN for a better prediction for path and trajectories planning of destination before starting the maneuver. This requires the use of ANN abstraction as an independent layer in the control module of the intelligent steering system for self-driving and pattern recognition for the steering commands. Table 5.3. shows the MSE and the R results with the SWA dataset as target.

Table 5.3. Training, validation and test results for the SWA target.

Results	Samples	MSE[-]	R[-]
Training	7775	1.31399e-1	4.58652e-1
Validation	1666	1.33399e-1	4.53627e-1
Testing	1666	1.47282e-1	4.52188e-1

One of the automotive applications' stringent requirements is the EUC sampling frequency when the vehicle is moving or maneuvering in the road. The critical safety controllers such as steering and braking actuation need to be executed every 2 msec which requires 500 Hz computation capabilities. Therefore, it is essential that the real-time ANN training yields the target dataset and samples the updated data in 2 msec. Let us assume a highway driving scenario when the ego vehicle is moving with the speed of 70 mph (equivalent to ~ 112.65 kph or 31.5 m/sec), the vehicle will move a distance of 0.315 m every 1 msec. Therefore, the ANN deployment is ADAS applications require

using NSP and accelerators to boost the computational performance of the controllers and execute in real-time of 1 to 2 msec.

5.5.2 Model Error Analysis

The error histogram with 20 bins was generated for training, validation and testing as shown in figure 5.12. The error was calculated as shown in Equation (5.3).

$$Error = Targets - ANN\ outputs \tag{5.3}$$

The error histogram figure shows that the data fitting errors distributed within a reasonably good range around zero denoted as orange vertical line for the training (blue), validation (green) and test (red) data. The number of bins of 20 represents the vertical bars observed in the error histogram ranging from -2.908 (leftmost bin) to 2.489 (rightmost bin). This error range is then divided into 20 smaller bins so each bin has a width of 0.269 as shown in Equation (5.4).

$$\frac{2.489 - (-2.908)}{20} = 0.269 \tag{5.4}$$

The vertical bar represents the number of samples from the dataset, which lies in a particular bin and their corresponding error. As can be seen that the higher number of the dataset plugged in ANN, the lower the error associated with it. As the number of instances (dataset combinations) decreases, the associated errors increase (positive and negative errors) which directly affects the ANN prediction performance.

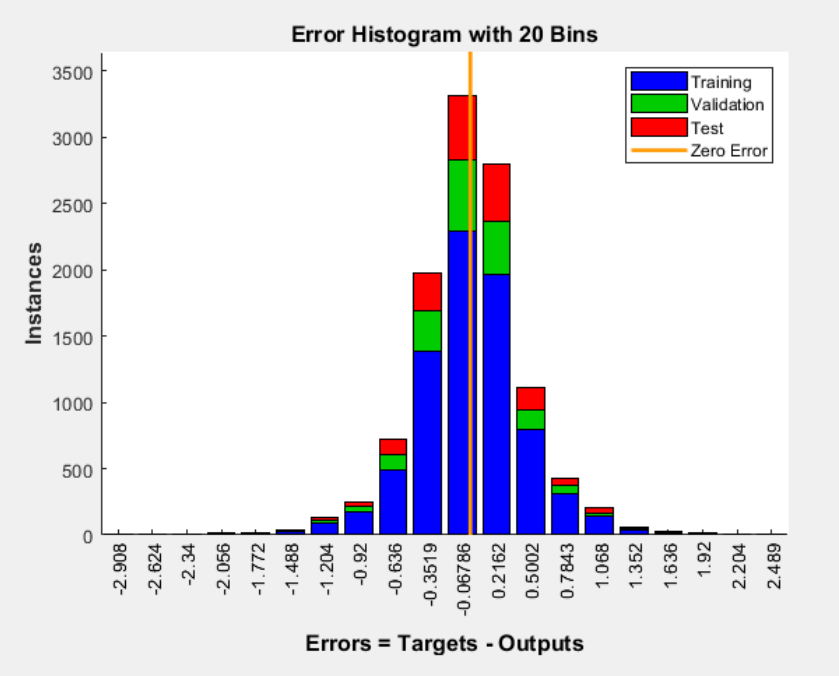

Figure 5.12. Error histogram of the ANN created with the simulation data.

The Simulink model was generated from the neural network toolbox as shown in figure 5.13. The block of NNET represents a model library that contains the hidden layer of the ANN.

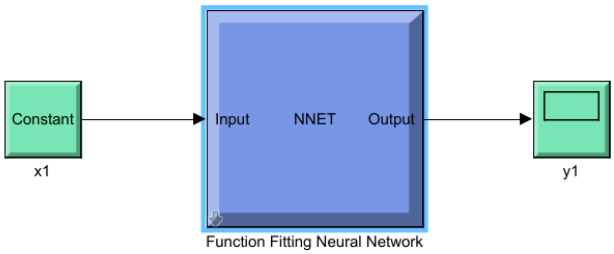

Figure 5.13. Artificial neural network Simulink model and interfaces input and output (IO).

A closer look inside the NNET block of the above Simulink model enables us to see the input and the output layers of the neural network as shown in figure 5.14. There is no feedback from the output of the ANN to the input and this is the reason this is call a feedforward type of control system.

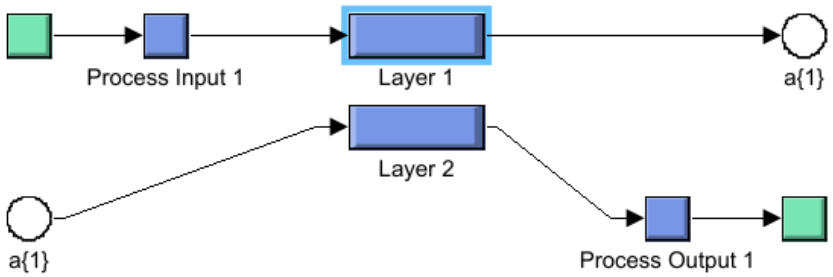

Figure 5.14. The topology of input and output layers of the neural network.

The Simulink model can be compiled and implemented in the embedded base software of the intelligent steering control module to enable the artificial neural network. This enables the automakers increasing the safety of the critical system controls module of the vehicle with the option to enable- disable the artificial neural network learning and training as desired.

5.5.3 Safety of the Artificial Neural Networks and Machine learning algorithms

Artificial neural network and machine learning algorithms, especially those using Deep Neural Networks, have demonstrated their excellent capabilities to resolve many critical control systems of autonomous vehicles control systems. They improved the quality of several non-safety related products in the past years and deployed in critical safety applications recently such as steering and braking systems. Their design and

development are so complicated that a number of hardly detectable systematic errors may occur, which may result in unintentional operation of the whole system. Therefore, functional safety standards or norms should be developed to allow for the safe implementation of these algorithms. ISO 26262 standard for functional safety in the automotive industry does not address the use of ANN and ML algorithms at all. A recent work analyzed safety lifecycle defined in ISO 26262 standard and proposed how currently defined work products can be adopted to cover specific aspects of ANN and ML algorithms. The proposed approach was presented in [99, 100] and proposed adaptation of ISO 26262 V-model workflow applied for ANN and ML algorithms to trace any potential failure before a dedicated standard for ANN and ML algorithms can be developed in the near future.

CHAPTER SIX

CONCLUSIONS

6.1 Research Summary

The new design guidelines proposed in this study serve to design a highly available EPS system architecture and accurately determine the ASIL for the sudden SLOA failure mode. The implementation of the control logic path for the EPS system that is compliant with the ISO 26262 Standard and PMHF metrics at the decision maker or microcontroller level. The recent market development of SUVs, BEVs and pickups showed increasing vehicles curb weight and more ADAS functionalities in the EPS system resulting in new challenges for potential SLOA of steering systems. The SLOA of steering system at higher rack forces and more ADAS functions leads to the recommendation to change the ASIL rating from ASIL B to ASIL C based on HARA and ISO 26262 metrics for the SLOA scenario. The proposed ASIL C mandates that the FIT to be less than 100 h^{-1} and the SPFM to be more than 97% as shown in table 3.11. It is possible to achieve ASIL C for EPS systems using various types of architectures at the level of control logic paths utilizing the redundancy concepts. ASIL C mitigation or risk reduction was achieved by incorporating a dual core microcontroller integrated with a power management and safety-monitoring unit at the same board. The proper implementation of this logic control path of dual core µc integrated with power management and safety monitoring makes the EPS system simpler, faster, reliable and more cost effective. This allows steering system designers to easily and effectively add

functional safety to EPS systems for higher levels of automated vehicles in the future. The combination of safe acquisitions, decision making and actuation along with ASIL decomposition simplify the hardware architecture for the market of highly available EPS systems and reduce the time to market highly available EPS systems compliant with the ISO 26262 Standard. Chapter three mainly covers the architecture design and hardware evaluation of the highly available EPS system. The model-based software design and implementation of highly automated driving systems was explained in chapter 4.

In chapter four, the analysis of model-based fault injection for the steering system of high-automated vehicles has shown that the steering wheel angle is of high importance and classified as ASIL D based on the risk assessment and control metrics that were developed in this study. The finding of chapter four modeling also redefined the controllability classes or categories of high automated vehicles based on the vehicle global position related to the lane marker lines to accommodate for the machine in the loop controlling the DDT in autonomous vehicle maneuvering. There are however, human factors challenge in SAE level 4 and 5 and the interaction between the driver and the automated control system of the vehicle that require HMI modalities as explained in table 4.6. The driver – automated control system engagement in the steering system of the vehicles is one of the crucial control complex scenario that add uncertainty and potential risk when handing over the steering control between the driver and-or the automated control system. Even when the driver is in full control of the steering system, the ESP is still responsible for approximately (~ 80%) of the SWT required to steer the vehicle. Therefore, the steering system design and functional safety metric requires specific

architecture redundancies in SW, HW and system level for high availability and risk mitigation mechanisms. Chapter four highlighted the need to define the driver intervention in high-automated vehicle of SAE level 4 and 5 in order to sustain the traffic safety and keep the vehicle in the intended trajectory. This can be addressed by HMI and the human factor implementation in ISO 26262 to standardize the driver-machine relation with the DDT in real time and interactive environment. Both manual and automated driving modes demand the functional safety implementation of the steering system to mitigate any system malfunction or failure. Therefore, the fault injection concept supports the safety mechanism implementation and correctness of the system architectural design with respect to faults and failures during the runtime. This improves the test coverage of developing safe control system to operate as designed and meet the safety requirements in compliance with the OEMs and government regulations. Another aspect to consider in the future work is to utilize the HMI in ASIL D systems in ISO 26262 in more detail and include the HMI in the safety mechanism of the vehicle control system.

The highly automated driving systems heavily rely on the artificial intelligence and the artificial neural network as the backbone of the control system. In chapter five, the problem of predicting the steering wheel torque commands for autonomous vehicles has been considered. This chapter research methodology used a collected dataset of steering system input and output parameters from vehicle level hardware-in-the-loop simulator of the high fidelity dSPACE bench to build the ANN for training and validation of the steering column torque commands. The performance of the artificial neural

network to predict the steering command based on the SWA, SWS and ego speed was validated with a regression value of ~ 96.5 % versus the measured steering torque commands. The results show that the artificial neural network can effectively predict the steering commands accurately given the fact that the non-linearity and complexity of the steering system control. This improves the safety highly automated driving system vehicles and confirm the feasibility of the concept of intelligent steering systems for path and trajectory planning based on the prediction patterns of the steering systems peripheral signals and parameters. Artificial intelligence finds its way to the most critical safety systems of the automotive for higher reliability and performance. Therefore, the ANN should be implemented as an abstraction layer in the control module to support sensor data fusion and support the prediction and pattern recognition.

6.2 Contributions

This dissertation demonstrated a significant contribution to the state of the art of the automated driving systems focusing on the steering systems and the human capabilities in the light of the emerging challenges of EV and AV. It provided an experimental assessment of utilizing an adaptive MPC for intended path follow and evaluated the failures in same model to improve the test coverage and assess the developed products in the early phase of the life cycle. The followings are the Contributions of this dissertation:

- Contribution to the understanding of the highly automated driving EPS systems and the design guide of the ASIL determination for the SLOA and LOF EPS systems.

- The second important contribution of this research and the hands-on experiment is to measure the human capability and controllability of the vehicle steering systems and define a new criteria for the controllability classes of the ASIL matrix because ISO 262626 uses a generic criteria that does not fit the highly automated driving systems. Based on the results of this research, the EPS systems developers can design the steering systems considering the human capability of steering wheel torque. The sudden loss of assistance of the EPS systems requires developing a highly available control system based on the new ASIL determined in this research given the fact that the vehicle curb weight is increasing in the EV and AV. The findings of the new ASIL determination and steering systems human controllability in the real product development of EV and AV will hopefully make the driving systems more reliable, safer and more comfortable. There is a strong need to address the human factors and the HMI of the highly automated driving systems and standardize the driver – machine with the DDT in real time and interactive environment.
- Also the controllability classes were redefined in chapter five based on the global position of the vehicle and related to the lane marker lines with the introduction of the wheel offset markers concept. The driving ecosystem of the vehicle position and the road environment were related to keep the vehicle in the intended path and defined the safety integrity of the highly automated driving vehicles of the SAE level 4 and 5.

- The ANN model developed in this dissertation with 98.5% performance results is a great success that the ML and ANN can be deployed in a critical safety systems of the AV. This will increase public trust and encourage OEMs and suppliers to adapt this technology in the automotive safety applications. This would save lives and reduce fatalities and make the driving experience more comfortable.
- Open the door for intelligent transportation systems development with EV, AV and PAV technologies to forge zero crashes, zero emissions and zero congestion.

6.3 Future Work

The future work should concentrate on the following aspects of the highly automated driving systems:

- Focus on the highly automated EPS signals and parameters optimization in different driving scenarios and maneuver environment such as intersections and roundabout and other complex driving scenarios. Consequently, this will cover a variety of situations and scenarios which increase the public trust towards hands-free driving systems across different ecosystems. These driving scenarios are very critical for the highly automated driving systems and the future of this technology to claim that the hands-free driving mode is safe and trustworthy with 100% coverage of the roads and scenarios.
- Another promising area is to focus on in the future is bridging the gap between ISO 26262 functional safety of the road vehicle and the artificial intelligence and the machine learning deployment in the automotive industry especially in the safety critical systems in the vehicle. The applicability of the V-model and the

required confidence in these new technologies in the safety critical systems and ASIL determination are still challenging in the absence of industrial standardization. These new technologies create lots of questions and concerns for meeting the functional safety requirements. For example, the validation process of the object detection systems uncertainties and probabilistic outcomes, which are hard to model and validate. In general, there is no formal specifications for these new technologies in the automotive industry.

- The implementation of the artificial intelligence and machine learning in the safety critical driving system will introduce the neural signal processing (NSP) which is different from the current analogue and digital signal processing. The deployment of the NSP and its interfaces with other signals need to be carefully studied and analyzed because the data layers and the time stamping are different from the analogue and digital types. The processing of the NSP requires accelerators and boosting the computational units and this creates more functional safety requirements and requires dedicated safety mechanisms to detect, mitigate and react for any malfunction in these signals and their serial data interfaces.

APPENDIX A

A PERMISSION TO CONDUCT INDOOR AND IN PERSON RESEARCH AT OAKLAND UNIVERSITY, IRB-FY2021-183

OAKLAND UNIVERSITY

Institutional Review Board

January 6, 2021

Protocol #: IRB-FY2021-183

Research Team:
Saif Salih
Richard Olawoyin

Based on applicable federal regulations, the following study, "Vehicle Steering System and Human Controlability " has been determined to be Approved, with the following categories 4. Collection of data through noninvasive procedures (not involving general anesthesia or sedation) routinely employed in clinical practice, excluding procedures involving x-rays or microwaves. Where medical devices are employed, they must be cleared/approved for marketing. (Studies intended to evaluate the safety and effectiveness of the medical device are not generally eligible for expedited review, including studies of cleared medical devices for new indications.)

This approval is based on an appropriate risk/benefit ratio and a project design wherein the risks have been minimized. All research must be conducted in accordance with this approved submission.

This letter along with the IRB date-stamped consent document can be found in Cayuse in the Submission Details page under Letters and Attachments, respectively.

Notes for Researcher(s):
Please note that Oakland University has mandated a temporary stoppage of all in-person human subjects research procedures. An exception to the stoppage may be obtained for research with special circumstances from the Vice President for Research, Dr. David Stone. Please contact Dr. Judette Haddad at haddad@oakland.edu to request to proceed with in person research procedures.

Permission from Research Site(s):
Please note the following:

- This IRB approval letter means that the research has met the federal criteria for approval per 45 CFR 46.111 Criteria for IRB Approval of Research.
- Before the research is initiated, permission to conduct research at a given site must be obtained from all

APPENDIX B

HUMAN SUBJECT RESEARCH CITI PROGRAM CERTIFICATE

CITI PROGRAM

Completion Date 04-Dec-2020
Expiration Date 04-Dec-2023
Record ID 39885244

This is to certify that:

Saif Salih

Has completed the following CITI Program course:

Not valid for renewal of certification through CME.

Human Subjects Research
(Curriculum Group)
Student and Faculty Advisor Basic/Refresher
(Course Learner Group)
1 - Basic Course
(Stage)

Under requirements set by:

Oakland University

CITI
Collaborative Institutional Training Initiative

REFERENCES

1. Fatality Analysis Reporting System (FARS), “https://www.nhtsa.gov/research-data/fatality-analysis-reporting-system-fars “National Highway Traffic Safety Administration, Washington, DC 20590.
2. USDOT, Bureau of Statistics, Motor and Vehicle Safety, https://www.bts.gov/content/motor-vehicle-safety-data, Washington, DC
3. National Center for Statistics and Analysis, “2018 fatal motor vehicle crashes: Overview. (Traffic Safety Facts Research Note. Report No. DOT HS 812 826),”, Washington, DC: National Highway Traffic Safety Administration.
4. Thorn, Eric, Shawn C. Kimmel, Michelle Chaka, and Booz Allen Hamilton. A framework for automated driving system testable cases and scenarios. No. DOT HS 812 623. United States. Department of Transportation. National Highway Traffic Safety Administration, 2018.
5. Singh, Santokh. Critical reasons for crashes investigated in the national motor vehicle crash causation survey. No. DOT HS 812 115. 2015.
6. Salih, Saif, and Richard Olawoyin. Computation of Safety Architecture for Electric Power Steering System and Compliance with ISO 26262. No. 2020-01-0649. 2020.
7. Marcano, Mauricio, José A. Matute, Ray Lattarulo, Enrique Martí, and Joshué Pérez. "Low speed longitudinal control algorithms for automated vehicles in simulation and real platforms." Complexity 2018 (2018).
8. Wang, Raymond, and Robert Charles Crimmins. "Autonomous Ground Vehicle Prototype via Steering-, Throttle-, and Brake-by Wire Modules." (2016).
9. FDIS, ISO. "26262 2nd. Edition: Road Vehicles–Functional Safety." The International Organization for Standardization (ISO), (2018).
10. SAE On-Road Automated Vehicle Standards Committee. "Taxonomy and definitions for terms related to driving automation systems for on-road motor vehicles." SAE International: Warrendale, PA, USA, 2020.
11. International Standards. ISO 26262 Functional safety for road vehicles. Part 1, Geneva, Switzerland, Second edition, 2018.
12. Palin, R., David W., Ibrahim H., and Roger R., "ISO 26262 safety cases: Compliance and assurance," 1-12, 2011.

13. International Standards. ISO 26262 Functional safety for road vehicles, Part 3 . Geneva, Switzerland, Second edition, 2018.

14. Schmid, T., “Safety Analysis for highly automated driving,” IEEE International Symposium on Software Reliability Engineering Workshops, pp. 154–157, 2018.

15. Forkenbrock, Garrick J., and Devin Elsasser. "An assessment of human driver steering capability." National Highway Traffic Safety Administration DOT HS 809: 875, 2005.

16. Trimble, Tammy E., Richard Bishop, Justin F. Morgan, and Myra Blanco. "Human factors evaluation of level 2 and level 3 automated driving concepts: Past research, state of automation technology, and emerging system concepts," 2014.

17. Schmid, T., “Safety Analysis for Highly Automated Driving,” in IEEE International Symposium on Sofware Reliability Engineering Workshops, 2018, 154-157.

18. Sampath Kumar, Varun. "P3/PPP in the Context of Autonomous Driving Vehicles." (2017).

19. Horani, Modar, and Osamah Rawashdeh. A Framework for Vision-Based Lane Line Detection in Adverse Weather Conditions Using Vehicle-to-Infrastructure (V2I) Communication. No. 2019-01-0684. SAE Technical Paper, 2019.

20. Al-Refai, Ghaith, Modar Horani, and Osamah A. Rawashdeh. "A Framework for Background Modeling Using Vehicle-to-Infrastructure Communication for Improved Candidate Generation in Pedestrian Detection." In 2018 IEEE International Conference on Electro/Information Technology (EIT), pp. 0729-0735. IEEE, 2018.

21. Horani, Modar, Ghaith Al-Refai, and Osamah Rawashdeh. Towards Video Sharing in Vehicle-to-Vehicle and Vehicle-to-Infrastructure for Road Safety. No. 2017-01-0076. SAE Technical Paper, 2017.

22. Raiyn, Jamal. "Road Intersection Intelligent Traffic Management Based on V2V Wireless Communication." In 2019 IEEE International Conference on Electrical, Computer and Communication Technologies (ICECCT), pp. 1-6. IEEE, 2019.

23. Ängskog, Per, Per Näsman, and Lars-Göran Mattsson. "Resilience to Intentional Electromagnetic Interference Is Required for Connected Autonomous Vehicles." IEEE Transactions on Electromagnetic Compatibility (2018).

24. Van ND, Kim GW. Fuzzy Logic and Deep Steering Control based Recommendation System for Self-Driving Car. In2018 18th International Conference on Control, Automation and Systems (ICCAS) 2018 Oct 17 (pp. 1107-1110). IEEE.

25. Bojarski M, Yeres P, Choromanska A, Choromanski K, Firner B, Jackel L, Muller U. Explaining how a deep neural network trained with end-to-end learning steers a car. arXiv preprint arXiv:1704.07911. Apr 25, 2017.

26. Kornhauser AL. Neural network approaches for lateral control of autonomous highway vehicles. InVehicle Navigation and Information Systems Conference, 1991 1991 Oct 20 (Vol. 2, pp. 1143-1151). IEEE.

27. Montanaro U, Dixit S, Fallah S, et al., “Towards connected autonomous driving: Review of use-cases,” Vehicle System Dynamics, 2018.

28. Koopman, Philip, Uma Ferrell, Frank Fratrik, and Michael Wagner. "A safety standard approach for fully autonomous vehicles." In International Conference on Computer Safety, Reliability, and Security, pp. 326-332. Springer, Cham, 2019.

29. Jonasson, Mats, and M. Thor. "Steering redundancy for self-driving vehicles using differential braking." Vehicle system dynamics 56, no. 5 (2018): 791-809.

30. Lin, Shih-Chieh, Yunqi Zhang, Chang-Hong Hsu, Matt Skach, Md E. Haque, Lingjia Tang, and Jason Mars. "The architectural implications of autonomous driving: Constraints and acceleration." In Proceedings of the Twenty-Third International Conference on Architectural Support for Programming Languages and Operating Systems, pp. 751-766. 2018.

31. Tlig, Mohamed, Mathilde Machin, Romain Kerneis, Emmanuel Arbaretier, Linda Zhao, Florent Meurville, and Jean Van Frank. "Autonomous Driving System: Model Based Safety Analysis." In 2018 48th Annual IEEE/IFIP International Conference on Dependable Systems and Networks Workshops (DSN-W), pp. 2-5. IEEE, 2018.

32. Lytrivis, Panagiotis, and Angelos Amditis. "Intelligent Transport Systems: Co-Operative Systems (Vehicular Communications)." Wireless Communications and Networks-Recent Advances (2012).

33. Gao, Yiqi. "Model predictive control for autonomous and semiautonomous vehicles." PhD diss., UC Berkeley, 2014.

34. Mayne, David Q., James B. Rawlings, Christopher V. Rao, and Pierre OM Scokaert. "Constrained model predictive control: Stability and optimality." Automatica 36, no. 6 (2000): 789-814.

35. Froisy, J. Brian. "Model predictive control: Past, present and future." Isa Transactions 33, no. 3 (1994): 235-243.

36. Morari, Manfred, and Jay H. Lee. "Model predictive control: past, present and future." Computers & Chemical Engineering 23, no. 4-5 (1999): 667-682.

37. Jiang-Yun Y, Feng K, Fang-Yuan W. Control strategy for front wheel angle of steer-by-wire based on variable steering ratio. InProceedings of 2011 International Conference on Computer Science and Network Technology 2011 Dec 24 (Vol. 2, pp. 852-856). IEEE.

38. Eski, Ikbal, and Ali Temürlenk. "Design of neural network-based control systems for active steering system." Nonlinear Dynamics 73, no. 3 (2013): 1443-1454.

39. Duau, Jie, Lei Zhang, Zhaoiinz Zhang, Jinzbo Zhao, and Yan Jiang. "Research on Automatic Steering System of Agricultural Machinery Based on Fuzzy Neural Network." In 2018 2nd IEEE Advanced Information Management, Communicates, Electronic and Automation Control Conference (IMCEC), pp. 1602-1605. IEEE, 2018.

40. Park, Seungjin, Wonteak Lim, and Myoungho Sunwoo. "Robust Lane-Change Recognition Based on An Adaptive Hidden Markov Model Using Measurement Uncertainty." International Journal of Automotive Technology 20, no. 2 (2019): 255-263.

41. Li, Zeyu, Jiangqiang Hu, and Xingxing Huo. "PID control based on RBF neural network for ship steering." In 2012 World Congress on Information and Communication Technologies, pp. 1076-1080. IEEE, 2012. J. Clerk Maxwell, A Treatise on Electricity and Magnetism, 3rd ed., vol. 2. Oxford: Clarendon, 1892, pp.68–73.

42. Farhat, Ana, and Ka C. Cheok. "Improving adaptive network fuzzy inference system with Levenberg-Marquardt algorithm." In 2017 Annual IEEE International Systems Conference (SysCon), pp. 1-6. IEEE, 2017.

43. Meng, Yanan, Xiuwei Fu, and Li Fu. "Application of neural network trained by adaptive particle swarm optimization to fault diagnosis for steer-by-wire system." In 2010 International Conference on Measuring Technology and Mechatronics Automation, vol. 1, pp. 652-655. IEEE, 2010.

44. Nowakowski, Christopher, Steven E. Shladover, and H-S. Tan. "Heavy vehicle automation: Human factors lessons learned." Procedia Manufacturing 3 (2015): 2945-2952.

45. Scheibenzuber, W., Franziska M., Julao Nimler E., Ovaldo B., Harald W., and Friedrich R., "Dual-Sensor Package Technology Supporting ASIL-D in Safety-Related Automotive Applications,".

46. Rao, Deepak, Plato Pathrose, Felix Huening, and Jithin Sid. "An approach for validating safety of perception software in autonomous driving systems." In *International Symposium on Model-Based Safety and Assessment*, pp. 303-316. Springer, Cham, 2019.

47. Inoue, S., Takumi O., Hideo I., Pongsathorn R., and Masao N.,"Cooperative lateral control between driver and ADAS by haptic shared control using steering torque assistance combined with direct yaw moment control," In 2016 IEEE 19th International Conference on Intelligent Transportation Systems (ITSC), pp. 316-321. IEEE, 2016.

48. Schneider, N., Christian, P., and Alexandra N.,"Comparison of steering interventions in time-critical scenarios," Procedia Manufacturing 3: 3107-3114, 2015.

49. Halvorson, B. “Electric Power Steering: We Ask An Insider Where It’s Headed,” 2012.

50. Chiriac, V., Ciprian-Romeo, C., and Dănut B., "Safety Concepts for Body Control Automotive Functionalities," In 2018 10th International Conference on Electronics, Computers and Artificial Intelligence (ECAI), pp. 1-4. IEEE, 2018.

51. Koopman, P., and Michael W.,"Challenges in autonomous vehicle testing and validation," SAE International Journal of Transportation Safety 4, no. 1 : 15-24, 2016.

52. Svancara, K., John, P., Tomislav, L., Joseph D., Maciej K., and William J.,"Advantages of the alternative method for random hardware failures quantitative evaluation-A practical survey for eps," SAE International Journal of Passenger Cars-Electronic and Electrical Systems 6, no. 2013-01-0190 : 377-388, 2013.

53. International Standards, ISO 26262 Functional safety for road vehicles. Part 4, Geneva, Switzerland, second edition, 2018.

54. International Standards, ISO 26262 Functional safety for road vehicles. Part 5, Geneva, Switzerland, second edition, 2018.

55. International Standards, ISO 26262 Functional safety for road vehicles. Part 3, Geneva, Switzerland, second edition, 2018.

56. Miller, B., “General Motors recalling more than 1 million trucks and SUVs,” the Business Journals News Network, https://static.nhtsa.gov/odi/rcl/2018/RCAK-18V586-6881.pdf, 2018.

57. Granig, W, Dirk, H., and Hubert, Z., "Calculation of failure detection probability on safety mechanisms of correlated sensor signals according to iso 26262," SAE International Journal of Passenger Cars-Electronic and Electrical Systems 10, no. 2017-01-0015: 144-155, 2017.

58. Damak, Youssef, Marija Jankovic, Yann Leroy, and Bernard Yannou. "Analysis of Safety Requirements Evolution in the Transition of Land Transportation Systems Toward Autonomy." 2018.

59. Robert Bosch GmbH, https://www.bosch-mobility solutions.com/en/solutions/steering/electrohydraulic-power-steering-pump/, USA, 2021.

60. US Department of Transportation, Federal Highway Administration FHWA, OHPI, NHTSA, “https://www.fhwa.dot.gov/ohim/onh00/bar7.htm”, 2020.

61. Driving Tests, NHTSA, “https://driving-tests.org/beginner-drivers/how-to-hold-a-steering-wheel/”, 2021.

62. Don, S., “Are We Losing Touch? A Comprehensive Comparison Test of Electric and Hydraulic Steering Assist,” https://www.caranddriver.com/features/a15122019/electric-vs-hydraulic-power-steering/, Jan 2018,

63. Edwad, G., “Fundamentals of Automotive Conventional-Powertrian Integration,” Chapter 3, 2018.

64. Sari, B., and Hans-Christian, R., “ASIL-Decomposition and Related DFA for Autonomous Driving Systems,” No. 2019-01-0135. SAE Technical Paper, 2019.

65. Klomp, M., Mats, Jonasson, L., Leon H., Enrico R., and Stefan S., "Trends in vehicle motion control for automated driving on public roads." Vehicle System Dynamics 57,” no. 7: 1028-1061, 2019.

66. Zifei, Y., “The International Council on Clean Transportation, ICCT,” https://theicct.org/blogs/staff/china-still-lagging-fuel- consumption-2014, Spet, 2015.

67. Harrer, M., and Peter P., “Steering handbook,” Switzerland: Springer International Publishing, 2017.

68. Pacejka, Hans, “*Tire and vehicle dynamics”* Elsevier, 2005.

69. Haupt, A., Fabian, W., Christian, B., and Barbara, H., "Automated generation of classifier based monitoring functions and its application to automotive steering control." IFAC Proceedings Volumes 43, no. 7: 721-726, 2010.

70. NHTSA. Preliminary Statement of Policy Concerning Automated Vehicle, http://www.nhtsa.gov/staticfiles/ rulemaking/pdf/Automated_Vehicles_Policy.pdf, May 2013.

71. Jonasson, M., and M. T., "Steering redundancy for self-driving vehicles using differential braking," Vehicle system dynamics 56, no. 5: 791-809, 2018.

72. International Standards, ISO 26262 Functional safety for road vehicles. Part 11, Geneva, Switzerland, second edition, 2018.

73. Wu, Z., Xiezu, S., and Yuan, Z., "Functional Safety System Design on EPS," In Society of Automotive Engineers (SAE)-China Congress, pp. 647-664. Springer, Singapore, 2016

74. Bernon-Enjalbert, V., Mathieu Blazy, W., Regis, G., David, L., Jean-Philippe M., and Mark O., "Safety Integrated Hardware Solutions to Support ASIL D Applications." (2013).

75. Montanaro U, Dixit S, Fallah S, et al., “Towards connected autonomous driving: Review of use-cases,” Vehicle System Dynamics, 2018

76. Sampath Kumar, Varun. "P3/PPP in the Context of Autonomous Driving Vehicles." (2017).

77. Alberto Bemporad, Manfred Morari, and N. Lawrence Ricker, “Model Predictive Control Toolbox: User's Guide (R2020a). MathWorks, 2020, https://instruct.uwo.ca/engin-sc/391b/downloads/mpc.pdf

78. Watzenig D., Horn M. “Introduction to Automated Driving.” Automated Driving. Springer, Cham. https://doi.org/10.1007/978-3-319-31895-0_1, 2017.

79. Wu, Jingda, Zhiyu Huang, and Chen Lv. "Uncertainty-Aware Model-Based Reinforcement Learning with Application to Autonomous Driving." *arXiv preprint arXiv:2106.12194*, 2021.

80. Lytrivis, Panagiotis, and Angelos Amditis. "Intelligent Transport Systems: Co-Operative Systems (Vehicular Communications)." Wireless Communications and Networks-Recent Advances (2012).

81. USDOT, Bureau of Transportation Statistics, Motor and Vehicle Safety, https://www.bts.gov/content/motor-vehicle-safety-data, Washington, DC

82. National Center for Statistics and Analysis, “2018 fatal motor vehicle crashes: Overview. (Traffic Safety Facts Research Note. Report No. DOT HS 812 826),”, Washington, DC: National Highway Traffic Safety Administration.

83. Kim, Wonhee, Chang Mook Kang, Young-Seop Son, and Chung Choo Chung. "Nonlinear steering wheel angle control using self-aligning torque with torque and angle sensors for electrical power steering of lateral control system in autonomous vehicles." *Sensors* 18, no. 12, 2018.

84. Regan, Michael A., Charlene Hallett, and Craig P. Gordon. "Driver distraction and driver inattention: Definition, relationship and taxonomy." Accident Analysis & Prevention 43, no. 5, 2013.

85. Marinik, Andrew, Richard Bishop, Vikki Fitchett, Justin F. Morgan, Tammy E. Trimble, and Myra Blanco. Human factors evaluation of level 2 and level 3 automated driving concepts: Concepts of operation. No. DOT HS 812 044. United States. National Highway Traffic Safety Administration, 2014.

86. Ellims, M., and H. E. Monkhouse. "Agonising over ASILs: Controllability and the in-wheel motor." (2012): 52-52.

87. Schneider, Norbert, Christian Purucker, and Alexandra Neukum. "Comparison of steering interventions in time-critical scenarios." Procedia Manufacturing 3 (2015): 3107-3114.

88. Thorn, Eric, Shawn C. Kimmel, Michelle Chaka, and Booz Allen Hamilton. A framework for automated driving system testable cases and scenarios. No. DOT HS 812 623. United States. Department of Transportation. National Highway Traffic Safety Administration, 2018.

89. Debouk, R., “Overview of the 2nd Edition of ISO 26262: Functional Safety–Road Vehicles.” General Motors Company, Warren, MI, USA, 2018.

90. Singh, Santokh. Critical reasons for crashes investigated in the national motor vehicle crash causation survey. No. DOT HS 812 115. 2015.

91. Khan, Muhammad Qasim, and Sukhan Lee. "Gaze and eye tracking: techniques and applications in ADAS." *Sensors* 19, no. 24, 5540, 2019..

92. Koopman, Philip, and Michael Wagner. "Challenges in autonomous vehicle testing and validation." SAE International Journal of Transportation Safety 4, no. 1 (2016): 15-24.

93. dSPACE manuals release 2016 A. “ControlDesk of dSPACE”, 2016.

94. Hansson, Anders. "Steering Angle Prediction by a Deep Neural Network and its Domain Adaption Ability." Master's Theses in Mathematical Sciences (2018).

95. Farhat, Ana, and Ka C. Cheok. "Improving adaptive network fuzzy inference system with Levenberg-Marquardt algorithm." In 2017 Annual IEEE International Systems Conference (SysCon), pp. 1-6. IEEE, 2017.

96. Demuth, Howard, and Mark Beale, and Martin Hagan. "Neural network toolbox." *For Use with MATLAB. The MathWorks In,c* 2020.

97. Ayala, Melvin, and Malek Adjoundi. "Artificial neural network design and evaluation tool." U.S. Patent 7,502,763, issued March 10, 2009.

98. Samadani, M., CA Kitio Kwuimy, and C. Nataraj. "Diagnostics of a nonlinear pendulum using computational intelligence." In Asme 2013 dynamic systems and control conference, pp. V002T24A006-V002T24A006. American Society of Mechanical Engineers, 2013.

99. Neural Network, https://www.mathworks.com/discovery/neural-network.html, 2019.

100. Radlak, Krystian, Piotr Serwa, Michał Szczepankiewicz, and Tim Jones. "Organization of ML-based product development as per ISO 26262." arXiv preprint arXiv:1910.05112, 2019.

LIST OF PUBLICATIONS

1. Salih, Saif, and Richard Olawoyin. "Fault Injection in Model-Based System Failure Analysis of Highly Automated Vehicles." IEEE Open Journal of Intelligent Transportation Systems (ITS) 2, 417-428, 2021.
2. Saif, Salih, and Richard, Olawoyin, "Computation of Safety Architecture for Electric Power Steering System and Compliance with ISO 26262," SAE Technical Paper 2020-01-0649, 2020, https://doi.org/10.4271/2020-01-0649.
3. Salih, Saif, and Dan DelVescovo. Design and Validation of a GT Power Model of the CFR Engine towards the Development of a Boosted Octane Number. No. 2018-01-0214, 2018.
4. Salih, Saif, and Richard Olawoyin. "Intelligent Performance Analysis of Automated Steering Systems for Autonomous Vehicles." In 2020 IEEE International Conference on Electro Information Technology (EIT), pp. 200-205. IEEE, 2020.
5. Salih, Saif, and Richard Olawoyin. "Twin Scroll Turbocharger Simulation and Engine Power Optimization." In IIE Annual Conference. Proceedings, pp. 670-675. Institute of Industrial and Systems Engineers (IISE), 2020.
6. Salih, Saif, Daniel DelVescovo, Christopher P. Kolodziej, Toby Rockstroh, and Alexander Hoth. "Defining the boundary conditions of the CFR engine under RON conditions for knock prediction and robust chemical mechanism validation." In Internal Combustion Engine Division Fall Technical Conference, vol. 51982, p. V001T02A005. American Society of Mechanical Engineers, 2018.
7. Salih, Saif. "Water-diesel emulsion: a review," International Journal of Advances in Engineering & Technology 10, no. 3: 429-436, 2017.